Measurement of the Sound Speed in Articular Cartilage *In-Vitro*

by

Sushil G. Patil

A Thesis Submitted for the Degree of
Master of Philosophy
in
Biomedical Engineering
(December 2004)

Jockey Club Rehabilitation Engineering Centre

The Hong Kong Polytechnic University

CERTIFICATE OF ORIGINALITY

I hereby declare that this thesis is my own work and that, to the best of my knowledge and belief, it reproduces no material previously published or written, nor material that has been accepted for the award of any other degree or diploma, except where due acknowledgement has been made in the text.

Sushil G. Patil

Dedicated

To

Love, Peace, Unity and Mankind

对于

爱、和平、团结　和　人类

प्रति,
प्रेम, शांती, एकता और मनुष्यमात्र

प्रति,
प्रेम, शांती, एकता आणि मनुष्यगण

Abstract

Articular cartilage (artC) is a biphasic biological soft tissue that covers the end of articulating bones within synovial joints. It plays an important role for joint lubrication and load transmission, and mainly consists of an organic composite matrix filled with liquids. The change of artC thickness, measured by various devices such as X-ray has been widely used as an indicator for its degeneration status. Recently, ultrasound (US) has been widely used to investigate the change of thickness and acoustic and mechanical properties of the degenerated artC.

The sound speed in artC is an essential parameter for the ultrasonic measurement, and its change is also an indicator of artC degeneration. Conventional methods of calculating the sound speed require the measurement of the artC thickness in addition to the detection of the flight time of sound. Therefore, different approaches including needle punching technique, optical measurements, magnetic resonance imaging (MRI), X-ray, etc., have to be used for the measurement of artC thickness, which increases the complexity of the assessment. The sound speed of artC can be affected by the variations of surrounding environment and its structure during *in-vitro* measurement. Environmental factors include the temperature and the concentration of saline surrounding the artC specimen, while the artC structural factors include its inhomogeneous structure, anatomic location, degeneration level and compression level. To better understand the variation of the sound speed in artC under various conditions is important to the US assessment of artC.

In the present study we first developed a non-contact US approach to measure the sound speed and the thickness of artC simultaneously using US (50MHz) alone. After

validation using different materials, this approach was then used to investigate the variations of the sound speed in artC at different tissue depths (n = 18 x 3) and locations (n = 10 x 25), treated with different enzymes (n = 20 x 5), and under different temperature (n = 20) and saline concentrations (n = 19). ArtC specimens from bovine patellar models were used in these *in-vitro* studies. The strain-dependence (n = 20) of the sound speed in artC was studied using a custom-designed US compression device, which allowed simultaneous measurement of the applied force, artC deformation, and US signal reflected from the artC surface.

Results showed that the sound speeds of artC at superficial, middle and deep regions were 1518±17 (mean±SD), 1532±26 and 1554±42 m/s with the US beam parallel to the artC surface, and 1562±23, 1623±33 and 1703±50 m/s with the US beam perpendicular to the artC surface, respectively. The differences among the different depths and between the two measurement directions were both significant ($p < 0.001$). The sound speed in artC ranged from 1681±50 m/s to 1816±54 m/s with the saline concentrations varied from 0M to 2.5M, while the sound speed in saline changed from 1521±03 to 1674±03 m/s. The sound speed in artC changed from 1430±39 to 1667±68 m/s when the temperature varied from 15°C to 40°C. In case of the digested specimens the sound speed in artC significantly ($p < 0.001$) decreased from 1653±40 m/s to 1577±32, 1564±33 and 1575±38 m/s in specimens digested by chondrotinase, collagenase and trypsin, respectively. It was noted that the sound speed in artC varied from 1507 – 1830 m/s at the 25 locations tested on the patella. Significant ($p < 0.01$) site dependence of the sound speed in artC was demonstrated between the inner region and the surrounding region of the patellae. It was also revealed that the sound speed in artC

increased from 1581±36 m/s at 0% compression to 1671±56 m/s at 20% compression. The sound speed in artC almost linearly increased at a rate of 11 m/s per 1°C increase in temperature. The overall mean of the sound speed in full-thickness artC was (1648±75 m/s, ranged from 1438 - 1984, 327 specimens and 87 patellae)

The present study introduced a non-contact approach to measure the sound speed in artC *in-vitro*. The results revealed that the sound speed in artC varied significantly with the variations in artC structure, environmental and pathological conditions. It is concluded that these variations play important roles in defining the accuracy and reliability of the ultrasonic measurements of artC and should be well considered during the experimental designs. Though the results were obtained *in-vitro* using bovine patellar models, they should also have reference values for the ultrasonic assessment of human artC *in-vitro* or *in-vivo*.

*Key Words**:*** ultrasound, sound speed, high-frequency US, articular cartilage, osteoarthritis, cartilage degeneration.

Acknowledgements

This study was carried out in the Jockey Club Rehabilitation Engineering Center, The Hong Kong Polytechnic University during the year 2002 – 2004. I wish to express my deepest gratitude to everyone who has contributed to my study and supported my work towards this thesis. Especially, I wish to mention the following persons.

First of all I would like to issue my warm thanks to my supervisor, Dr. Yong Ping Zheng. He has supported and inspired me throughout this project. I am very grateful for the opportunity given to me to work under his professional and dynamic guidance. His truly constructive criticism, as well as optimism and encouragement, serve as a model to any researcher. His valuable comments and enthusiasm on this study have been important factors in helping me to complete this study. Prof Arthur Mak also deserves my sincere gratitude especially for his support in studies concerning the use of his laboratory and sharing his immense knowledge of tissue biomechanics. I am blessed to have a supervisor who shares endless expertise and has given support during every point of research project. I wish to express my sincere thanks to Dr. Daniel Chow and Dr. Raymond Tong for assessing my progress on this study, and enriching my thoughts with their useful comments and guidance. I also want to address my gratitude to Dr. Aaron Leung, Dr. Nakkeeran Kaliyaperumal, Dr. Andrew Holmes, Dr. Ameersing Luximon and other academic faculty members for the academic as well as emotional support provided during my stay in HK.

I owe my deepest thanks especially to Mr. Shi Jun, Mr. Huang Qing Hua, Dr. Chen Xin, PhD., and Mr. Huang Yan Ping for the invaluable cooperation in software

development. I cherish all members of biomedical US team including Mr. Choi Pong Chi, Miss Wang Qing, Miss Lu Min Hua for their ever friendly and helpful attitude.

I would like to acknowledge Dr. Tam Wing Cheung, Mr. Chen Kung Chee and Mr. Tin Chi Fai for allowing me to use the workshop and their invaluable help in the development of US instrument. My sincere appreciation to Dr. Jian-Yong Wu of the Department of Applied Biology and Chemical Technology for the opportunity to use the facilities of his laboratory. I convey my thanks to all friends in my department for the support they provided right from day one in this laboratory. It would have been difficult for me to get along in a foreign country without their guidance and caution every now and then. I would like to thank my friends in Polytechnic University and in Hong Kong for being there whenever I needed. Special thanks to my brother Dr. Sandeep Patil, Mr. Kannan Ranganath, Miss Candy Yung and Miss Cris Liu for their encouragement, generous support, and friendship throughout my stay in Hong Kong. Lastly, but not the least, I would like to convey thanks to my friends back in India who are and will be for me. Their support, motivation, kindness etc are much appreciated. Good luck to all of you in the career you chose for yourself. Special thanks to my family members back home.

The project was jointly funded by the Research Grant Council of Hong Kong and the Hong Kong Polytechnic University.

Sushil G. Patil Hong Kong, November 2004

Table of Contents

Abbreviations and Nomenclature

artC	articular cartilage
US	ultrasound
PG	proteoglycan
GAG	glycosaminoglycan
PBS	phosphate buffered saline
OA	osteoarthritis
MRI	magnetic resonance imaging
CT	computed tomography
MU	medial upper
ML	medial lower
LU	lateral upper
LL	lateral Lower
PC	personal computer
A/D	analog to digital
LVDT	linear variable differential transducer
RF	radio frequency
SD	standard deviation
E	Young's modulus
Φ	diameter
σ	stress
ε	strain
H	equilibrium aggregate modulus
v	Poisson's ratio
F	applied force
a	radius of the indenter
w	deformation
κ	theoretical correction factor for the finite artC thickness in indentation
h	artC thickness
K	bulk modulus
G	shear modulus
ρ	density of the material
c_{AC}	sound speed in artC
c_S	sound speed in saline
hrs	hours
min	minutes
sec	seconds
ns	nano seconds
N	Newton
MPa	mega pascal
mm	millimeter
eqn	equation

List of Figures

List of Tables

1. Introduction

1.1 Articular Cartilage (ArtC)

1.1.1 Brief Overview of ArtC

ArtC is a highly specialized, avascular and aneular translucent tissue that covers the ends of articulating bones within synovial joints. It is a special fibrous connective tissue that has limited potential for repair. It mainly consists of an organic composite matrix filled with liquids. Functionally, artC has to perform its obligatory physiological functions without suffering any damage over the lifespan of a living being. ArtC has a important mechanical task to transmit load across joints and it provides almost frictionless surfaces to allow unhampered locomotions (Kempson 1980; Mow et al 1991).

1.1.2 Structure of ArtC

Structurally, artC can be considered as a proteoglycan (PG) gel reinforced by a network of fine collagen fibrils and swollen with a multi-ionic electrolytic aqueous solution (Mow et al 1991; Mankin et al 1994). The biomechanical properties of artC are mostly determined by the interactions among the three organic composite matrix namely collagen, PG and chondrocytes (Toyras et al 2003). Its material composition is a mixture of cells imbedded in an extra cellular matrix, permeated by the network of collagen fibers. Due to the spatial variation of the water content, the PG concentration and the orientation of the collagen fibrils, the mechanical properties of the artC are different at different depths as shown in Fig 1 (Mow et al 1991; Mankin et al 1994). Therefore, artC is referred as structurally inhomogeneous and exhibits anisotropic mechanical properties.

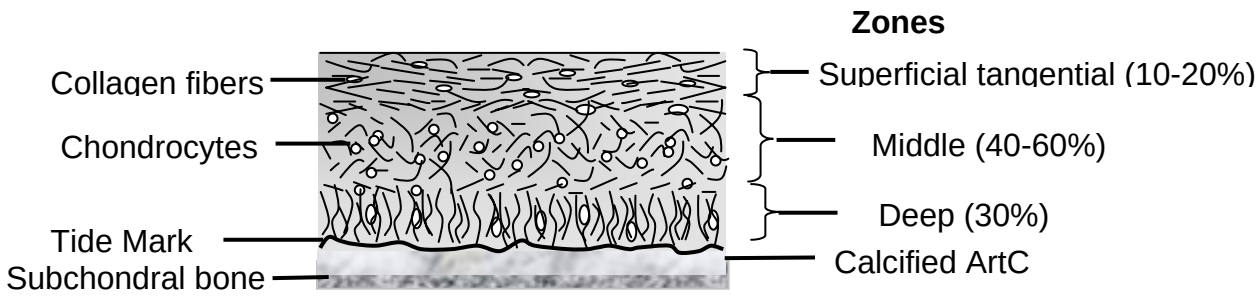

Figure 1. Schematic representation of the layered stucture of artC (Mow et al 1991).

Table 1. Composition of artC (Mow et al 1991).

Phase		Superficial (Tangential)	Middle (Transitional)	Deep (Radial)
Solid	Collagen fiber orientation	Parallel to artC surface	Random	Perpendicular to artC surface
	Chondrocyte structure orientation	Elongated, parallel to artC surface	Circular	Elongated, perpendicular to artC surface
	PG content	Lowest	In-between	Highest
Fluid	Water content	Highest	In-between	Lowest

The three zones shown in Fig 1 are widely understood to be distinct from each other based on the orientation of the different components of artC. Fig 1 and Table 1 illustrates the artC components and their orientation in different layers. ArtC consists mainly of a solid phase (chondrocytes that occupy about 1% of the tissue wet weight and the extra cellular matrix (ECM) i.e. the collagen network and the PG that account for 20-30% of weight) and a liquid phase (the interstitial water that comprises 60-80% of the wet weight) (Mow et al 1991). Collagen fibers, mainly of type II collagen, form a highly organized and isotropic three dimensional fibrous network in artC. The collagen is one of the major constituent in artC accounting for the largest portion of organic material in the

tissue, 15-22% of the tissue wet weight (Mow et al 1991). The orientation of collagen fiber is different in the three zones of artC. The collagen fibers are arranged parallel, random, and perpendicular to the surface of artC in the superficial, middle, and deep layer, respectively. They are anchored to the artC-bone interface. PG is another major macromolecular constituent of artC in addition to the collagen and accounts for 4-7% of the tissue wet weight. PG consists of a core protein bonded with glycosaminoglycan (GAG) chains. PG monomers combine to form aggregates. They are produced by chondrocytes and secreted into the matrix. Together with collagen network, PG accounts for the complex physiochemical interactions in artC (Grodzinsky 1983). The functions of collagen (Armstrong and Mow 1982) and PG (Harkness RD 1968; Kempson et al 1973) are to establish the tensile property and the compressive stiffness of artC, respectively. Chondrocytes are specialized cells that manufacture and maintain the ECM. The cells occupy 1-10% of the tissue volume, yet relatively few chondrocytes are capable of producing the fibril-reinforced gel structure of the collagen and the PG. The space surrounding the macromolecules and chondrocytes is filled with water and multiple ions. A small amount of water is contained in chondrocytes. About 30% of water is in the intrafibrillar space within collagen fibrils, while the remainder exists in the solution form by water and PG (Mow et al 1991). The water content of the tissue is governed by (1) the concentration of PG and the resulting swelling pressure, (2) the organization of collagen network and (3) the strength and stiffness of the collagen network that resist PG swelling (Maroudas 1976). Thus, the tropic structure and composition of ECM results in an inhomogeneous distribution of water. The water content is highest in the superficial tissue and decreases towards the deep tissue (Muir 1995).

1.1.3 Degeneration of ArtC

Osteoarthritis (OA) is very common joint disorder affecting millions of elderly individuals all over the world. The general understanding of the process of OA is a source of inflamed synovium that stimulates the degeneration of artC (Fukui et al 2001). OA can result in pain, swelling and progressive loss of motion (Buckwalter and Mankin 1997). In advanced OA, artC gets completely damaged and the bones of the femur, the tibia, and the patella come in direct contact. This is generally accompanied by significant pain leading to a decrease in motion, muscle weakness and difficulty in walking. The common symptoms of artC degeneration are tissue softening (Lane et al 1979), fibrillation of the superficial layer, changes in the organization of artC components and disruption of the organization of collagen fibers (Weiss and Mirow 1972; McDevitt 1973). The measurement of mechanical properties of artC is important for investigating the reasons behind the degeneration and the approaches for its diagnosis.

1.2 Assesment of ArtC

1.2.1 Conventional Approaches for ArtC Assessment

In recent years, a number of different approaches have been introduced to improve the assessment of artC *in-vivo* as well as *in-vitro*. These methods include magnetic resonance imaging (MRI) (Burstein et al 2000; Nieminen et al 2000; McGibbon 2003), X-Ray (Adam et al 1998), calibrated microscope (Myers et al 1995; Jurvelin et al 1995), micrometer installed with microscope (Modest et al 1989), needle penetration technique (Swann and Seedhom 1989; Jurvelin et al 1995; Yao and Seedhom 1999; Toyras et al 1999), Stereophotogammetry (Athesian et al 1992), CT arthrography

(Buckland-Wright et al 1995), optical coherence tomography (Herrmann et al 1999), mechanical indentation (Armstrong and Mow 1982; Lyyra et al 1995; Duda et al 2000), electromechanical evaluation (Sachs and Grodzinsky 1995; Garon et al 2002), as well vibroarthrography, i.e. analysis of sound generated during the motion of the joint (Tavathia et al 1992; Zhang et al 1994; Shen et al 1995).

X-ray is routinely used to confirm the diagnosis of OA disease by measuring the gap between bones, but unable to directly visualize the artC tissue. In addition, because of their low resolution, current clinical noninvasive imaging modalities such as X-Ray, CT arthorgraphy and MRI are able to detect only the late stages of the artC degradation. Another nondestructive and noninvasive approach is the vibroarthrography. The sound generated by the stimulation with a finger tap over the mid-patella or the swinging movement of the leg was collected around the knee joint and analyzed using different signal processing approaches. This convenient and noninvasive approach shows great potential in the assessment of artC degeneration, but it is difficult to provide localized assessment. Arthroscopy is another approach that can be used to assess artC *in-vivo* with its telescope inserted into the joint through a small hole in the skin and other soft tissue (Fu et al 1998). Due to the limitation of the conventional optical imaging, arthroscopy can only assess the surface condition of artC, such as fibrillation, which again is a later indication of OA. The Optical techniques such as stereomicroscope can also be used to measure the thickness of artC, but only for *in-vitro* assessment for isolated artC specimens. Recent development of optical coherence tomography provides a tool for the assessment of artC not only on the surface but also along cross-sectional area. Together with arthroscopy, it has good potential for the diagnosis of OA, but researchers showed

that it cannot detect the artC-bone interface clearly, thus difficulty for the precise measurement of artC thickness (Jurvelin et al 1995). In the case of the needle punching technique, artC is penetrated perpendicularly to the surface by a sharp needle which is normally fixed to a material testing machine. The measured force and displacement signals allow the detection of artC thickness. Due to its destructive nature, it can only be used for *in-vitro* assessment. In addition, since the artC-bone interface is irregular, the thickness of artC may not be measured very accurately even in the *in-vitro* situation. Since softening is one of the early signs of OA, measurement of the mechanical properties of artC becomes an important approach for the assessment of artC. It has already been demonstrated that an indentation probe together with the arthorscope can be used for the assessment of artC *in-vivo* (Lyyra et al 1995). However, the indentation probe alone cannot provide the thickness of artC, which may affect the stiffness measurement. It will be further elaborated in the following section. Due to its nondestructive nature and penetration capability, US techniques have recently widely investigated for the assessment of artC, which will be introduced in detail later on.

1.2.2 Mechanical Characteristics of ArtC

During the joint movement, artC is subject to repetitive loading and unloading. Therefore, artC's mechanical properties play an important role in defining its life span. Stress-relaxation is a typical phenomenon of the viscoelastic behavior of artC. In the stress-relaxation test, a deformation is applied on artC instantaneously or during a short time then maintained as a constant. The deformation results, initially, in a stress rise followed by a period of fall in stress until equilibrium is reached. During the stress-

relaxation phase, the water gradually moves out of the artC. At the equilibrium state, no fluid flow or pressure gradient subsist, and the load is therefore controlled completely by the solid matrix. After the load is removed, the artC gradually reaches its original dimensions at the rate that is dependent on the artC properties. There are three commonly used methods for the mechanical measurement of artC including indentation test, unconfined compression, and confined compression (Mow et al 1991). All of them can be associated with the stress-relaxation test to measure the viscoelastic mechanical properties of artC.

For the unconfined and confined compression, the artC sample has to be isolated from the joint and used for the *in-vitro* testing. ArtC has to be further removed from its subchondral bone in the unconfined compression. In the confined compression, the artC sample is inserted into a confined chamber and the artC surface is compressed with a porous compressor. During the confined compression, the water content of artC may flow freely only via the porous compressor. In the unconfined compression, the artC sample is compressed between two smooth impermeable platens (metallic or glass) and the fluid flow is allowed only in the lateral direction. In the indentation test, artC is compressed with a plane-ended (or spherical-ended) indenter and it can be applied for *in-situ* assessment of artC as the test can be conducted on the articulating surface of the joint. The indenter may be permeable or impermeable. Among the three tests, only the indentation test can be used for the *in-vivo* assessment of artC.

For an elastic material that is compressed in an unconfined condition, Young's modulus (E) is determined as the ratio of stress (σ) and strain (ε):

$$E = \frac{\sigma}{\varepsilon} \qquad (1)$$

This equation is commonly known as a generalization of the Hooke's Law. Based on the assumption of material isotropy, the aggregate modulus (H_a) is related to E and Poisson's ratio (v) (Mow et al 1991; Jurvelin et al 1995):

$$H_a = \frac{(1-v)}{(1+v)(1-2v)} \times E \qquad (2)$$

Hayes et al (1972) proposed an indentation model for the assessment of artC. Considering artC as an elastic material with a fixed rigid underlying surface, the Young's modulus E is determined by eqn (3):

$$E = \frac{(1-v^2)}{2a\kappa(v, a/h)} \times \frac{F}{w} \qquad (3)$$

where F is the applied force, v is the Poisson' ratio of artC, a is the radius of the indenter, w is the deformation, and $\kappa(v, a/h)$ is the theoretical correction factor for the finite artC thickness, h. The applied deformation is assumed to be infinitesimal and the contact between the indenter and the artC is assumed to be frictionless. Table 2 gives typical values of equilibrium Young's modulus, the equilibrium aggregate modulus, and the equilibrium Poisson's ratio of the human and bovine artC. Table 3 shows the various measurements conducted to measure the mechanical properties of artC. The measurement includes unconfined compression and indentation test. The information of the measurement type, nature of experiment, maximum strain, ramping rate, steps of compression are included. It has been widely reported that the Young's modulus of artC depends on its measurement direction, tissue depth, anatomical site, and degeneration status. This is further elaborated in the section of the sound speed variations.

Table 2. Typical values of the material parameters of the human and bovine artC in compression as determined by the unconfined, confined compression or indentation test.

Measurement site	H_a (MPa)	E (MPa)	ν	Reference
Human artC				
Patellar groove	0.5 – 0.9	0.6	0 – 0.16	Jurvelin et al 2003
Patella	0.9			Appleyard et al 2001
Medial condyle	0.6		0.07	Athanasiou et al 1997
Bovine artC				
Patellar groove	0.5		0.25	Athanasiou et al 1997
Patella	0.6	0.5 – 0.8	0.10 – 0.36	Korhonen et al 2002
Medial condyle	0.3 – 0.9	0.3 – 0.6	0.21 – 0.43	Korhonen et al 2002

(*E:* Equilibrium Young's modulus, H_a: equilibrium aggregate modulus, and ν: Poisson's ratio).

Table 3. A summary of the recent measurements of the equilibrium Young's modulus of artC reported in the literature. The information of the measurement type, nature of experiment, maximum strain, ramping rate, steps of compression are included.

Authors (Year)	Measurement	Nature of experiment	Maximum strain	Ramping rate	YM (MPa)
Jurvelin et al (1997)	Unconfined Compression	Stress Relaxation	20%	1 μms^{-1} 10 steps (4% / step)	0.754±0.198
Toyras et al (1999)	Indentation Test	Stress Relaxation (450 s)	20%	1 μms^{-1} 10 steps (40μm/step)	1.039±0.333
Lyyra et al (1999)	Indentation Test	Stress Relaxation (780 s)	20%	2 mms^{-1} 10 steps (4% / step)	0..094 – 1.6
Koehonen et al (2002)	Unconfined Compression	Stress Relaxation (<100 Pa / min)	20%	1 μms^{-1} 4 steps (5% / step)	0.56±0.19
Toyras et al (2003)	Indentation Test	Stress Relaxation (2400 s)	10%	2 mms^{-1} 3 steps (1% strain /step)	0.29±0.30

1.2.3 Ultrasound Measurement of ArtC

US has been widely used for the measurement of thickness, and acoustic, and mechanical properties of artC (Rushfeldt et al 1981; Modest et al 1989; Agemura et al 1990; Jurvelin et al 1995; Myers et al 1995; Yao and Seedhom 1999; Toyras et al 1999, 2003; Joiner et al 2001; Suh et al 2001). In the following sections, literatures were reviewed for the US measurement of the thickness, sound speed, and stiffness of artC.

1.2.3.1 Measurement of Thickness and Sound Speed

Rushfeldt et al (1981) used A-mode US (20 MHz) for the measurement of thickness of artC. Later, many studies used similar US techniques to measure artC thickness, with an underlying assumption in all measurements that the second reflection used in thickness calculations was from the artC-bone interface. Indirect measurement of artC was conducted by Modest et al (1989) using two techniques namely: the optical and the ultrasonic technique. The measurements established that the second reflection was from the artC-bone interface and validated the ultrasonic technique as a method of mapping the thickness distribution of artC in synovial joints *in-situ*. Later, Jurvelin et al (1995) conducted thickness measurements of artC using needle punching, ultrasonic, and optical technique to evaluate the suitability of these measurement techniques for thickness measurement. Myers et al (1995) used high frequency US (25MHz) to measure sound speed in artC wherein the thickness of artC was measured using optical technique. They concluded that high frequency ultrasonic images obtained *in-vitro* provided highly accurate and reproducible measurements of the thickness of artC. However, Yao and Seedhom (1999) suggested that a constant sound speed for measuring artC thickness may

introduce serious limitations. The measurements were conducted based on extensive locations including ankle and hip joints. Their measurement methods included needle punching technique and US.

The tissue thickness is a crucial parameter for the measurements of biomechanical properties of artC using indenation test as shown in eqn (3). The change of artC thickness is also an indicator to its degeneration. The thickness of artC was conventionally measured using the calibrated microscopes (Myers et al 1995; Jurvelin et al 1995), the micrometer installed with microscopes (Modest et al 1989), and the needling technique (Swann and Seedhom 1989; Jurvelin et al 1996; Yao and Seedhom 1999; Toyras et al 1999). Most of the above techniques can only be used *in-vitro*. The artC thickness can also be measured using other techniques such as X-ray (Adam et al 1998). Recently, US techniques have been widely used for the measurement of artC thickness. There has been growing evidence that US can potentially provide a non-destructive approach for the *in-vivo, in-situ and in-vitro* measurements of the artC thickness (Rushfeldt et al 1981; Macirowski et al 1994; Chen and Sah 2000; Toyras et al 2001; Youn and Suh 2001; Nieminen et al 2002; Laasanen et al 2002; Zheng et al 2004). Most of these approaches involved the measurement of the sound speed and thickness of artC. However, measurement of artC with US alone is notoriously difficult. Measurement of the sound speed needs the knowledge of the tissue thickness and vice versa. Therefore, earlier US studies on artC were performed by either assuming constant sound speeds reported in the literature (Jurvelin et al 1995) or measuring thickness by needling technique (Mow et al 1989; Jurvelin et al 1995; Swan and Seedhom. 1999; Toyras et al 1999; Nieminen et al 2002). The techniques used with US for the measurement of the sound speed and

thickness are summarized in Table 4. The approaches that include different techniques to measure the sound speed and thickness separately may affect the accuracy of the measurements. Potential errors may also occur with the difference in the needle and transducer orientations and the uneven artC-bone interface (Mann et al 2001). Yao and Seedhom (1999) measured the sound speed of human artC, the thickness of which was measured using a needling technique. Their study demonstrated that the sound speed of human artC varied widely and hence concluded that US measurement of artC thickness using a constant sound speed was not reliable.

The sound speed in artC is an important parameter for the measurement of artC thickness using US (Rushfeldt et al 1981; Modest et al 1989; Adam et al 1998; Toyras et al 1999). Constant sound speeds were frequently used in these studies based on the values reported in the literature. However, many studies have demonstrated that the change of the sound speed can be used as an indicator of artC degeneration (Myers et al 1984 and 1995; Agemura et al 1990; Wilson et al 1993; Toyras et al 1999; Suh et al 2001; Joiner et al 2001). Yao and Seedhom (1999) reported a very large variation of sound speed in human artC. In their study, the thickness was measured using the needle punching technique. The accuracy of the sound speed measurement might be affected by the mismatch of the precise measurement locations or directions, with the needle punching and the US method. Suh et al (2001) measured the sound speed and thickness of artC tissues simultaneously *in-situ* by applying an indentation on the artC surface. Using this technique, the sound speed of artC could be measured without the knowledge of the artC thickness. Since the stiffness of artC tissues significantly depends on the depth (Guilak et al 1995; Schinagl et al 1996; Zheng et al 2001, 2002; Wang et al 2002), artC is

compressed non-uniformly during indentation. Thus the knowledge about the dependence of the sound speed in artC is critical to this new approach.

Table 4. A summary of the sound speed of full-thickness artC reported in the literature. The information of the specimen type, US frequency, and testing temperature were included. In addition, the methods used for thickness measurement were also described.

Authors (Year)	ArtC Specimen	US Frequency	Testing Temperature	Thickness Measurement	Sound speed
Modest et al (1989)	Human femoral head	7.5 MHz	Room temperature	Microscope and needle insertion	1760 m/s
Jurvelin et al (1995)	Canine and bovine femoral and tibial condyles	10 MHz	Room temperature (22.5°C)	Microscope and needle insertion	1760 m/s (verified)
Agemura et al (1990)	Bovine patella	100 MHz	Room temperature	Optical method	1617 ~ 1720 m/s
Myers et al (1995)	Human femoral condyle	25 MHz	Room temperature	Microscope	1658±185 m/s
Yao and Seedhom (1999)	Human hip and ankle joint	20 MHz	Room temperature	Needle insertion	1892±183 m/s
Toyras et al (1999)	Bovine patella	22 MHz	37°C	Needle insertion	1654±82 m/s
Joiner et al (2001)	Bovine femoral condyle Human femoral condyle	30 MHz	37°C	Saline sound speed with specimen in contact with the bottom	1666±16 m/s 1664±7 m/s
Suh et al (2001)	Bovine patellar and femoral condyle	10 MHz	Room temperature	Microscope	1735±35 m/s
Toyras et al (2003)	Bovine femoral condyle, patella, patello femoral groove and talus joint	10.3 MHz	Room temperature (20°C)	Microscope	1627 m/s (1532 ~ 1754 m/s)

The sound speed may vary in artC due to its heterogeneous structure throughout its depth. Agemura et al (1990) studied the propagation of US through various sections of

artC at difference depths with only few specimens. They demonstrated the depth dependence of the sound speed in artC. They also demonstrated that the sound speed in artC was related to the orientation of collagen fibrils. In the osteoarthritic artC, specific changes were observed in the echo pattern of the superficial tissue attributable to the depth of fibrillation beneath the artC surface. Toyras et al (1999) characterized artC using high frequency US. In their study, different components of artC were selectively digested by enzymes to characterize the relationships among the structural, mechanical and acoustical properties of artC. It was reported that the sound speed of full-thickness artC significantly correlated with the equilibrium Young's modulus, the water content and the other AC composition. Table 4 illustrates a summary of the sound speed of full-thickness artC reported in the literature. The information of the specimen type, US frequency, and testing temperature are included. In addition, a few indirect methods used for thickness measurement were also described.

In summary, sound speed in artC has been reported either as constant values referred from literature or measured with the thickness obtained using another approach indirectly. An ultrasonic technique which can measure the sound speed as well as the thickness of artC simultaneously could be considered ideal for the measurement of artC.

1.2.3.2 Measurement of Stiffness

In addition to the measurement of the artC thickness, US have also contributed to the measurement of the artC stiffness together with compression or indentation tests (Jurvelin et al 2000; Kawchuk et al 2000; Toyras et al 2001; Youn and Suh 2001; Mann et al 1999; 2001; Zheng et al 2002). Measurement of mechanical properties of artC is

important for investigating the reasons behind its degeneration and diagnosis. Several indentation devices have been developed for the evaluation of artC *in-vitro* (Berkenblit et al 1994; Appleyard et al 2001) and arthorscopically *in-vivo* (Lyrra et al 1995). These instruments are based on mechanical indentation without the knowledge of artC thickness. According to the indentation model in eqn (3), the indentation measurement of Young's modulus depends on the artC thickness and the unknown thickness may induce uncertainty in the results. Recently, an US indentation technique, which combines US measurement and the indentation test, was introduced (Zheng and Mak 1996; Suh et al 2001; Laasanen et al 2002). Laasanen et al (2002) integrated US with the indentation instrument developed earlier by Lyrra et al (1999) to measure the mechanical and the acoustical measurements of artC. The instrument was found to be sensitive to the artC thickness and feasible for the detection of structural and mechanical changes in early OA. The results revealed a minor decrease in the sound speed of artC between degraded and healthy artC and they suggested that a constant sound speed in artC was acceptable for diagnosis of artC. However, Suh et al (2001) measured the sound speed and thickness of artC simultaneously and demonstrated the dependence of the sound speed on tissue degradation. Their measurement method is discussed in detail in the following section. The US indentation allows the simultaneous measurement of the thickness of artC by US and the stiffness by indentation.

1.2.3.3 Simultaneous Measurement of Sound Speed and Thickness

Suh et al (2001) developed a technique by which the sound speed and the thickness of artC were measured simultaneously using an indentation test (Fig 2). Hence

it is not necessary to use another device to measure the thickness of artC. Using this technique, a preload was first applied to the surface of artC with the US transducer acting as an indenter. After the preloading was fully equilibrated, the echo time t_1 of the US signal was measured. The transducer was then perpendicularly indented into the artC by a predetermined distance, d using a micrometer head. After the indentation force was fully equilibrated, the echo time t_2 was again measured (Fig 2).

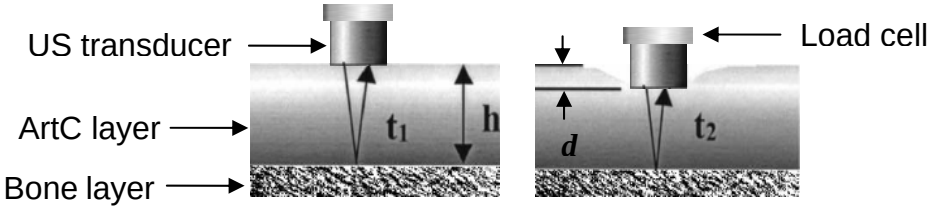

Figure 2. Indentation of artC layer to measure sound speed in artC (Suh et al 2001)

The sound speed c_{AC} was then calculated from the two echo times using eqn (4):

$$c_{AC} = \frac{2d}{t_1 - t_2} \tag{4}$$

The artC thickness *h*, was obtained using the measured sound speed c_{AC} and the initial US echo time using eqn (5):

$$h = \frac{c_{AC} t_1}{2} \tag{5}$$

They reported an averaged sound speed of 1735±35 m/s for the artC of bovine patella and the femoral condyle using 10 MHz US transducer. It was noted that the force applied by the transducer on the specimen and its perpendicularity are critical to the accuracy of the measurement. The sound speed measured using this approach mainly

represent the value of the indented portion rather than that of the entire tissue layer. Therefore, the depth dependence of sound speed in artC might affect the measurement.

Joiner et al (2001) introduced a method to measure the sound speed in artC using a non-contact pulse-echo method (Fig 3). A substitution ultrasonic approach (30MHz) was used to calculate the sound speed. The artC sample was placed on the bottom of a container which was filled with saline solution. A resinite membrane was used to hold the specimen and avoid any movement inside the container. By measuring the US echoes with and without the specimen the sound speed of artC can be calculated. The calculation of the sound speed in artC with this method is explained as follows.

T_1 to T_3 represent the flight times of the round trips of US from the transducer to the upper surface of the artC slice (T_1), the lower surface of artC slice (T_2) (contacting with the container bottom), and the container bottom without the sample (T_3). The sound speed in saline was calculated using eqn (6):

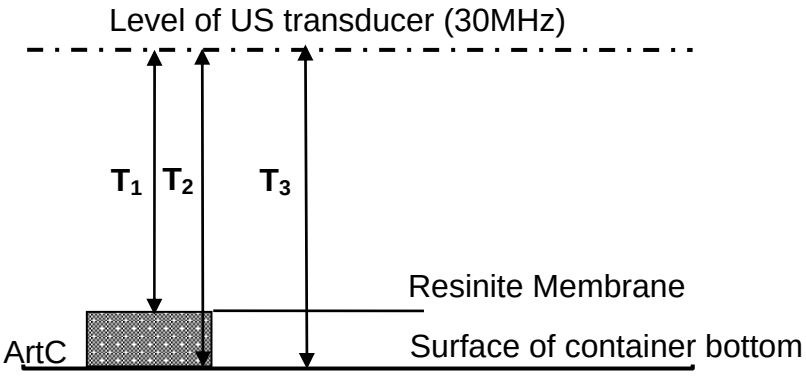

Figure 3. Schematic representation of sound speed measurement by Joiner et al (2001).

$$c_s = \frac{2d_s}{T_s} \qquad (6)$$

where, c_S is the sound speed in saline. In Joiner's study the sound speed measurement in saline solution was not explained. However, this measurement can be conducted in several ways; for instance, the sound speed in saline solution can be measured by placing the resinite membrane at a known distance d_S from the container bottom and collecting US echoes from the resinite membrane and the container bottom. The sound speed in saline can be calculated as the ratio of the distance d_S and the time difference T_S, which is obtained from the US echoes reflected from the resinite membrane and the container bottom. Further, keeping the distance between the transducer and the specimen constant, T_S equals $T_3 - T_1$, and the sound speed in artC can be calculated as,

$$c_{AC} = \frac{T_3 - T_1}{T_2 - T_1} \times c_S \qquad (7)$$

where, $T_2 - T_1$ and $T_3 - T_1$ are the time taken by the US echoes with and without the specimen for a distance same as the artC thickness; c_{AC} is the sound speed in artC.

They used this method to study the effects of degeneration on the sound speed in artC. The measured sound speeds in the artC of the femoral condyle were 1666±16 m/s for the bovine and 1664±7 m/s for the elderly human. With this non-contact method the sound speed the thickness of artC can be measured simultaneously. However the specimen might not be totally in contact with the bottom of the container due to the rough and uneven surface of artC.

In Joiner's study they used a plastic membrane to cover the artC specimen so as to make it in a better contact with the container. However it would be very difficult for artC specimen, as curling is a very common phenomenon after it is removed from the subchondral bone. A large enough compression provided by the membrane may be able

to make a total contact between the artC specimen and the container, but this may affect the artC thickness as well as its sound speed, which will be described in the next section.

If the US measurement is conducted at the region where the artC does not make total contact with the container, then the measured region contains a portion of saline. Because the sound speed of saline is generally smaller than that in the artC tissues, the effect of including a portion of the saline might reduce the measured sound speed of artC slices. Even though Joiner et al (2001) did not use it, this non-contact method can provide the measurement for the thickness of artC using the measured sound speed and US flight time in artC (Hsu and Hughes 1992). The thickness measurement may also be affected by the potential gap between the artC specimen and the container bottom. To void this drawback an improved non-contact approach was developed in this study for the measurement of the sound speed in artC *in-vitro*.

1.3 Variations of Sound Speed in ArtC

1.3.1 Depth and Direction Dependences

Due to the structural and compositional differences in different layers of artC, the mechanical properties of artC vary with its depths and along different directions (Guilak et al 1995; Schinagl et al 1997; Zheng et al 2001; Wang et al 2002). The tensile properties of artC are conventionally determined for slices that are cut from the different layers (zones) of artC. The sliced samples are stretched in the lateral direction in the tension test (Kempson et al 1973, 1980; Roth et al 1980; Akizuki et al 1986). In human femoral condyle artC, the typical reported equilibrium tensile modulus of the human artC ranged from 1- 40 MPa modulus (Akizuki et al 1986; Elliot et al 2002). It has been

reported that the compressive modulus of bovine humeral artC is up to 10 times lower than the tensile modulus in the direction perpendicular to the artC surface (Korhonen et al 2001). The high tensile stiffness of the artC is attributed to the tendency of the collagen fibrils to resist tension only (Kempson et al 1991).

Despite the wide use of US in the assessment of artC, US propagation in artC, such as its depth-dependency and anisotropy, has not been well understood. Due to the spatial variation of the water content, the PG concentration and the orientation of the collagen fibrils, the mechanical properties of the artC are different at different depths (Fig 1; Mow et al 1991; Mankin et al 1994). Therefore, artC is referred as structurally inhomogeneous and exhibits anisotropic mechanical properties. Wu and Herzog (2001) reported that the orientations of the collagen fibres and chondrocytes were responsible for the anisotropic mechanical property of artC. Some studies reported the anisotropy of artC in compression (Jurvelin et al 1996; Koehler et al 2001; Wang et al 2003). Toyras et al (2003) reported that the sound speed of the full-thickness artC significantly depended on the equilibrium Young's modulus, water content and other artC composition.

Agemura et al (1990) measured sections of bovine artC prepared both parallel and perpendicular to the artC surface using a scanning laser acoustic microscope with an US frequency of 100 MHz. Their preliminary study with two specimens demonstrated that the sound speed of artC tissue measured with the US beam parallel to the artC surface depended on its depth. They reported that the differences in sound speed among different regions of artC to its dissimilar fibril organization. In the superficial, middle and deep region, the collagen fibers are parallel, random, and perpendicularly oriented to the surface of the artC, respectively (Mow et al 1991; Mankin et al 1994). They concluded

with a limited number of specimens that the US appeared to propagate faster across the long axis of collagen fibrils than along them. Measuring the depth-dependent and anisotropic properties of artC is important not only for the investigation of artC structure but also for finding the reason behind its degeneration as well as for the tissue engineering of artC (Risbud and Sittinger 2002). The depth and direction dependences of the sound speed in artC have not been well understood yet.

1.3.2 Site Dependence

A number of studies have been conducted to investigate the site-dependent acoustic and mechanical properties of artC (Lyyra et al 1999; Jurvelin et al 2000; Korhonen et al 2002a, 2002b; Laasanen et al 2003a, 2003b; Toyras et al 2003). Yao and Seedhom (1999) measured the sound speed in artC at different sites on the ankle and hip joints of human *in-vitro*. The thickness of artC was measured using a needling technique. Their results demonstrated that the sound speed varied widely (1419–2428 m/s; mean: 1892 m/s; SD 183 m/s) and therefore a large error was induced in the measurement of the artC thickness. They suggested that the measurement of the artC thickness with a constant sound speed was not reliable. Their measurements were performed at extensive locations ranging from ankle to knee joints. Even though their study may have procedural variation due to the use of the needling technique for the thickness measurement (Mann 2001), the possible site-dependent variation of the sound speed in artC may affect the accuracy of the measurement of the thickness and stiffness of artC using the ultrasonic indentation technique (Zheng et al 1996; Laasanen et al 2002). Recently, US indentation was used to quantify the site-dependent variation in the

mechano-acoustic properties of bovine knee artC (Laasanen et al 2003). The measurement was conducted on the femoral medial condyle, the lateral facet of the patella-femoral groove and the medial tibial plateau. They demonstrated significant site-dependent variations of the dynamic modulus (measured before stress relaxation) and the US reflection coefficient. Similar site-dependent variation of the dynamic modulus was obtained earlier with the canine artC using unconfined compression and indentation test (Arokoski et al 1999; Korhonen et al 2003).

In addition to the mechanical and acoustic properties of artC, the thickness of artC also depends on the anatomical site (Lengsfeld 1993; Heegard et al 1995). However, uniform distribution of artC thickness throughout the artC surface was assumed in some earlier computer modeling of joint biomechanics (Blankevoort et al 1991; Nambu et al 1999). Adam et al (1998) measured artC thickness using A-mode US (12.5 MHz) at 36 different locations on the human patella. They reported that the mean patellar artC thickness was 2 mm. Their results revealed that the maximum thickness of artC was in the middle and lateral patellar facet. In the same year, Adam's group investigated the normal distribution of artC thickness in the major joints of the lower limb in elderly individuals.

Despite these earlier studies, the knowledge of the site dependences of the thickness and sound speed of artC is still lacking to date. In this study, the thickness of artC at different locations of the bovine patella were measured *in-situ* on the patellar surface and *ex-situ* on the excised artC specimen by using a contact and non-contact US approaches, respectively. The distribution of the sound speed was also obtained using the non-contact approach.

1.3.3 Saline Concentration Dependence

Many researchers have used normal saline solution during experiments to provide a physiological condition to artC as well as propagating medium for US. It has also been reported previously that the change in the bathing saline concentration causes the swelling of artC (Setton et al 1998). They used five saline solutions with different concentrations ranging from 0.015M to 2M. The artC was studied in free-swelling experiment in which ionic variation due to the concentration change in the saline solution was used to modulate the concentration of counter-ions and hence interstitial swelling pressure in the artC matrix. It was suggested that swelling effect was a potential mechanism for the existence of residual stresses (interlocked stresses) and strains in cartilaginous tissue (Fry and Robertson 1967). It was also reported that the residual stresses and strains played an important role in the biomechanical function of artC tissues as well as their physiological responses which were directly related to the artC structure (Fung 1968). The swelling properties of artC were studied under mechanical tension (Grodzinsky et al 1981; Guilak et al 1995) and compression (Eisenberg and Grodzinsky 1987) and electromechanically (Berkenblit et al 1994). An ultrasonic technique was recently developed to monitor the transient and inhomogeneous swelling behaviour of artC by changing the concentration of the bathing saline solution (Zheng et al 2004). Their result demonstrated that the artC shrinked and recovered when the saline concentration was changed from 0.15 M to 2 M and back to 0.15 M, respectively. The maximum deformation of the artC was observed during the first few minutes. It has been reported earlier that the sound speed in saline increased with the increase of the concentration (Marks 1959). It was also noted that the sound speed in artC changed as the

change of bathing saline concentration. However, to the best of our knowledge, there is little information in the literature about the variation of the sound speed in artC induced by the change of the bathing saline concentration of artC.

1.3.4 Degeneration Dependence

It has been widely reported that changes in the original structure and composition of artC can cause swelling, which forms one symptom of OA. During OA, the collagen network and PG matrix degrade and the water content in artC increases (Mow et al 1984; Buckwalter and Mankin 1997). The diagnosis of artC degradation can be performed using MRI (Burstein et al 2000), US evaluation (Disler et al 2000), mechanical indentation (Appleyard et al 2001), etc. Several studies were carried out to investigate the interrelationship between the sound speed, composition, degenerative state and structure of artC (Agemura et al 1990; Myers et al 1995; Toyras et al 1999; Joiner et al 2001; Suh et al 2001; Nieminen et al 2002). Agemura et al (1990) suggested that the orientation of the collagen fibrils might affect the sound speed whereas the content of PG had minor effect on the sound speed. Myers et al (1995) found that the sound speed decreased during artC degeneration. Similar results were obtained by Joiner et al (2001) and they reported that the sound speed decreased after degrading artC with interleukin -1α or papain. A significant decrease of sound speed in artC was also observed by Toyras et al (1999) and Nieminen et al (2002) after it was digested by various enzymes. It has been demonstrated in the literature that the changes in the structure and the composition of artC can cause changes in the propagation of US. However, different groups of artC specimen were normally used to investigate the digestion effect of different kinds of

enzymes in the previous studies. Due to the site and other variations of acoustic properties of artC, it is difficult to make a solid conclusion about the difference of the sound speed change induced by the different enzyme digestion. In addition, in the previous studies, the control group of the artC specimen was normally not stored under the same condition as that of the digestion group during the process of digestion. Therefore, it is not very clear yet whether the change of the environmental condition such as temperature for a certain period may induce the variation of the sounds speed in artC. In the current study, 5 pieces of artC specimen were collected from the same artC-bone plug. Three of them were treated with different enzymes, while the other two pieces were used as controls. During the digestion process, the first control was stored at -20°C and the second control was stored under the same condition with that of the digestion ones.

1.3.5 Temperature Dependence

It was noted that most of the sound speed of artC reported in the literature was measured at either room temperature or 37°C. In many studies, the degree of room temperature has not been reported. The variation in temperature might also cause a change in the sound speed in artC particularly for *in-vitro* measurements. Significant change in sound speed was demonstrated in the measurement of cadaveric foot tissues with the temperature ranging from 15 to 40°C (Pocock et al 2000). Similar correlation between the sound speed and the temperature was observed in the calcaneus bone *in-situ* (Njeh et al 2002). As more ultrasonic studies on artC *in-vitro* have been conducted under room temperature, it is very necessary to document the relationship between the sound speed in artC and the environmental temperature, which can vary significantly from

laboratory to laboratory. To the best of our knowledge, no study had been reported on the investigation of the effect of the temperature on the sound speed of artC and thickness.

1.3.6 Strain Dependence

Routine physical motion of human body involves joint knee flexion. During the daily activities, artC is stressed by the force applied by various parts of joints including patellar artC on femoral and tibial artC. This loading and unloading may cause structural deformation of artC. Cooper et al (1994) reported that high repetitive loading is a major risk factor for OA. Adam et al (1998) reported that when artC was subjected to sustained or repetitive loading, the loss of the equilibrium thickness and the water content increased with the increase of applied stress. Recently, a number of studies have been reported on the combination of the US measurement and the mechanical testing including compression and indentation for assessment of artC.

Zheng et al (2001) developed an US-compression system (50 MHz) to investigate the layered biomechanical properties of artC. They reported that the compression moduli of digested and undigested artC were significantly different. Using a focused US transducer and a specially designed compression device, the depth-dependent equilibrium compressive material properties of artC were reported (Zheng et al 2002a). This technique was later improved for the investigation of the transient measurement and the 2D mapping of the mechanical properties of artC (Zheng et al 2004b, 2004c). Fortin et al (2000) used 50 MHz US to measure the transient lateral displacements of artC at different depths under an axial compression with two flat plates. The dimensions of the specimen were in the order of 1 mm. It was demonstrated that the transient depth-dependent

Poisson's ratio could be measured using this method. In these US-compressions as well as the US-indentation methods (Zheng et al 1996; Suh et al 2001; Laasanen et al 2002) described in the earlier section, the potential change of the sound speed under different stress or deformation conditions have not been well considered. It has been widely reported that artC could become stiffer as the increase of the applied stress (Bursac et al 1999; Fortin et al 2000; Legare et al 2002). The knowledge of such structural and functional alteration due to the change of the applied load on artC is important for the assessment of artC and the development of theoretical models. Many studies have shown that the strain change induced by the mechanical loading (axial or lateral compression or impact loading) influences the normal function of artC, as its structure may change such as the breakdown of collagen (Repo and Finlay 1977; Broom 1986; Jeffery et al 1995; Borelli et al 1997; Kerin et al 1998; Quinn et al 1998; Chen et al 1999; Torzilli et al 1999). This change may affect the mechanical and acoustical properties of artC including the sound speed (Chen et al 1999). While few studies have been reported on the relationship between the sound speed in artC and its applied stress, the correlation between the stiffness of artC and its sound speed has been investigated by several groups (Suh et al 2001; Toyras et al 2003). The strain dependence of the sound speed in artC is important for the further development and application of US-compression and US-indentation for the assessment of artC, as the stress induced change of the sound speed could directly affect the measurement of mechano-acoustical properties of artC. In this study, a US-compression device was developed, which was capable to measure the sound speed, stress, and strain in artC simultaneously. The relationship between the sound speed and stress, strain, and modulus were studied. A summary of several recent studies

conducted to measure the Young's modulus of artC has been illustrated in Table 4.

1.3.7 Summary

During the last decade, US assessment of artC has been widely investigated. It not only provides a direct measurement for the artC thickness, sound speed and other acoustical properties but also assists the measurement of artC mechanical properties through techniques of US-compression and US-indentation. As reviewed above, these techniques require a better understanding of the sound speed in artC for its depth-dependence, site-dependence, degeneration-dependence, saline concentration-dependence, temperature-dependence, and strain-dependence. Accordingly, the present study was designed to systematically investigate the variations of the sound speed in artC to environmental, morphological, pathological, structural, and locational variations.

1.4 Objectives of the Study

The overall aim of the study was to conduct a systematic investigation of the sound speed in artC *in-vitro* under various conditions using bovine patellar models. The specific objectives can be summarized as follows:

- To develop a non-contact US method for the simultaneous measurement of the sound speed and thickness of artC.
- To develop a US-compression device for the simultaneous measurement of the sound speed, thickness, and the Young's modulus of artC.
- To investigate the depth-dependence and anisotropy of the sound speed in artC.

- To investigate the change of the sound speed in artC induced by the digestion of collagenase, chondrotinase, and trypsin, which selectively degrade the collagen and PG in artC using groups of well matched specimens.
- To investigate the site dependence of the sound speed in artC by measuring at 25 different locations on the bovine patella.
- To investigate the change of the sound speed and thickness of artC induced by the change of the bathing saline concentration from 0 M to 2.5 M.
- To investigate the change of sound speed induced by the change of the surrounding temperature from 15°C to 40°C.
- To investigate the strain dependence of the sound speed in artC by changing the strain from 0 – 20% and to correlate the sound speed with the mechanical properties of artC.

Fig 4 shows the overall diagram of the contents of this thesis. It also represents how the above objectives were achieved.

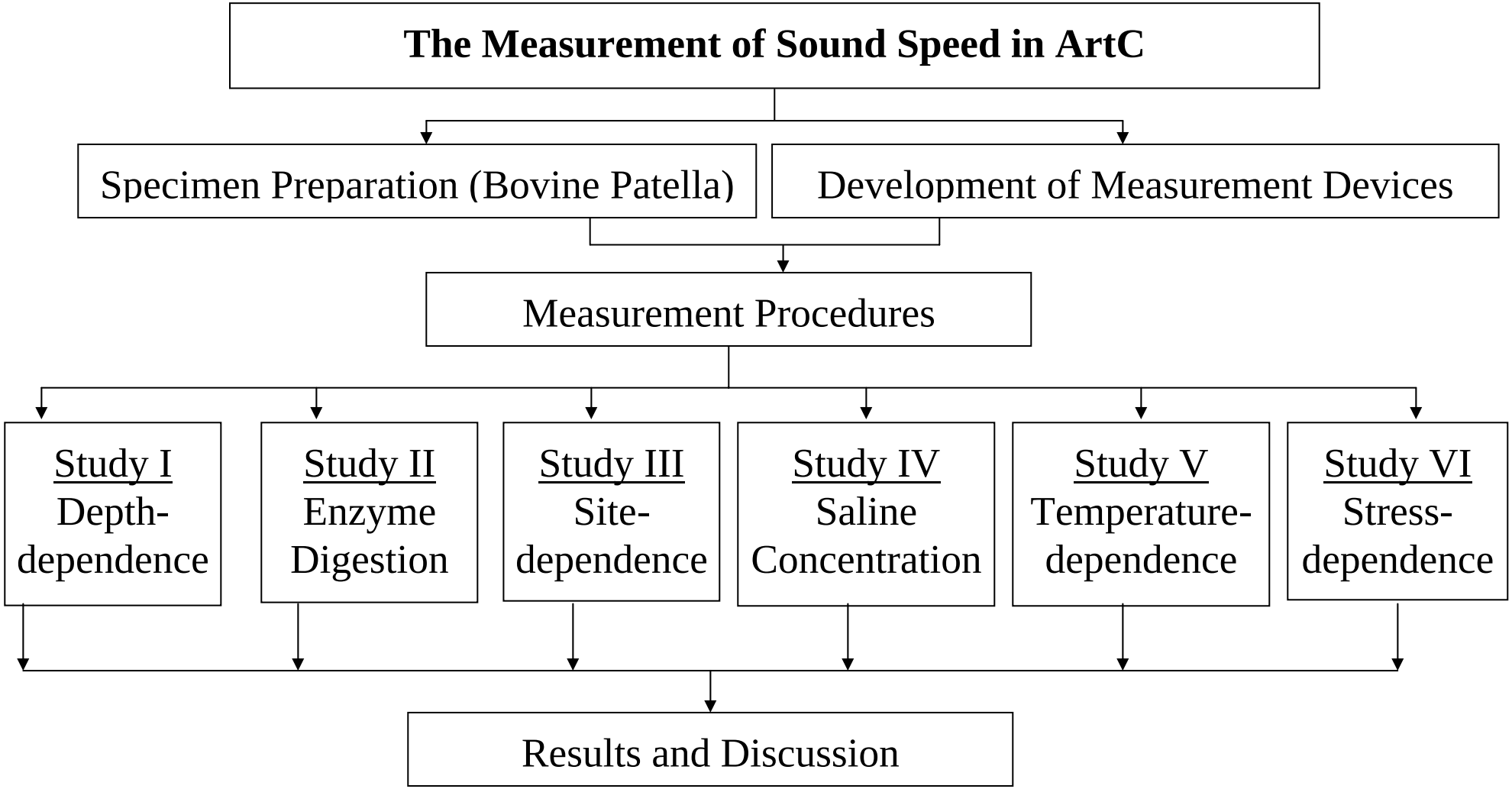

Figure 4. A Schematic representation of the contents of this thesis.

Table 5. Summary of the material and methods used in the study.

Study	Specimen Type	Specimen Location	Specimen Dimension	Number of Patellae	Measurement Mode	Remarks
Depth dependence and anisotropy	Semicircular Full thickness	Medical Upper (MU)	6.4 mm	n = 18	Scanning	3 slices with approximately equal thickness, 1 vertical slice and 1 horizontal slice were used. The scanning interval was 0.05 mm.
Enzyme digestion	Semicircular Full thickness	Medial Lower (ML)	9.0 mm	n = 20	Scanning	Chondrotinase, collagenase and trypsin were used for digestion. Specimens were digestied for 24h at 37°C. Two control groups were included.
Site dependence	Circular Full thickness	25 sites on a patella	3.0 mm	n = 10	Scanning	Patella with similar size were selected.
Saline concentration variation	Semicircular Full thickness	Lateral Upper (LU)	6.4 mm	n = 19	Scanning	Saline concentration used: 0, 0.0075, 0.082, 0.15, 0.3, 0.75, 1.25, and 2.5 M. Measurements were conducted at 22±1°C.
Temperature dependence	Semicircular Full thickness	Lateral Lower (LL)	6.4 mm	n = 20	Continous monitoring	Measurement range: 15°C - 40°C. Measurements were conducted during the change of temperature.
Strain dependence	Circular Full thickness	Medial Upper (MU)	6.4 mm	n = 20	Continous monitoring	Applied strains: 0, 0.025, 0.050, 0.075, 0.100, 0.125, 0.150, 0.175, and 0.200.

2. Materials and Methods

2.1 Specimen Preparation

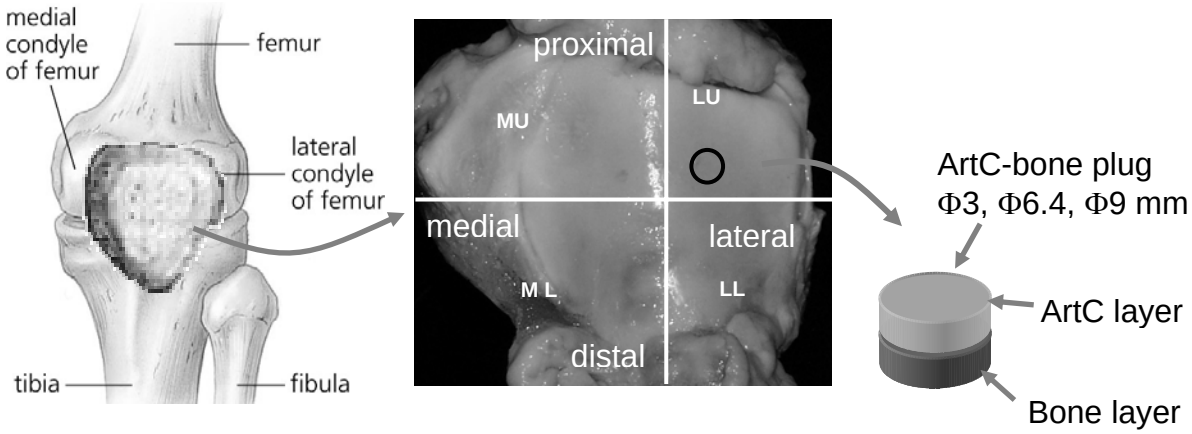

Figure 5. Schematic representation of the initial phase of the preparation for the osteochondral cylinders. The specimens would be further prepared for each measurement (Fig 6).

Bovine knee patellae without obvious lesions were obtained from a local slaughter shop within 6 hrs of decease and stored at -20°*C* until further specimen preparation. It has been reported that cryopreservation (Kiefer et al 1989), freezing, and thawing (D'Astous and Foster 1986; Agemura et al 1990; Kim et al 1995) of artC specimens would not affect its mechanical and acoustic properties such as the sound speed, attenuation, and backscatter. Specimen preparation in this phase consists of excising the patella into 4 quadrants using a bend saw machine (Fig 5). The four parts were named according to the medial or lateral side of the patella. As shown in Fig 5, the four quadrants were named as MU (Medial Upper), ML (Medial Lower), LU (Lateral Upper), and LL (Lateral Lower). During excising, it was made sure that the patellae were kept moist with the saline solution. For each measurement listed in Fig 4 and Table 5, one

quadrant was used to extract artC-bone plugs for further specimen preparation (Refer to Fig 5). The dimension of the plugs was 6.4 mm in diameter with approximately 3 mm thick bone layer for all experiments except the site dependence experiments (3 mm diameter) and enzyme-digestion experiments (9 mm diameter). Table 5 summarized the number of patellae used in each measurement, the diameter of the artC-bone plug, the location of the specimen, as well as the measurement modes, which were described in details in the following sections. Fig 6 illustrates the specimen preparation in phase II according to the different studies. The details were described in following sections.

2.1.1 Specimens for Depth and Direction Dependences

The artC-bone plug obtained for the depth-dependent study from the MU quadrant was further prepared to get three different categories of artC slices using a thin surgical blade in the 2nd phase of the specimen preparation as shown in Fig 6. One specimen from each patella (n = 18) was tested in this study. The surgical blade was used manually to obtain a small portion of artC with a width of approximately 2 mm for the full-thickness measurement (n = 18). A lateral vertical slice with a width of approximately 1 mm was then prepared (n = 10), and the artC surface was marked as an indicator for this block. The remaining portion of the artC was cut into three horizontal slices (n = 18 x 3) parallel to the artC surface, each of approximately equal thickness. These three groups of specimens were then used for the US measurement within 15 minutes after the preparation.

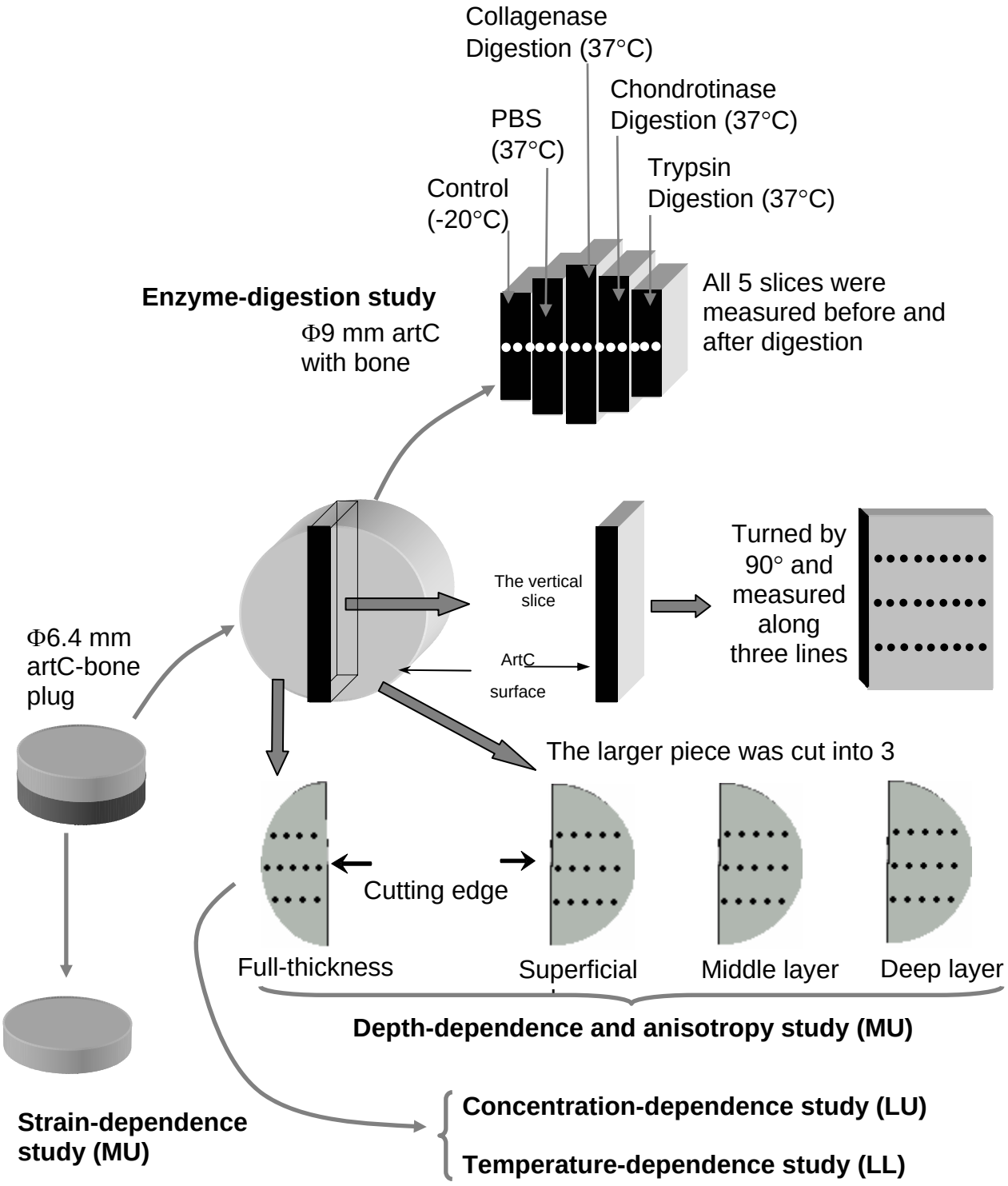

Figure 6. Schematic of the specimen preparation for the different measurements carried out in this study.

It was a concern whether the sound speed of artC would change as a function of time due to the swelling effects after it was detached from its subchondral bone. Additional 5 artC-bone plugs were prepared for investigating the swelling effects of artC after the specimens were detached from the bone. The artC disks were first thawed in normal saline for at least 2 hrs before further preparation. For each artC-bone plug, a full-thickness portion was first removed from one side; then a full-thickness slice was prepared from the remained portion and was installed onto the specimen platform immediately after detaching. The whole procedure was completed within 1 min. After the test of this specimen, another full-thickness artC specimen was prepared from the same artC disk. The procedure was the same as that for the first full-thickness slice, but obtaining the artC slice from the opposite direction of the disk so as to avoid the potential effects caused by the previous cut.

2.1.2 Specimens for Strain, Temperature, and Saline Concentration Dependences

For the studies of stress, concentration, and temperature dependences, full-thickness specimens were obtained from the artC-bone plugs of the MU, LU and LL quadrants of the patella, (n = 20, 19, 20), respectively (Fig 5 and Fig 6). The artC was detached from the bone to get a full-thickness circular artC disk. The disk thus obtained was used for *strain dependence study*. The artC disks were selected such that the surface of the artC remained plat and parallel to the bottom throughout the whole disk. For the *temperature and saline concentration dependence* studies, the disks were cut into two hemispheres and one hemisphere was used for US measurement.

2.1.3 Specimens for Enzyme Digestion Study

Three different enzymes were used in this study to remove different components in artC for the enzyme digestion measurement. Collagenase solution (30Uml^{-1}, Type VII, Lot No. 60K8618, C-0773, Sigma, USA) was used for the degradation of the collagen network (Shingleton et al 1996). Chondrotinase ABC (0.1 U ml^{-1}, Lot No. 122K4036, C-2905, Sigma, USA) was used for the digestion of the PG (Yamagata et al 1968). Trypsin solution (Lot No. 102K2379, T4549, Sigma) was used for the digestion of PG with minor simultaneous degradation of the collagen network (Harris et al 1972).

The 9-mm plugs were obtained from the ML quadrant of the patella (n = 20). As shown in Fig 5, the full thickness disk was detached from the bone. The disk was further cut into five full thickness vertical portions. Three slices would be digested with different enzymes. Each slice was measured with US before and after the enzyme digestion. The remained two slices were used as control, which were described in details in the procedure section.

2.1.4 Specimens for Site Dependence

Bovine patellae (n = 10) of similar size and shape were selected for this study. A transparent plastic sheet with a dimension of 100 × 100 mm^2 was firstly placed on the patella with a marked scale on its boundaries (Fig 7). The scale at the left and bottom of the plastic sheet was used as a reference for marking the sites to be punched on the patellae. The plastic sheet consisted of 25 holes arranged in rows and columns. The alignment of the plastic sheet on the patella was assured according to the four points marked diagonally on the surface of each patella in MU, ML, LU, and LL quadrants,

approximately at equal distance from the boundary of artC. These four points were used as reference points on each patella for marking the location of specimens. The specimen locations were then marked with a marker (N50, Pentel pen marker, Pentel Co. Ltd. Japan). The same sheet was used for all the 10 patellae used in this study.

Each patella was measured at the marked points *in-situ* using a contact US method, which was described in the procedure section. After this *in-situ* measurement, a custom made mechanical device was used to secure the patella in order to avoid the movement while punching. ArtC-bone plugs with a diameter of 3 mm were punched out from the marked portions on the patella. These artC-bone plugs were thawed in saline solution after the punching. Then the full-thickness artC disks were sliced from the bone layer and used for the non-contact US measurement (Fig 7).

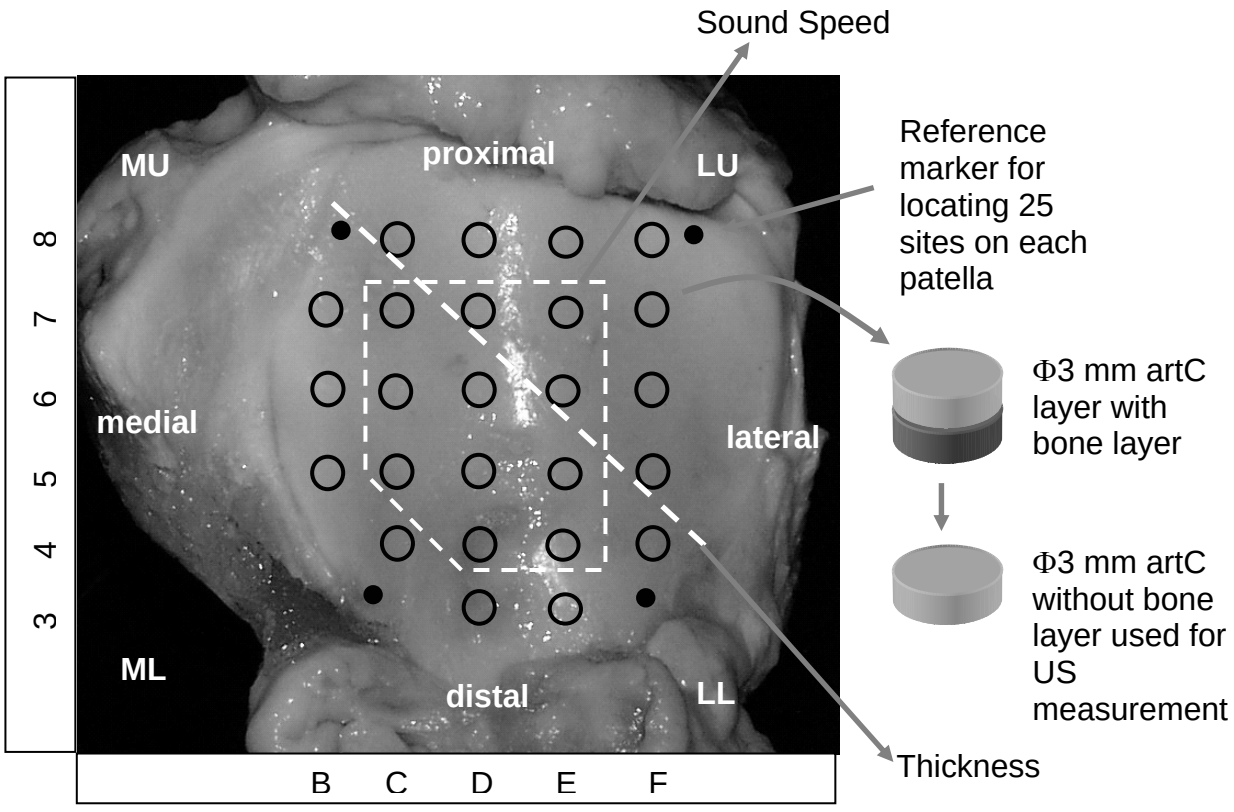

Figure 7. A schematic of the specimen preparation for site dependence study.

2.2 Experimental Setups

2.2.1 Setup for Non-contact Measurement of ArtC Sound Speed

Fig 8 shows schematic representation of the experimental setup for the non-contact measurement of artC. This setup was used to study the dependences of sound speed on depth, site, enzyme digestion, temperature, and saline concentration. A focused US transducer (Panametrics Inc., Waltham, MA, USA) with a nominal frequency of 50 MHz and a focal length of 12.8 mm was fixed on a vertical translating device (Model R301MMX, Ball Slide Positioning Stages, Deltron Precision Inc.). The US transducer could be translated vertically in one dimension. The artC slices were placed on three pairs of plates with equal thickness and with a gap between them on the bottom of the container, which was filled with saline solution.

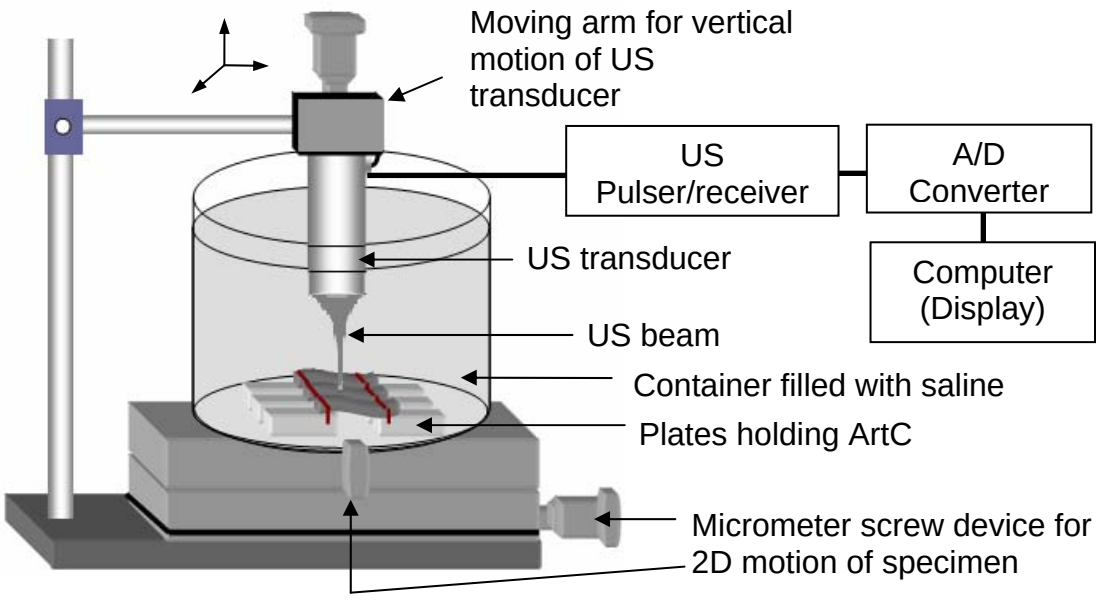

Figure 8. Schematic representation of the experimental setup (Kuo et al 1990; Hsu and Hughes 1992).

During the measurement, the focal zone of the US transducer was located approximately in the middle of the specimen by moving the transducer vertically. The specimen was translated in two dimensions using two orthogonal translating devices (Model 2201MMXY, Ball Slide Positioning Stages, Deltron Precision Inc.) with 0.01 mm precision and US-measurement was performed at different sites.

The US system used in this study has been introduced previously (Zheng et al 2001, 2002). An US pulser/receiver (Model 5601A, Panametrics, Waltham, MA, USA) was used to drive the US transducer and to amplify the received US echoes. The received US signals were digitized by an A/D converter card (CompuScope 8500PCI, Gage, Canada) with a sampling rate of 500 MHz installed in a PC. The signals were displayed on the monitor in real time and saved into the hard disk for offline signal analysis (Zheng and Mak 1996; Zheng et al 2002). The setting of pulser/receiver including transmitting energy, receiving gain, attenuation and damping were selected according to pilot experiments and maintained constant for all the measurements. This experimental setup was used for all experiments except strain-dependent study.

The experimental setup was slightly modified from its original version for temperature-dependent study. A plastic coil was curled along the inner wall of the container. The coil entirely covered the side walls of the container so that uniform heat distribution was assured surrounding the specimen. One end of the coil was connected to a hot water source. The hot water passing through the coil was set and assumed to be at a constant rate. It was used to increase the temperature of the saline solution inside the container gradually from 15°C to 40°C.

2.2.2 Setup for Strain-dependent Study

The strain dependence study involved the contact between the artC specimen and the transducer, as a compression on the specimen was required. Therefore, the instrumentation was different from the one used in other studies. The specimens used in this study were different from other studies, where slices or semicircular specimens were used. This study involved the full thickness circular disk of artC. The instrument used in this study was modified from its original form of US-compression configuration, where a focused 50 MHz transducer was used (Zheng et al 2002). Fig 9 shows a schematic diagram of the US-compression system used in this study.

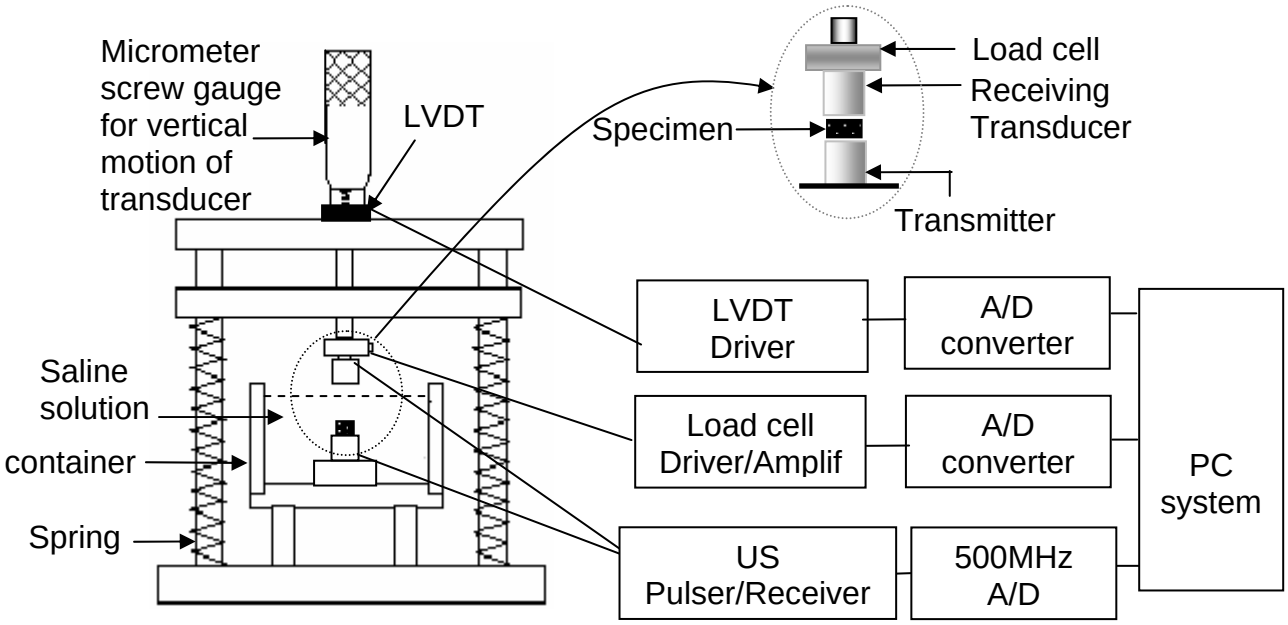

Figure 9. The US-compression system for the study of the strain dependence of the sound speed in artC.

During the experiment, the container was filled with saline solution. The specimen platform (transmitting transducer) as well as the compressor (receiving

transducer) were located in the middle of the container. The specimen was located between the transmitting and the receiving transducers (unfocused, 5 MHz, Panamaetrics Inc, Waltham, MA, USA). The diameter of transducers was 8.9 mm, and the diameter of the specimen was 6.4 mm. It was assured that the US-compression system was rigid enough during the compression test so that the deformation was only applied on the artC specimen. The movement of the compressor was manually driven with a micrometer adjustor installed on the top of the testing device as shown in Fig 9. The compressor was connected in series to a 25 N load cell (model ELFS-T3E-5L from Entran, NJ, USA). The amplified load signal was digitized by an A/D card (NI-DAQ 6024E, National Instruments, USA) installed in the PC. The broadband US pulser/receiver (model 5601A, Panametrics Inc., Waltham, MA, USA) was used to drive the US transducer and to amplify the received US echoes. The US reflection signals were digitized by another A/D converter card at a sampling rate of 500 MHz (Model CompuScope 8500PCI from Gage, Canada) installed in the PC. In addition, a Linear variable displacement transducer (LVDT, DFg 5 (guided), Solartron, RS components Inc., Hong Kong) was used to measure the axial displacement of the compressor. The LVDT signal was also digitized by the A/D card (NI-DAQ 6024E, National Instruments, USA). A custom made computer program was used to collect the load signals, LVDT signals and ultrasonic signals digitized by the A/D converter cards. To improve the ultrasonic signal condition for the cross-correlation algorithm applied later for the signal analysis, the US echo trains were averaged for 30 times to enhance the signal-to-noise ratio. Similarly, the load and LVDT data were averaged for 100 times. Normal saline solution was used for minimizing the friction between the artC sample and the transducer surfaces during the measurement.

2.3 Sound Speed Calculation

2.3.1 Calculation of Non-contact Measurement

US reflections were collected by the custom made program in real time and analyzed offline. Fig 10a shows one typical US echo trains collected from the artC specimen using the non-contact configuration. The three radio frequency (RF) echo signals were reflected from the upper and lower surface of the artC specimen and the surface of the container bottom, respectively. The corresponding envelope signals were obtained using Hilbert Transform and are shown in Fig 10b.

In the beginning of this study on the depth dependence sound speed, both the RF and envelope signals were used for the signal processing to calculate the sound speed and thickness of the artC specimen. It was noted that similar accuracy was achieved using both types of signals. However, the phase change of the echoes sometime was very obvious and the echo tracking based on RF signals were not very reliable under such situation, particularly when the artC specimen was digested by the enzymes. Therefore, the envelope signals were finally selected for the further signal processing to calculate the sound speed and the thickness. A similar approach was applied for the contact measurements in the strain dependence and site dependence studies. As shown in Fig 10b, three pairs of tracking windows were used to track the signals reflected from the interfaces of the specimen and the container. Each tracking cursor could be moved individually with a time resolution of 2 ns as defined by the sampling rate (500 MHz) of the A/D converter. In the present study, a cross-correlation algorithm was used to match the echoes reflected form the different interfaces so as to calculate the corresponding flight time.

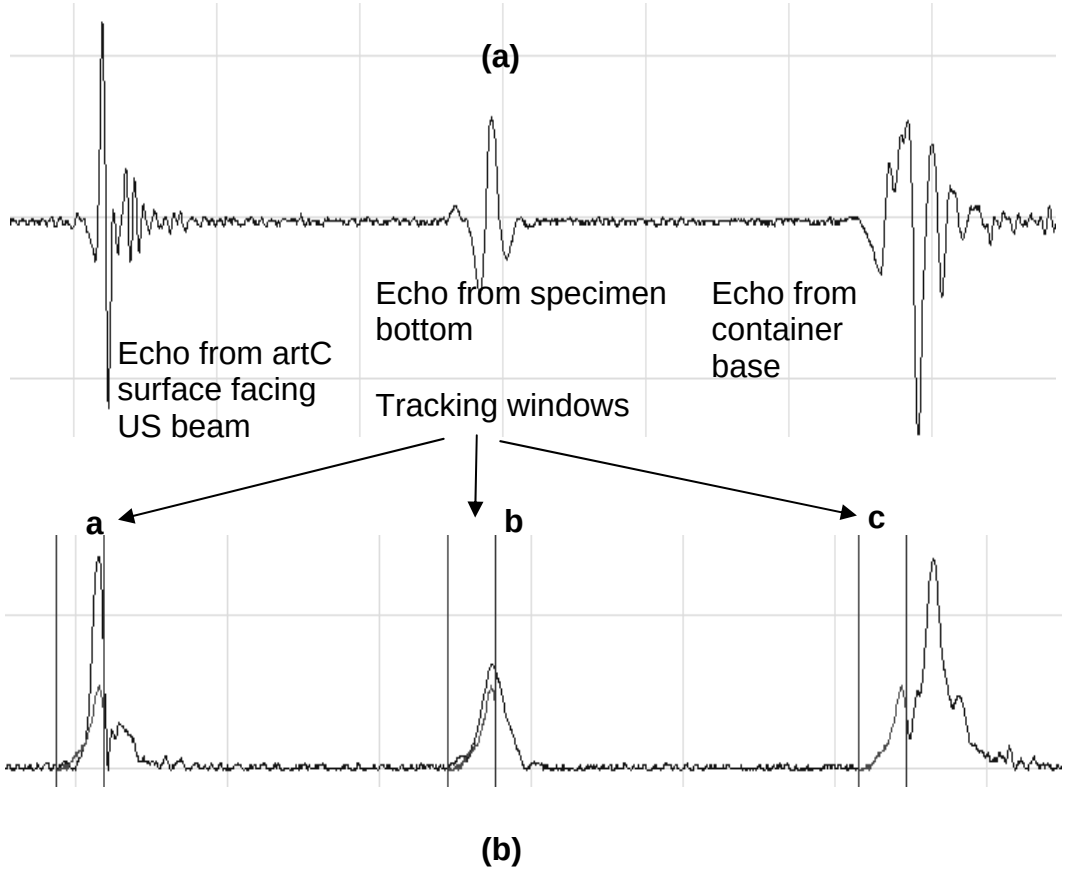

Figure 10. (a) Typical RF US echoes from interfaces. **(b)** Typical envelope signal converted from the RF signals. It was observed that the phases of the US echoes from various interfaces of artC changed considerably such as in the enzyme digestion study. The RF wave was converted to envelope signal to obtain better correlation. A cross-correlation technique was used to track the echoes. The echoes indicated by ‘c’ represents the reference signal and echoes indicated by ‘a’ and ‘b’ were located by the cross-correlation tracking. The echoes to be matched were overlapped with the reference echo in ‘a’ and ‘b’.

The reference echo was normally selected as the echo reflected from the upper surface of the artC specimen. Two corresponding full cycles of RF signals were marked by the tracking windows on the echoes reflected from the two interfaces of the artC slices, respectively. This echo matching processing was repeated for each measurement

point on the artC specimen. The sound speed and the thickness of the artC specimen were calculated at each measurement point using the method described as follows and the results were averaged. Fig 11 shows a schematic representation for the US paths and flight times involved in the calculation of the sound speed in artC. T_1, T_2, and T_3 represent the flight times of the round trips of US from the transducer to the upper surface of the artC specimen, the lower surface of artC specimen, and the bottom of the container through the specimen. T_4 represents the round trip from the bottom of the container without the presence of the specimen. The sound speed in the saline solution was measured by moving the transducer vertically down for two steps of 0.5 mm and then back to the original position in another two steps. T_5 represents the position of the transducer after it was moved from its original position. The difference between the flight times obtained at the four positions was used to calculate the sound speed in the saline solution (eqn 8).

$$c_S = \frac{2d_T}{(T_4 - T_5)} \tag{8}$$

The sound speed in the saline, calculated after each step of transducer movement was averaged. The sound speed in artC was calculated as follows (refer to Fig 11):

$$\frac{T_3}{2} = \frac{d_{ab}}{c_S} + \frac{d_{bc}}{c_{AC}} + \frac{d_{cd}}{c_S} \tag{9}$$

$$\frac{T_4}{2} = \frac{d_{ab}}{c_S} + \frac{d_{bc}}{c_S} + \frac{d_{cd}}{c_S} \tag{10}$$

Also

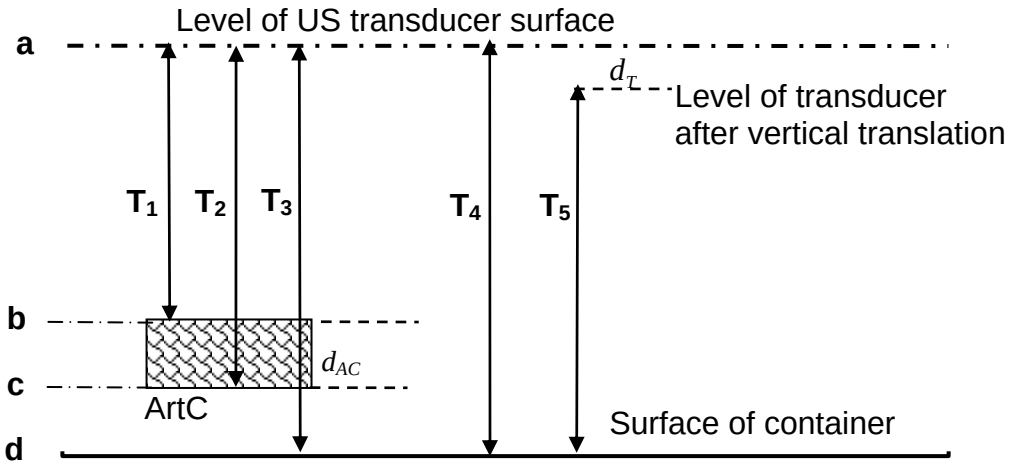

Figure 11. Schematic representation for the elements involved in the calculation of the sound speed in artC and saline. d_{AC} is the thickness of artC slice, which is equal to the distance between b and c, i.e d_{bc} (The subscripts $_{bc}$ and $_{AC}$ are used interchangeably for understanding the equations better); T_1 to T_5 are the flight times of the round trips of US from the transducer to different interfaces. T_4 is measured after a vertical movement of the transducer and used to calculate the sound speed in the saline solution.

$$\frac{T_1}{2} = \frac{d_{ab}}{c_S} \tag{11}$$

$$\frac{T_2}{2} = \frac{d_{ab}}{c_S} + \frac{d_{bc}}{c_{AC}} \tag{12}$$

$$\frac{d_{cd}}{c_S} = \frac{T_3}{2} - \frac{T_2}{2} \tag{13}$$

where d_{ab}, d_{bc}, and d_{cd} represent the distance between the transducer and the specimen upper surface, the specimen thickness, and the distance between the specimen lower surface and the surface of the container base, respectively. By substituting eqn 9 and 10 into eqn 12 and 13, we get:

$$d_{bc} = \left(\frac{T_2}{2} - \frac{T_1}{2} \right) * c_{AC} \tag{14}$$

$$\frac{T_4}{2} = \frac{T_1}{2} + \frac{d_{bc}}{c_S} + \frac{T_3}{2} - \frac{T_2}{2} \tag{15}$$

By substituting eqn 14 into eqn 15, we get:

$$c_{AC} = \frac{T_4 - T_3 + T_2 - T_1}{T_2 - T_1} * c_S \tag{16}$$

$$d_{AC} = c_{AC} * \frac{T_2 - T_1}{2} \tag{17}$$

where c_{AC} is the sound speed in artC and d_{AC} is the thickness of the artC slice.

2.3.2 Calculation of Strain-dependent Sound Speed in ArtC

A schematic representation of the US echoes passing through the specimen is shown in Fig 12. The sound speed in the artC was determined after the two platens were in contact with the specimen (indicated by the force measured by the load sensor) using the pulse-echo technique. The time-of-flight was determined as the travel time of the maximum amplitude of the US pulse back and forth through the artC specimen, while the artC thickness was determined as the distance between the surface of the two transducers. The distance was accurately measured using the calibrated LVDT fixed on the moving micrometer. The cross-correlation algorithm was used to match the two echoes obtained at each compression level so as to obtain the time-of-flight of US in artC specimen. The first echo was selected as the reference using a tracking window and the position of the second echo was automatically searched according to this reference (Fig 12b).

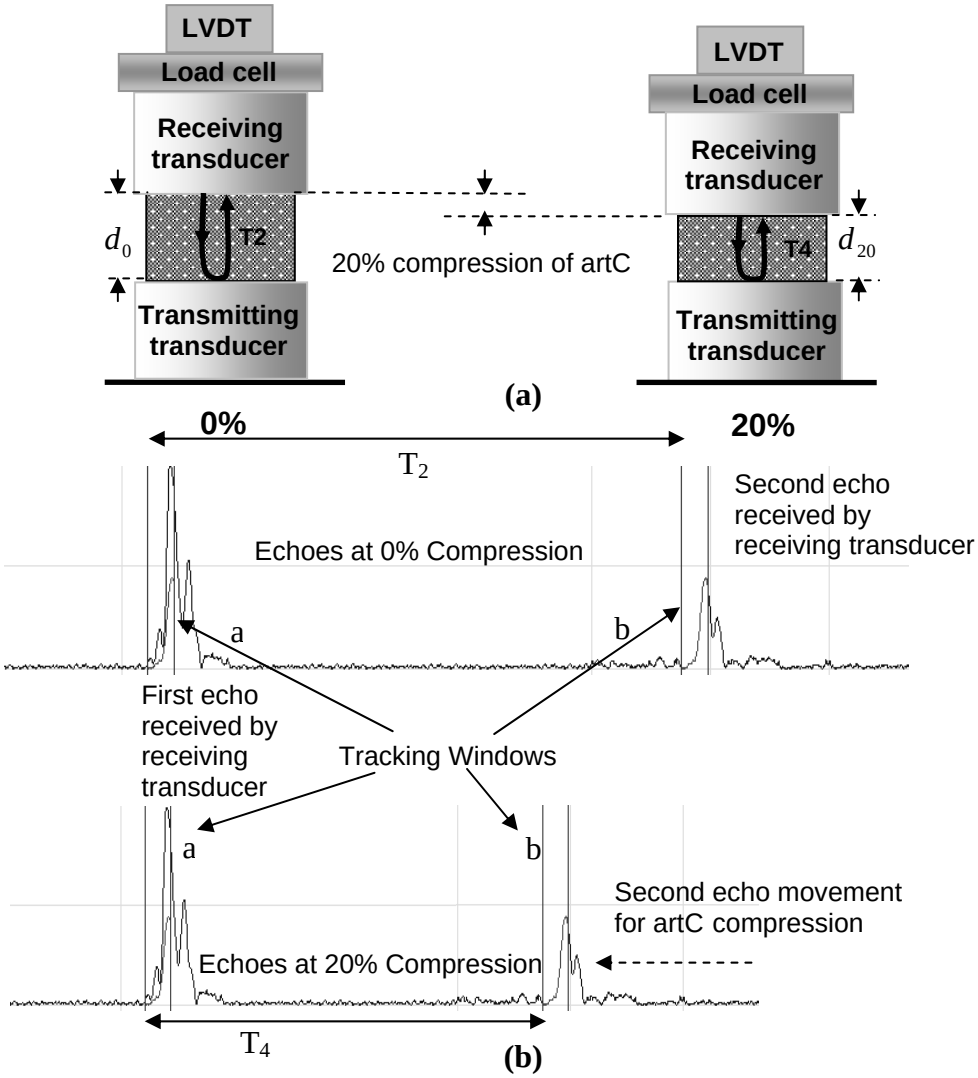

Figure 12. **(a)** Schematic representation of the US propagation through the artC specimen. **(b)** Typical US echoes received by the US receiving transducer. The cross-correlation algorithm was used to match the two echoes obtained at each compression level. The echo indicated by 'a' represents the reference signal and the echo indicated by 'b' was located by the cross-correlation tracking. The echo to be matched was overlapped with the reference echo.

Fig 12b shows the echoes obtained under compression levels of 0% and 20%.

T_2 and T_4 represents the round trip between the transmitting and the receiving, i.e. the round trip inside the artC specimen under two different compression levels, respectively.

The artC specimen was compressed upto 20% of its original thickness at steps of 2.5%. Therefore, the sound speed in artC under these two compression levels can be calculated by eqn 18 and 19, respectively.

$$c_0 = \frac{2d_0}{T_2} \tag{18}$$

$$c_{20} = \frac{2d_{20}}{T_4} \tag{19}$$

where d_0 and d_{20} is the uncompressed and compressed (20%) thickness of artC, respectively. The artC thickness at 0% compression was measured as the distance between the surfaces of the two transducers when they were just touching artC. It was noted that the quality of US echo remained almost the same under different compression levels and a good correlation was obtained among echoes.

2.4 Measurement Procedure

2.4.1 Validation of the Non-contact Measurement

The non-contact US technique introduced in this study has been previously used to measure the sound speed and thickness of hard materials like plastic and steel (Kuo et al 1990; Hsu and Hughes 1992). To further validate the accuracy of the measurement, different materials including steel, rubber, silicone phantoms, glass, and plastic were tested in the present study to determine the sound speed and the thickness of the samples. These materials were all with flat surfaces. The sound speed of the samples was also measured with a direct contact US method, i.e. using a flat unfocused transducer to contact the sample materials. The sound speeds obtained from the two measurements were compared. The thicknesses of the samples were measured by a Vernier caliper (0.01

mm resolution, Mitutoyo corporation, Japan). The thickness measured by the two approaches was also compared.

2.4.2 Procedure for Depth and Direction Dependence Study

The artC specimens were placed on the plates inside the container filled with saline solution. The vertical and full-thickness slices were first placed on the plates in the container. The superficial layer of the full-thickness slice and one of the vertical cutting surfaces of the vertical slice was arranged to face the US beam. The specimen was fixed on the supporting plate using a fine rubber band across the two edges. The US beam was first located approximately 2 mm away from the edge of the first artC specimen and the US signal reflected from the bottom of the container was collected. Then the US transducer was moved horizontally towards the specimen in 0.25 mm intervals and a total of eight sites on the container bottom were measured. The US beam was then moved to pass through the vertical slice specimen and the US signals were recorded at intervals of 0.05 mm. The US signals collected included echoes from the upper and lower surfaces of the specimen, and the bottom of the container (Fig 8 and Fig 10). As shown in Fig 8 (the dots on the specimen represent the measurement sites), the US beam was scanned along the vertical cutting interface of the artC specimen and the measurement were made on a number of sites located from the superficial layer to the deep layer. The position of each measurement site was recorded from the micrometer screw gauge. After the US beam passed the specimen region, US signals were collected from the gap between the vertical slice and the full-thickness slice at intervals of 0.25 mm. Similarly, US signals from the full-thickness slice were collected at a distance of 0.05 mm. beyond the full-thickness

specimen, US signals were recorded again at eight sites on the bottom of the container with 0.25 mm intervals. Three scans were performed across each specimen at a distance of 0.5 mm (Fig 6). The horizontal artC slices with the cutting parallel to the artC surface were measured in a similar way. Three slices from a single specimen were placed on the three pairs of plates. The US beam was scanned along the container bottom at equal intervals of 0.25 mm and along the specimens at equal intervals of 0.05 mm. An example of the US reflections from the upper and lower surfaces of the specimen and the surface of the container base is shown in Fig 10. The experiments were conducted at room temperature (21°C±1).

The mean value for the full-thickness and horizontal slices was obtained by averaging the data from the US scanning. This averaged value was used for the further data analysis of the superficial, middle and deep slices. For the vertical slice, the sound speeds measured at different sites along a scanning line were equally separated into three groups representing the superficial, middle and deep regions. The sound speeds of the measurement sites of each region were averaged, and the result was further averaged with those obtained along the other two scanning lines.

Baseline Drift Amendment. In the course of scanning it was noticed that the distance between the US transducer and the container bottom was not uniform. Despite of many careful adjustments, it was still difficult to ensure the uniformity. The baseline of the container was corrected by using US echoes reflected directly from the bottom of the container on the measurement sites and beyond the artC specimens. A pair of tracking cursors was used to track the shift of the echoes reflected from the bottom of the container directly or passing through the artC specimen. Since the horizontal positions of

the measurement sites were recorded with the micrometer screw gauge, a linear regression between the position and the flight time shift was made for the measurement sites without the presence of artC specimen. The regression line represented the slope of the container bottom and was used to correct the flight time of the echoes reflected from the bottom of the container for the measurement sites on the artC specimen. This procedure was also applied for the other studies using this device.

Measurement of swelling effects. The two full-thickness slices prepared from each of the 5 patellae were immediately installed onto the specimen platform and monitored for 1 h with US beam parallel and perpendicular to the artC surface, respectively. The monitoring site was located approximately at the middle of the surface facing the US beam. The transient thickness and the sound speed of artC specimen were calculated using the method introduced in the section 2.3.1, where T_4 in eqn 16 was measured after the specimen was removed from the platform.

2.4.3 Procedure for Saline Concentration Dependence Study

Full-thickness specimens with a semicircular shape were used for the measurement of the sound in artC under different saline concentrations. The specimens were first placed on the supporting plates and thawed in 0.15 M saline for 30 min. Then distilled water (0 M) was used to replace the 0.15 M saline in the container and the specimen was thawed for another 30 min. During the process, the saline was removed from the container quickly with the help of a syringe. Proper precaution was taken to make sure that the specimen did not move while the saline was removed. The US beam was first located approximately 2 mm away from the edge of the first artC specimen and

the sound speed in saline was measured using the method introduced in the last section. After that, scanning was performed at different locations on and between the specimens at an interval of 0.05 mm. The detailed scanning procedure has been explained in the last section. After the measurement, the distilled water was removed and the 0.0075 M saline solution was then poured gently into the container and the specimens were allowed to thaw for 30 min. Subsequently, US measurements were carried out.

Similar procedure was carried out for the remaining saline concentrations including 0.082, 0.15, 0.3, 0.75, 1.25, 2, and 2.5 M. Specimens were allowed to thaw in all saline solution for 30 min before the measurement. The selection of the concentrations of the saline solution and the thawing period was decided based on pilot studies on a number of specimens. It was noted that thawing for 30 min was well enough for the specimens to reach equilibrium after the change of saline concentration. The experiments were conducted at room temperature (22°C±1).

2.4.4 Procedure for Degeneration Dependence Study

The artC layer was first excised from the bone layer and was further cut into 5 full-thickness specimens as mentioned earlier (Fig 6). All the 5 slices were first measured in normal saline solution using non-contact US scanning method described earlier. After the measurement was completed, the first specimen was stored in a refrigerator at -20°C and used as the first control specimen. The remained 4 pieces of the artC specimen were placed in one row of a multi-well array (24 Well Plate, Arraycote, NUNC, Roskilde, Denmark). The second slice was immersed in PBS solution, as the second control specimen followed by the third, fourth and fifth in collagenase, chondrotinase and trypsin

solutions for digestion, respectively. The multi-well array plate was kept in an incubator (Incucell-V111, Nunc, Denmark), at 37°C for 24 h. The reason behind placing the second slice in PBS solution at 37°C was to find out whether there was any effect, of storing the specimen under 37°C for a certain period, on the acoustical properties in artC. Hence, the effects of storage and enzyme digestion can be separated. After the digestion, the specimens were scanned again after thawing in the normal saline solution for 1 h. The detailed measurement procedure was similar to that explained in section 2.4.2.

2.4.5 Procedure for Temperature Dependence Study

The specimen was thawed for 30 min in the normal saline solution at room temperature before the experiment commenced. A bottle of the normal saline solution was reserved in a refrigerator to allow its temperature to drop below 15°C. The saline solution in the container used for thawing the specimen was replaced by the reserved saline solution. A flow of hot water was passed through the coil at a constant rate to increase the temperature of saline in the container from 15°C to 40°C. US echoes were collected and saved by the custom made program at a rate of 2 frames per second. The frame number and temperature was recorded manually at an interval of 20 frames that approximately equaled to 10 s. After the temperature reached 40°C in approximately 90 min, the US monitoring was stopped and the specimen was removed. While removing the specimen from the container, precaution was taken that the settings of the experimental setup were not disturbed. After that, the saline solution in the container was replaced with the normal saline solution with a temperature of 15°C to collect the US echo from the bottom of the container without the specimen (T_4) (Fig 11). Then the above heating

process was repeated and the saline solution inside the container was allowed to reach up to 40°C. The US echoes from the container bottom was continuously monitored and recorded at a rate of 2 frames per second. After the measurement, the heating was stopped and saline finally reached the room temperature. The transducer was then moved vertically for 0.5 mm at 4 steps and the US echoes were collected at each step so as to calculate the sound speed in saline at the room temperature, which was recorded. Based on the shift of the US echo from the container bottom as the change of the temperature and the measured sound speed in saline at one temperature, i.e. the room temperature, the sounds speed at all the measured temperature could be calculated.

2.4.6 Procedure for Site Dependence Study

Before punching the artC patella at the marked sites, it was measured using an unfocused flat US transducer (10.5 MHz, Φ 3 mm, XMS-310, Panametris Inc., Waltham, USA) at each selected points. A traditional pulse echo method was used to measure the artC thickness *in-situ.* A gentle force was applied to make sure a contact between the transducer and the artC surface. During the measurements, the patella was immersed in physiological saline solution. Three measurements were taken at each location of the patella. The time-of-flight of US obtained in the three measurements was averaged to calculate the artC thickness using the sound speed, later measured with the non-contact method. The patella was then punched to obtain the artC-bone plugs at the selected points. The detached artC specimen was then measured using the non-contact method described earlier. After the sound speed in each artC specimen was measured, it was

applied to calculate the *in-situ* thickness at the corresponding site using the time-of-flight measured with the contact method earlier.

2.4.7 Procedure for Strain Dependence Study

The circular artC disk with a diameter of 6.4 mm was first thawed for 30 min in the normal saline solution (Fig 6 and Fig 9). The two US transducers acting as the compressor and the specimen platform were initially brought in contact with each other and the reading on the LVDT obtained at this position was recorded as a reference for the measurement of the artC thickness. The specimen was then placed on the transmitting transducer and the compressor was moved vertically down to make an initial contact with the specimen. The reading of the load cell indicated the initial contact of the compressor with the specimen. It was observed that the excised specimens were slightly curled. Therefore the compressor was further driven by 0.05 mm for each specimen, so that the surfaces of the two US transducers could make a full contact with the specimen surface. It was observed that the stress at this state was normally below 0.001 N at 15 min after the displacement was applied. It was assumed that this was 0% compression state. The friction between the artC surface and the two compressors was assumed negligible as the setup was immersed in physiological saline solution. Before further compression the specimen was allowed to rest in the normal saline for 30 min. Then stepwise stress-relaxation measurements (step 2.5% of artC thickness) were carried out up to a total strain of 20%. A relatively shorter relaxation time of 15 min was allowed between the steps, in comparison with traditional mechanical measurement of artC for equilibrium parameters, though shorter relaxation time has been used in some earlier studies (refer to

Table 3). Short relaxation time could save the overall experiment time, as 8 steps were used in the compression test for the 20 specimens. Additional 5 specimens were tested with a single compression step of 2.5%, but with a relaxation time of 60 min, to test whether the sound changed significantly during the stress-relaxation period. US signals were collected continuously at a rate of one frame per two seconds during the compression and stress-relaxation phases. We noted that the signal to noise ratio of the LVDT signal was relatively low due to the small deformation applied during each compression. Therefore, data averaging (30 point moving average) was used to enhance the LVDT readings and the related results. The instantaneous Young's modulus and sound speed were calculated at the moment with the maximum stress after each ramp compression. The Young's modulus and the sound speed after 15 min stress-relaxation were also calculated for compression. In the case of the additional 5 specimens tested with 60 min stress-relaxation, the sound speed was calculated for each 5 min.

2.5 Data Analysis

The statistical tests used for analyzing the results of the various studies are summarized as follows:

The Interclass correlation tool (SPSS v11.0.0, SPSS Inc.) was used to test the reproducibility of the non-contact method used in this study. Two-factor ANOVA (SPSS v11.0.0, SPSS Inc., Chicago, IL) was used for analyzing the significant differences in the following comparisons:

- Among the sound speeds measured at different depths and between the sound speeds measured along the two orthogonal directions;

- Among the sound speeds measured for specimens before and after digestion using trypsin, collagenase, and chondrotinase. Similarly, among the 2 control specimens stored at different temperatures;

One factor ANOVA (Microsoft Excel 2002, Microsoft Corporation, USA) was used for analyzing the statistical significance of differences in the sound speeds under following situations:

- Among the 25 different sites on patellae and among the 4 quadrants;
- Among different saline concentrations;
- Among different temperatures;
- Among different strains applied on artC;

Correlation analysis was performed for following pairs of data:

- Sound speed measured by the contact method and the non-contact method;
- Thickness measured by the caliper and the non-contact US method;
- Sound speed in artC and its depths;
- Sound speed in artC and different saline concentrations;
- Percentage change of artC thickness and different saline concentrations;
- Sound speed in artC and saline solution, with different temperatures;
- Thickness of artC measured with contact US method *in-situ* and non-contact US method *ex-situ* at 25 sites of each patella;
- Applied strain on artC and its Young's modulus after stress-relaxation for 15 min;
- Applied strain on artC and its sound speed;
- Applied strain and induced stress on artC;

- The stress and strain relation at the instantaneous and last 3 min of stress-relaxation phase;
- The change of the sound speed in artC and its Young’s modulus;

3. Results

3.1 Validation Results

The sound speeds of the various materials measured by the non-contact technique correlated highly with the results obtained by the contact technique (Fig 13a, $p < 0.001$, $R^2 = 1$, $n = 6$). The thickness measured by the same technique also correlated well with the reference thickness obtained by the vernier caliper (Fig 13b, $p < 0.001$, $R^2 = 1$ and 0.9924, $n = 12$). The error bars in both figures represent the standard deviations of the results of three measurements for each sample. The validation results demonstrated that the non-contact US technique was very reliable for the measurement of the sound speed and thickness measurement.

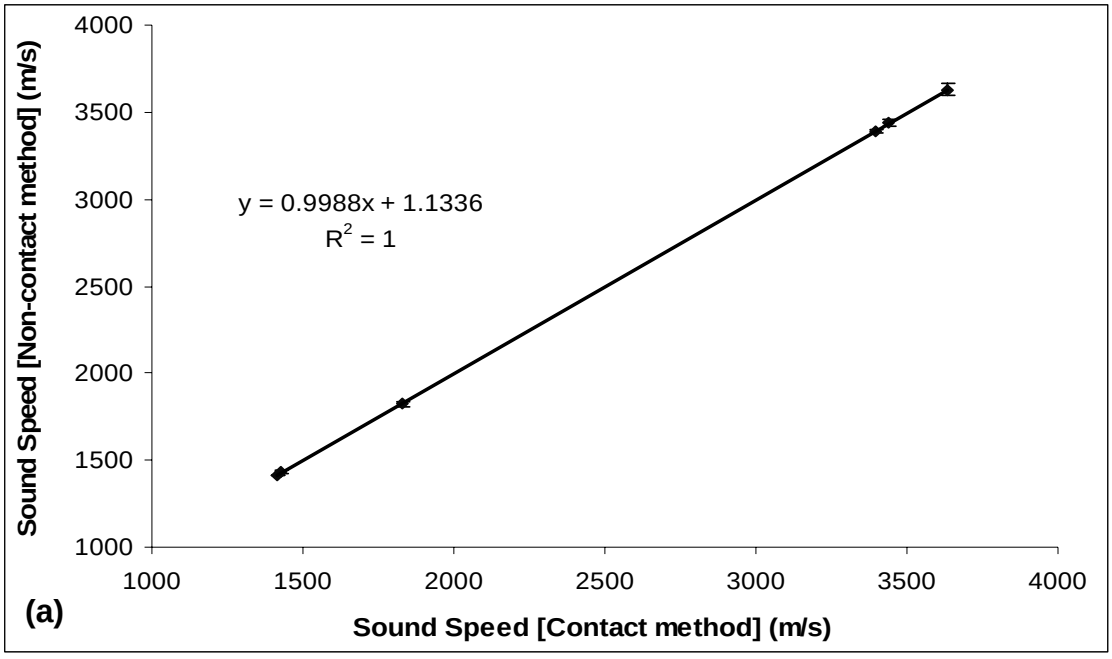

Figure 13. (a) The sound speed measurement using US non-contact technique correlated highly with the reference contact method.

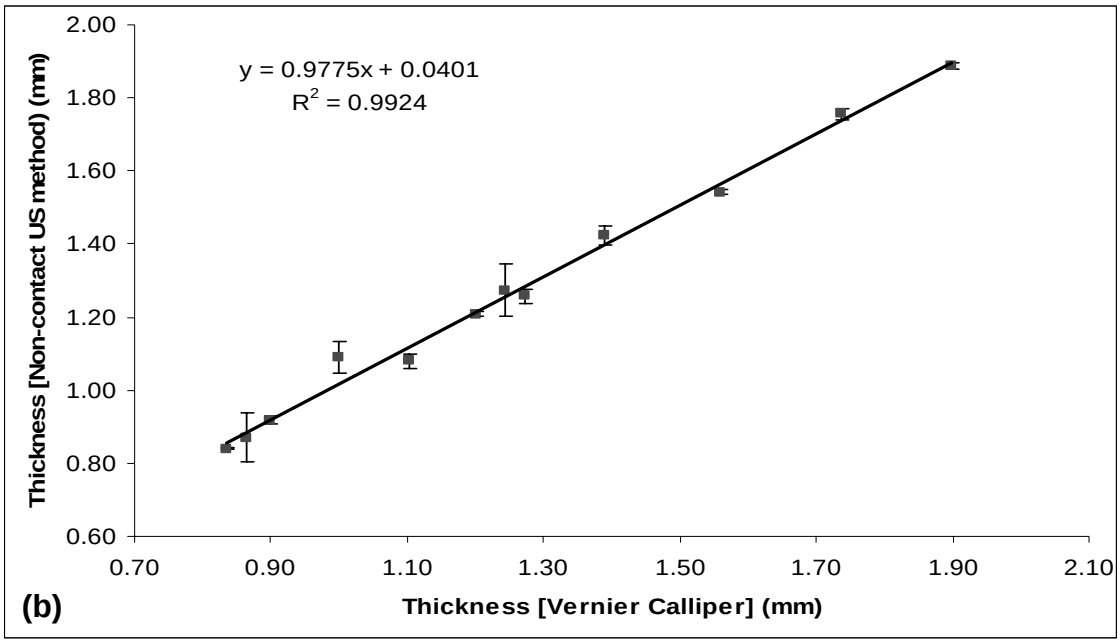

Figure 13. (b) The thickness measured using non-contact US technique also correlated significantly with that measured using a vernier caliper. The error bars in the figures represent the SD.

3.2 Depth Dependence Results

Reproducibility. To test the reproducibility of the technique, the sound speeds measured along the three scan lines (0.5 mm apart) for each slice were compared using Interclass correlation. The mean of the percentage SD for the three measurements of each slice was also calculated as an indicator for reproducibility. The reproducibility test showed that the sound speed measured along the three different scanning lines for each slice agreed well with a mean percentage SD of 2.2%. The Interclass Correlation coefficient for a 95% confidence level was r = 0.9721 ($p < 0.001$), which showed a very high reproducibility.

Sound Speed. The sound speeds of artC tissues at the superficial, middle, and deep regions were 1518±17 m/s (mean±SD), 1532±26 m/s, and 1554±42 m/s with the US beam parallel to the artC surface (n = 18), and 1562±23 m/s, 1623±33 m/s, and 1703±50 m/s with the beam perpendicular to the artC surface (n = 10) (Fig 14). The sound speeds of artC tissue significantly increased from the superficial to middle and deep regions for both measurement directions ($p < 0.001$, Two-factor with replication ANOVA). The sound speeds of artC measured in the two orthogonal directions were significantly different ($p < 0.001$, Two-factor with replication ANOVA). There was a quadratic relationship ($r^2 = 0.9982$) between the sound speed and the tissue depth for the measurements of the vertical slices (Fig. 15). The error bars in Fig. 15 represent the SD among the results of the 10 specimens.

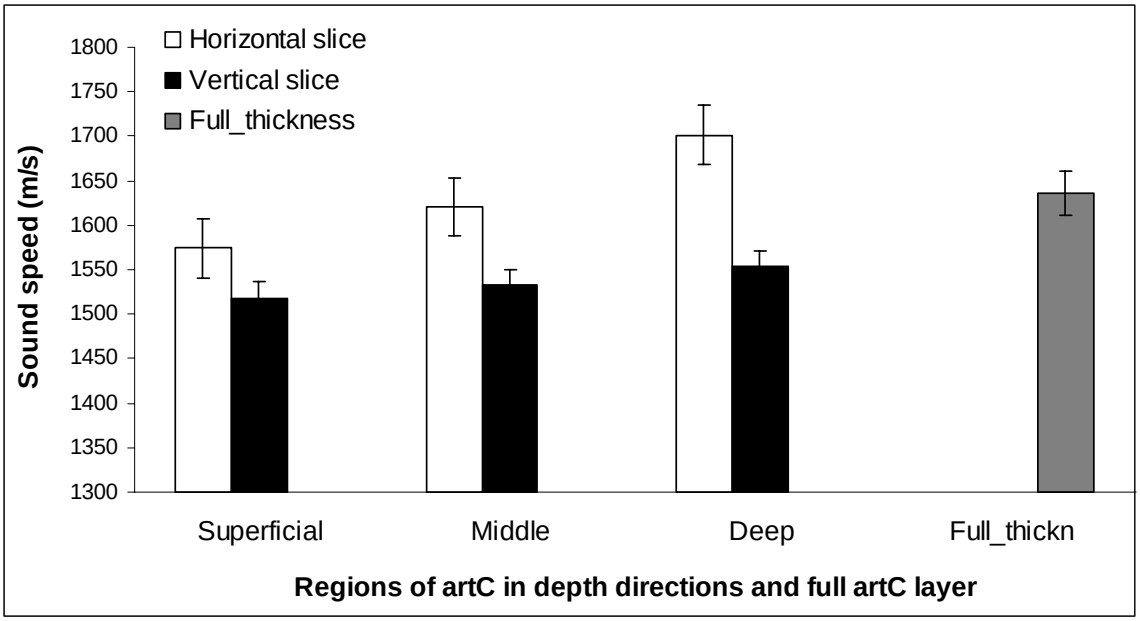

Figure 14. Depth-dependent sound speeds in artC tissue. The error bar represents the standard deviation. The vertical slice was measured with the US beam parallel to the artC surface, while the horizontal and full-thickness slices were measured with the beam perpendicular to the artC surface.

The variation among the specimens as shown in Fig. 15 was similar to that in Fig. 14, although the scale was changed in Fig. 15 to better represent the quadratic relationship. The sound speed increased from 1518 m/s to 1559 m/s (2.7% increase) when the measurement region moved from the most superficial to the deepest zone of the artC layer. The sound speed of the full-thickness artC layer (n = 18) was 1636±25 m/s (ranging from 1598 m/s to 1721 m/s).

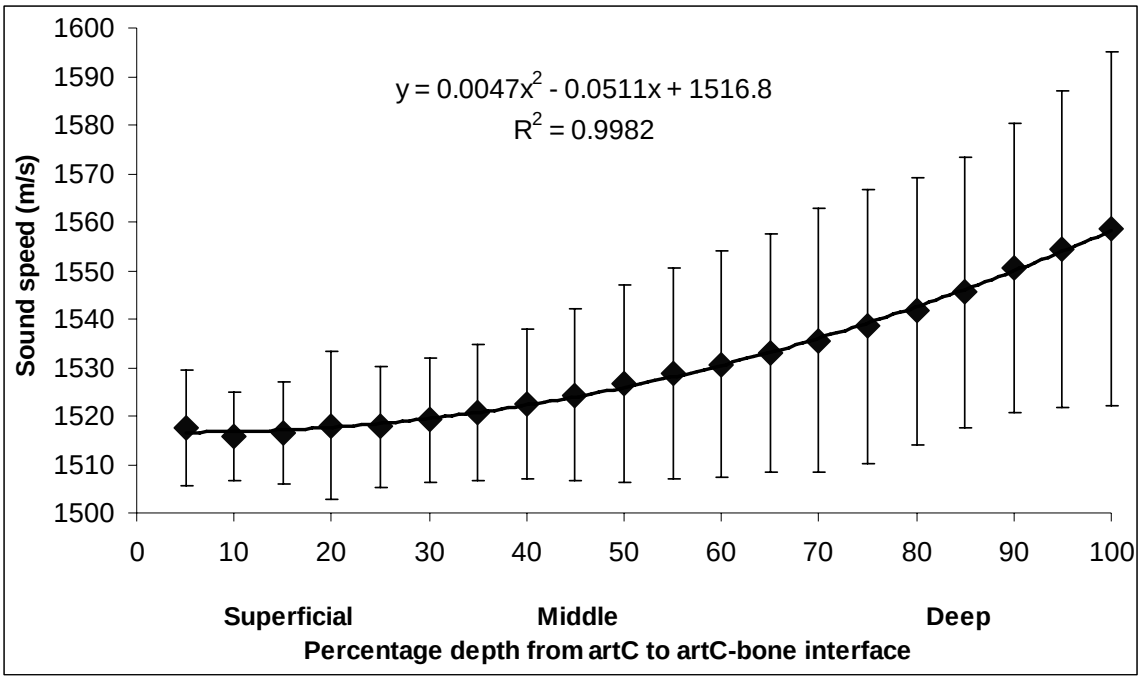

Figure 15. The sound speed measured in the vertical slice throughout the full thickness of artC. The presented data were the average of the ten specimens and the error bars indicated the standard deviations. It was demonstrated that the sound speed significantly depended on the depth of artC.

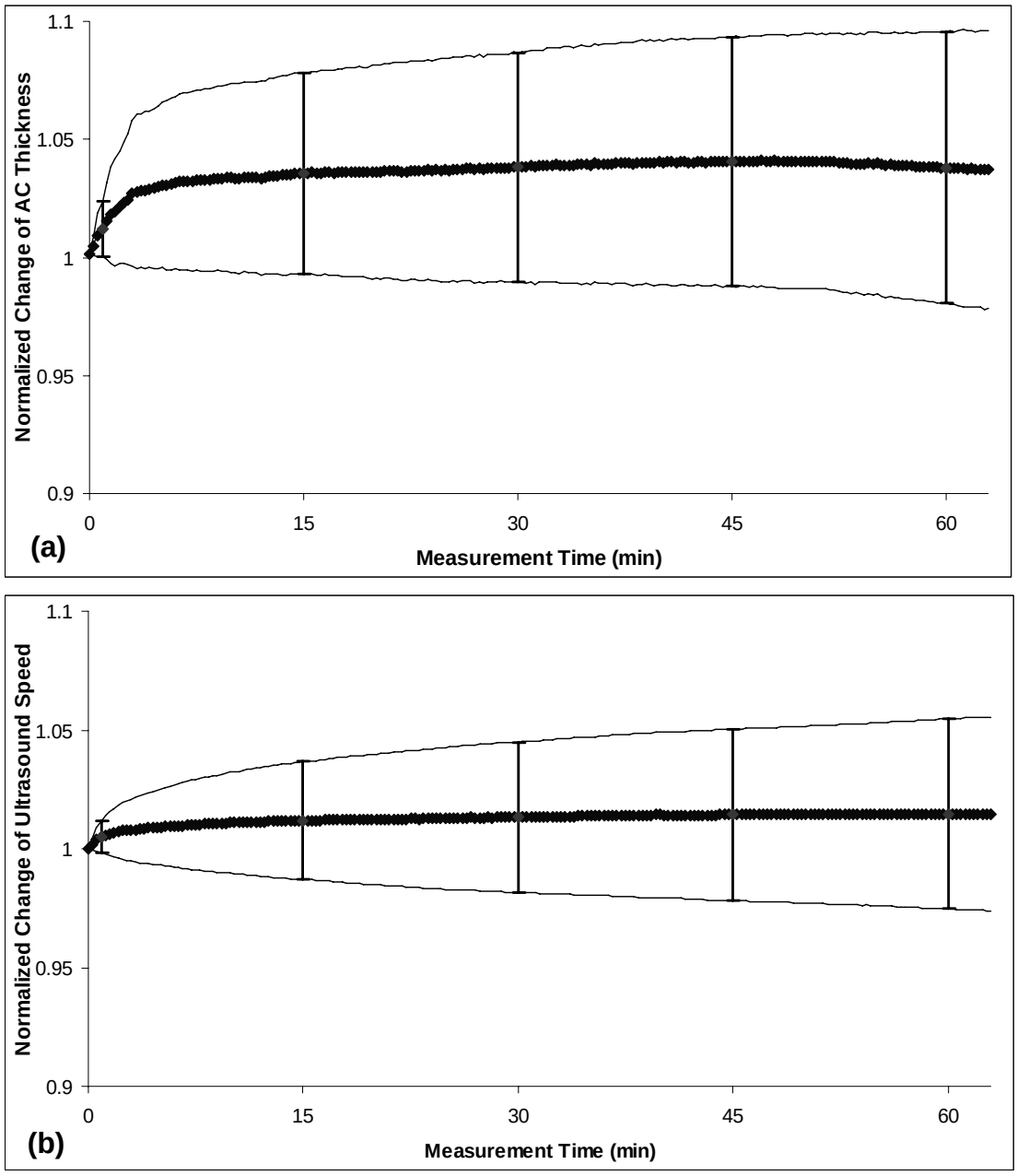

Figure 16. The changes of **(a)** normalized artC thickness and **(b)** normalized sound speed as a function of time after the specimen was detached from the bone. Ten full-thickness slice specimens were prepared from 5 disk specimens, which were cored from 5 different bovine patellae. The 2 slices from each disk specimens were tested in two different orthogonal directions, respectively. No distinguished difference was noted between the results measured in the two directions. Hence the results shown in the figure were the combined data of all the 10 slices from the 5 patellae.

Table 6. The mean normalized sound speed and thickness of artC slice specimens measured at different time after they were detached from their subchondral bones and installed on the specimen platform (corresponding to Fig 16).

Time (min)	Normalized Speed		Normalized Thickness	
	Mean	SD	Mean	SD
1	1.005	0.007	1.012	0.012
15	1.012	0.025	1.036	0.043
30	1.013	0.032	1.038	0.049
45	1.014	0.036	1.041	0.053
60	1.014	0.040	1.038	0.058

Thickness. The mean thickness (mean±SD) of the superficial, middle, and deep horizontal slices (n = 18 × 3) were 0.64±0.18 mm, 0.50±0.18 mm, and 0.59±0.18 mm, respectively. The mean thickness for the full-thickness layers (n = 18) was 1.64±0.30 mm, which was slightly smaller than the sum of the three slices (1.73±0.31 mm). The increase (5.5%) of the summed thickness of the slices was possibly due to the artC swelling after slicing. This swelling issue will be further discussed in the following section.

Swelling Effects. It was demonstrated that there was an increasing trend for the artC thickness for both measurement directions for the five specimens after they were detached from the subchondral bone (Fig 16a). No difference was noted between the results measured in the two directions. Hence, the results shown in Fig 16a were the combined data of all the 10 slices from the five specimens. This change of the artC thickness was believed to be caused by the swelling effect of artC due to its excision from the subchondral bone. Most of the increase in thickness was observed within the first 5 min. At time points 1, 15, 30 and 60 min, the mean increases of the thickness are

summarized in Table 6. The artC thickness changed by 3.6% after 15 min. It appeared that the measurement performed at 15 min was just slightly different from that performed at 60 min (changed by 0.2%). Large variations among specimens were observed. Considering the results of individual specimens, most of them showed different degrees of increase, but a few of them showed a slight decrease as time went on.

The sound speed results showed a similar, but smaller, increasing trend in comparison with that of artC thickness (Fig 16b). No distinguished difference was observed for the changes of the sound speed between the results obtained in two different directions. Most of the changes also happened within the first 5 min. At time points 1, 15, 30 and 60 min, the mean increases of the sound speed are summarized in Table 6. The sound speed changed by 1.2% after 15 min. It appeared that the measurement made at 15 min were just slightly different from that made at 60 min (changed by 0.2%). Considering the results of individual specimens, the majority of them showed different degrees of increase, but some of them showed decrease as time went on.

3.3 Saline Concentration Dependence Results

Sound Speed. The measured sound speed in the artC specimens (n = 19) and the saline solutions (19 groups) with different concentrations are shown in Table 7. Significant differences in sound speed were observed in the saline as well as the artC specimens with the change of the saline concentration (Single-factor ANOVA, $p < 0.001$).

Table 7. The sound speed (mean±SD) in the artC and saline measured under various concentrations of saline. Significant differences (Single-factor ANOVA, $p<0.001$) were observed among the sound speed in artC measured under different saline concentration. Similar results were demonstrated for the sound speed in saline.

		Concentration (Moles)								
		0	0.0075	0.082	0.15	0.3	0.75	1.25	2	2.5
Sound speed in artC(m/s)	Mean	1681	1673	1678	1675	1675	1707	1734	1781	1816
	SD	50	47	44	51	51	50	46	48	54
Sound speed in saline (m/s)	Mean	1521	1522	1529	1532	1532	1571	1601	1646	1674
	SD	3	3	3	5	3	4	4	3	3

A linear increasing relationship was observed for the sound speed in the saline ($r^2 = 0.99$) as well as in the artC specimens ($r^2 = 0.98$) with the increase of the concentration (Fig 17). When the saline concentration was changed from 0M to 2.5M, the sound speed changed from 1681±50 m/s to 1816±54 m/s, and 1521±03 m/s to 1674±05 m/s in the artC and in the saline solution, respectively. The measured sound speeds of 1532±05 m/s in the normal saline solution (0.15M) and 1675±51 m/s in the artC specimens were similar to those previously reported *(Refer to Table 3 for various studies conducted in the past for the investigation of the sound speed in artC).* It was observed that there was a 7.4% and 9.1% increase in the sound speed of artC and saline solution, respectively, when the concentration of saline solution was changed from 0M to 2.5M. The error bars in Fig 17 represent the SD among the results of the 19 artC specimens and the 19 groups of saline solutions (the saline solution of each concentration was obtained from the same batch). The variation of the sound speed in artC was higher than that of the saline. This maybe

due to the fact that the specimens were obtained from different patellae whereas the saline solution remained same (Fig 17).

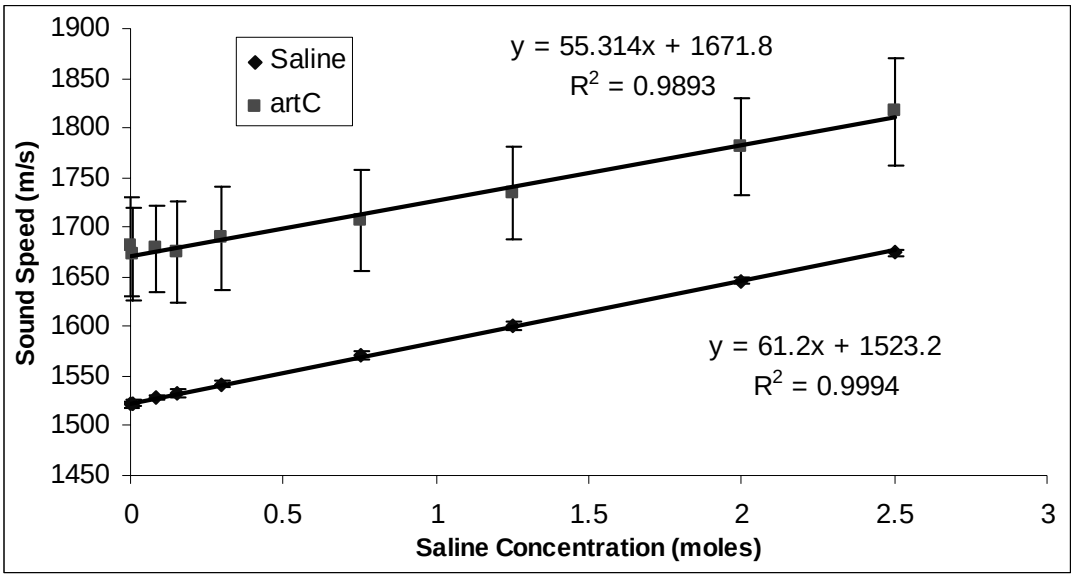

Figure 17. The sound speed in artC and saline solution increased with the increase of saline concentration. A linear relationship were observed and high correlations were obtained for both the sound speed results ($r = 0.9$, $p < 0.001$).

Thickness. The thickness of the artC specimens decreased almost linearly with the increase of the saline concentration (Fig 18). It was noted that there was a sudden change (1.1%) from 0M to 0.0075M. From the concentration of 0.082M to 2.5M, there was linear decrease for the artC thickness. However, no significant difference was demonstrated. In addition, the variation among the specimen was very large. Such a large individual variation has also been described for the artC thickness change during the swelling process after the specimen was detached from the bone and submerged in the normal saline solution.

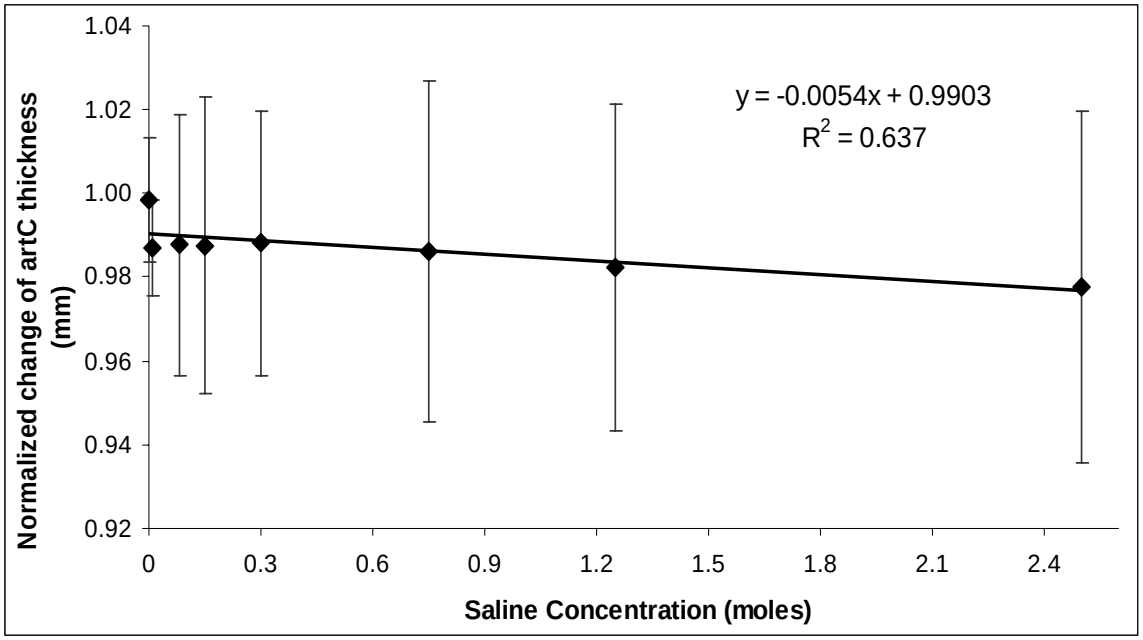

Figure 18. The thickness of artC decreased with the increase of the saline concentration. The thickness decrease was minor and not significant.

3.4 Temperature Dependence Results

Fig 19 shows the relation between the sound speed and the temperature and Table 8 presents the sound speeds in the saline and artC at the minimum and maximum temperature values. An increasing trend of sound speed was observed for artC with the increase of the temperature of the saline solution from 15°C to 40°C. Similar results were observed for the sound speed in the saline solution. A high correlation coefficient was obtained for artC (r^2 = 0.99) and saline (r^2 = 0.98) sound speed when linear regressions were used. The sound speed obtained in artC was 1430±39 m/s at 15°C and 1667±68 m/s at 40°C. There was a 9% difference in the sound speed measured at 21°C (the room temperature used in our study) and 37°C (for *in-vivo* study). The sound speed in the saline was 1360±38 m/s and 1606±64 m/s at 15°C and 40°C, respectively. The

percentage change of the sound speed in artC (14.2%) and saline (15.5%) was similar when the temperature was changed from 15°C to 40°C. The rates of the sound speed change in artC and saline were approximately 11 m/s per 1°C.

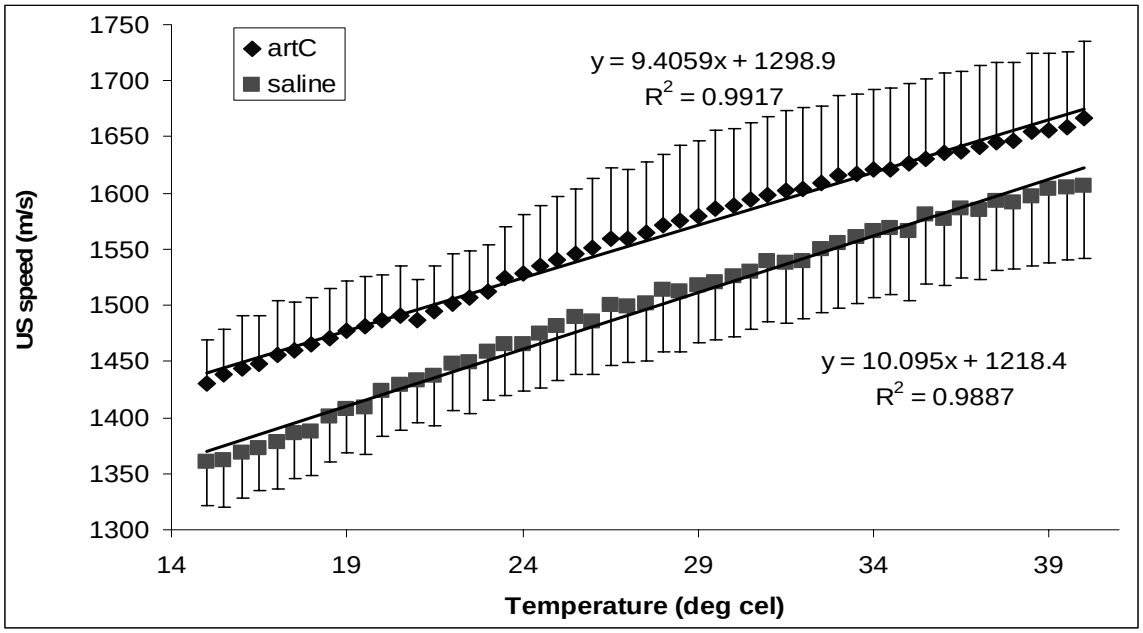

Figure 19. Sound speed of artC and saline solution increased with increase in temperature. A linear response was observed and high correlation was obtained for both sound speed results (r = 0.9).

Table 8. The sound speed in artC and saline solution at 15°C and 40°C

	Minimum (15°C) Mean±SD	Maximum (40°C) Mean±SD
Sound speed in artC (m/s)	1430±39	1667±68
Sound speed in saline (m/s)	1360±38	1606±64

3.5 Enzyme Digestion Results

It was noted that both sound speed and thickness of the 5 slices before any treatment matched very well (Tables 9 and 10, Fig 20a and 20b). The maximum variations of the sound speed and the thickness of artC were 5% and 11%, respectively. The results indicated that there was no bias between the control groups and the treatment groups of the specimens. It was found that the sound speed and the thickness of artC remained nearly constant for the first group of control specimens before and after storage at -20°C for approximately 24 hrs. The second control group showed results before and after the storage in PBS solution under 37°C for 24 hrs. Although the sound speed in artC tended to increase after storing at 37°C but no significant difference was demonstrated. However, the sound speed as well as the thickness in artC significantly decreased after the digestion with any of the three enzymes ($p < 0.0001$, Two-factor with replication, ANOVA). No significant difference was observed among the results of the three specimens treated by chondrotinase, collagenase, and trypsin.

After the enzyme digestion, the maximum decrease in the sound speed was observed in the specimen digested by collagenase and the minimum decrease was observed in the specimen digested by chondrotinase. The percentage decrease of the sound speed in artC after enzyme degradation was 4.46±1.74%, 5.39±2.31%, and 4.76±2.04% in the chondrotinase, collagenase, and trypsin solutions, respectively. This decrease did not correspond to the percentage decrease in the thickness of artC. The percentage decrease in the thickness of artC after enzyme degradation was 10.8±4.5%, 11.5±5.1%, and 11.3±5.0% in the chondrotinase, collagenase, and trypsin solutions, respectively.

Table 9. The sound speed of artC before and after storing at -20°C or 37°C (A and B) or digestion with chondrotinase, collagenase, or trypsin for 24 hrs (C, D, and E). The mean and SD was calculated from 20 specimens.

		Sound speed of artC (m/s)			
Specimen Group		**Before**		**After**	
		Mean	SD	Mean	SD
A	**Control (20°C)**	1651	40	1648	42
B	**PBS (37°C)**	1651	42	1662	43
		Enzyme Digested			
C	**Chondrotinase (37°C)**	1652	40	1577	32
D	**Collagenase (37°C)**	1654	42	1564	33
E	**Trypsin (37°C)**	1654	40	1575	38

Table 10. The thickness of artC before and after storing at -20°C or 37°C (A and B) or digestion with chondrotinase, collagenase, or trypsin for 24 hrs (C, D, and E). The mean and SD was calculated from 20 specimens.

		Thickness of artC (mm)			
Specimen Group		**Before**		**After**	
		Mean	SD	Mean	SD
A	**Control (20°C)**	1.52	0.27	1.51	0.26
B	**PBS (37°C)**	1.52	0.27	1.54	0.27
		Enzyme Digested			
C	**Chondrotinase (37°C)**	1.54	0.28	1.37	0.27
D	**Collagenase (37°C)**	1.53	0.27	1.36	0.27
E	**Trypsin (37°C)**	1.53	0.27	1.36	0.25

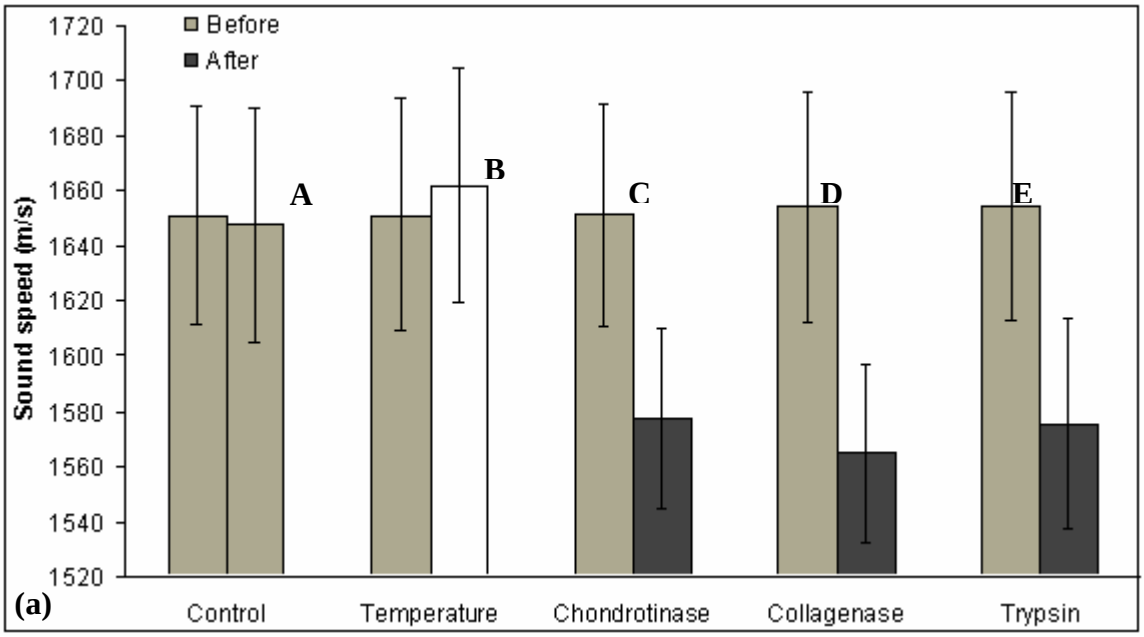

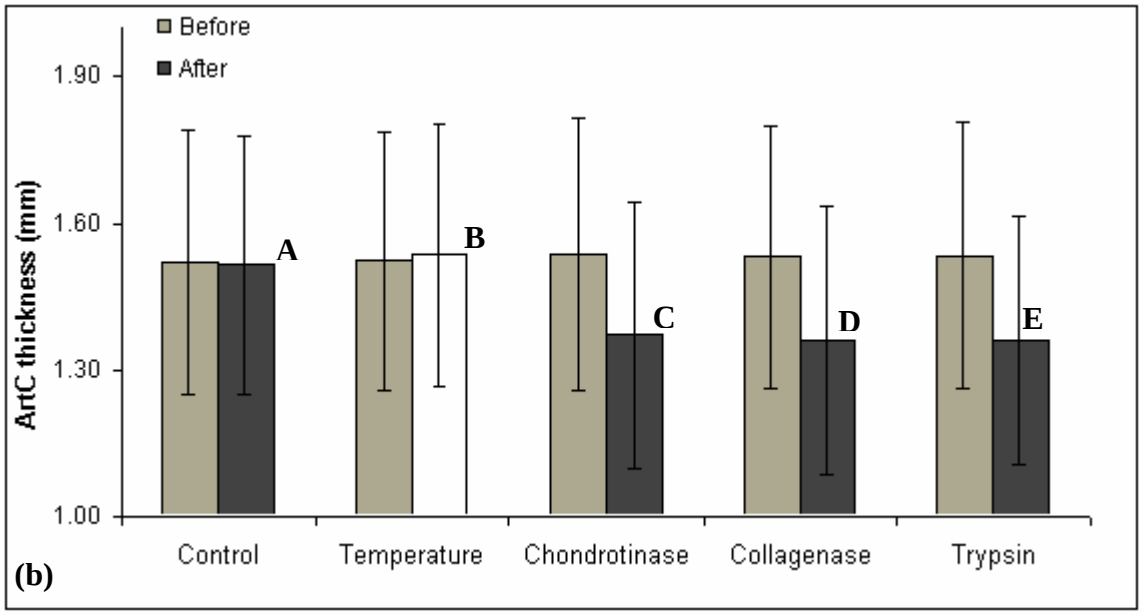

Figure 20. **(a)** The sound speed of artC and **(b)** the thickness of artC before and after storage or digestion. (A) represents the results of the 1st control specimen before and after storage at -20°C for 24 hrs. Similarly (B), (C), (D), and (E) represent the specimens before and kept in the incubator at 37°C in PBS, chondrotinase, collagenase, and trypsin solution before and after digestion, respectively.

3.6 Site Dependence Results

Sound Speed. No statistical significant difference in the sound speed was observed among the 25 locations on the patella surface ($p > 0.05$, Single-factor ANOVA). Hence the sound speed values were divided into 4 quadrants, namely ML, MU, LL and LU (Fig 21a), and were averaged to get overall values for each quadrant. However, no significant difference was demonstrated among these four sound speed values. The overall mean value of the sound speed in artC at the 25 points of the patella was 1626±86 m/s (range: 1507 – 1830 m/s). It agreed with the sound speed measured in the previous studies. The highest sound speed (1834±74 m/s) was obtained at the medial upper (MU) quadrant and the lowest value (1507±74 m/s) at the medial lower (ML) quadrant. Percentage coefficient of variance (% CV) of the sound speed measured at the 25 points was 5.2% (0% describing a homogeneous distribution and a higher % CV indicating a inhomogeneous pattern). To produce a topographical distribution of the pattern of the sound speed and thickness of artC, a computer program was developed (Matlab, The Mathworks Inc, USA). Linear Interpolation was used for the measured data points to construct maps of the sound speed and the thickness with intervals of 0.2 mm throughout the patella surface. Figs 22a and 22b shows the topographical distribution of the sound speed on the patella. The grey level indicates the value of the sound speed. It appears that the sound speeds in artC at the surrounding regions were distinctively smaller than those at the central region. After re-grouping the data according to the two regions indicated by the circle in Fig 22, it was found that the sound speeds in artC at the central region (1633±21 m/s) was significantly ($p < 0.01$) larger that those at the surrounding regions (1621±22 m/s).

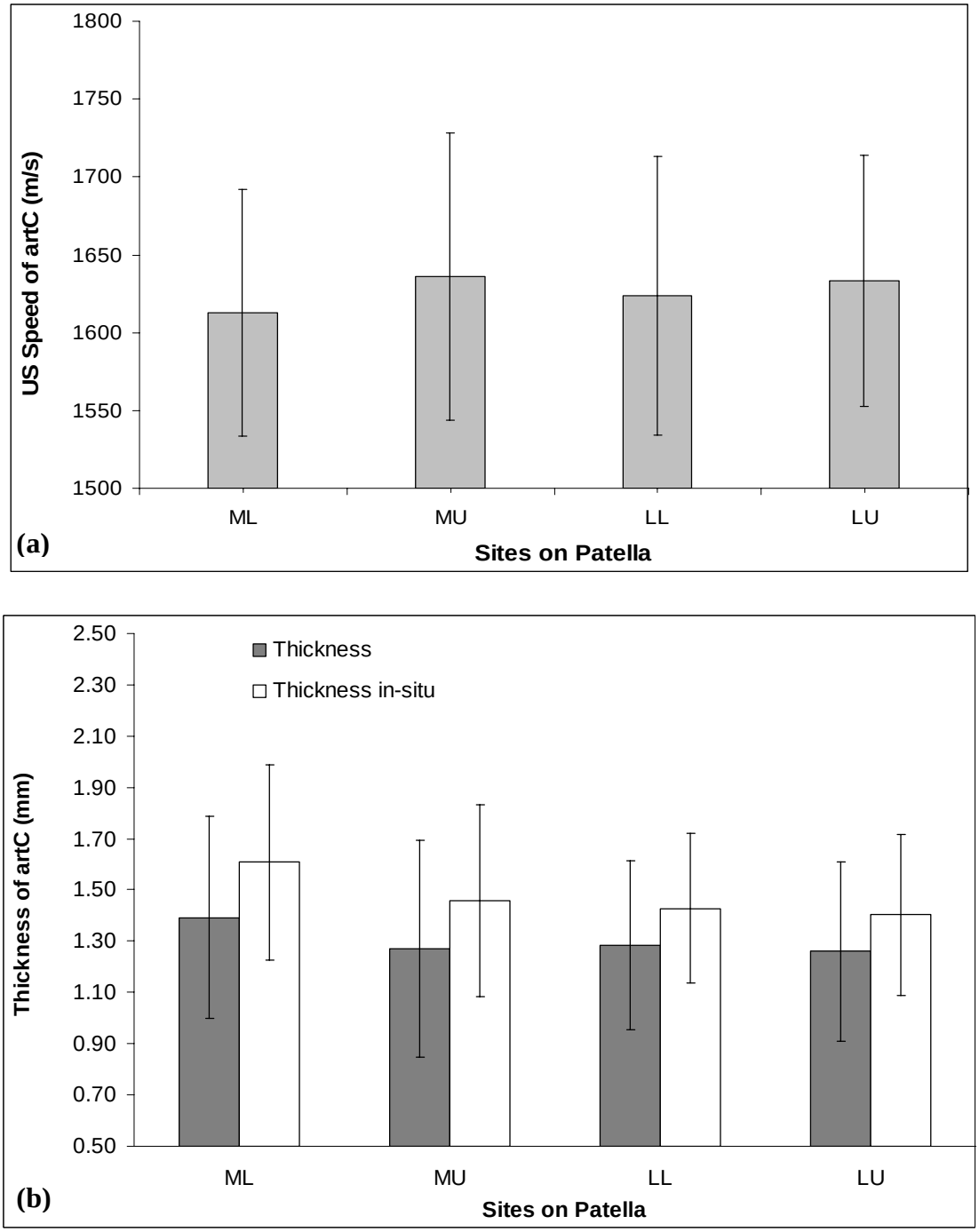

Figure 21. (a) The speed of sound in artC at the four quadrants after grouping from the 25 measurements points of the patella. **(b)** Topographical variation of the thickness of the patellar artC.

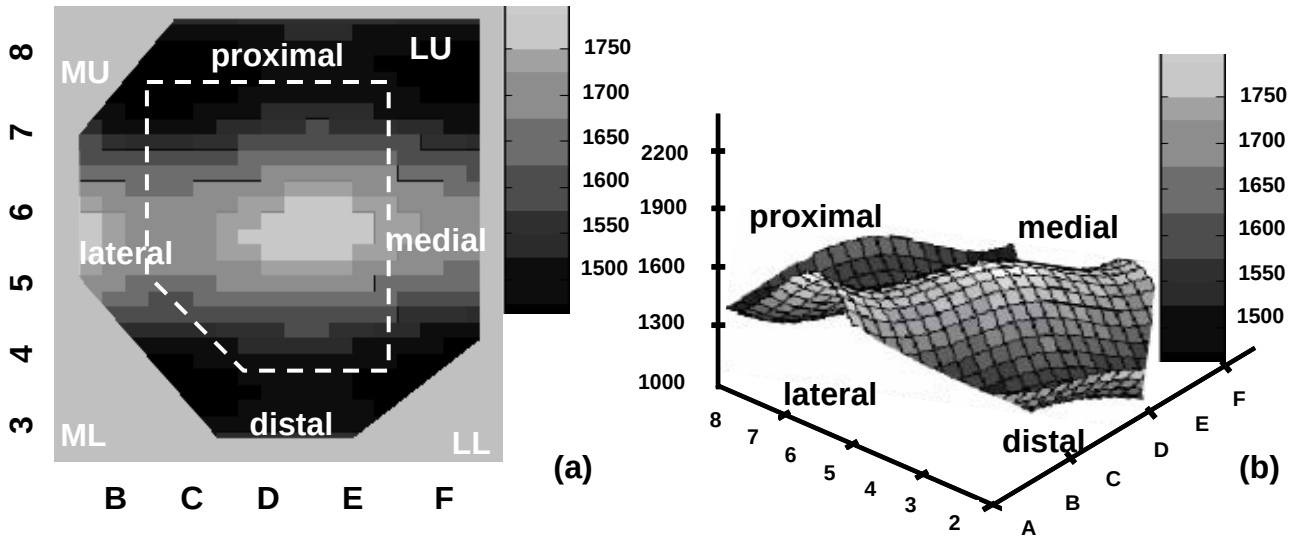

Figure 22. The topographical distribution pattern of the sound speed in the patellar artC. **(a)** 2D representation with the grey level indicating the values of sound speed; **(b)** contour representation of the artC sound speed distribution.

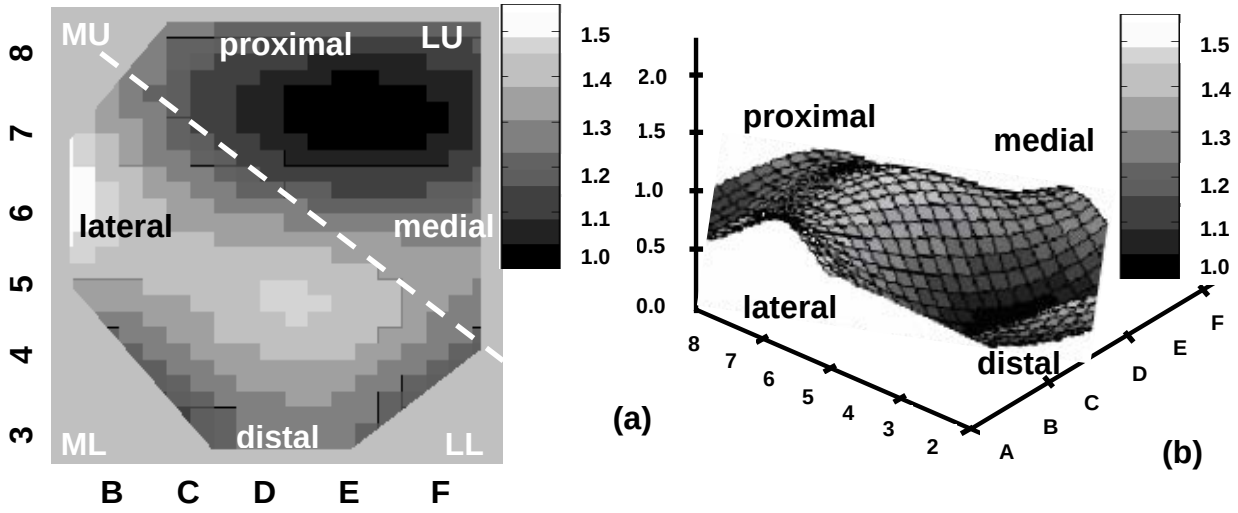

Figure 23. The topographical distribution of the thickness of the patellar artC. **(a)** 2D representation with the grey level indicating the thickness value, and **(b)** 3D contour representation of the artC thickness distribution.

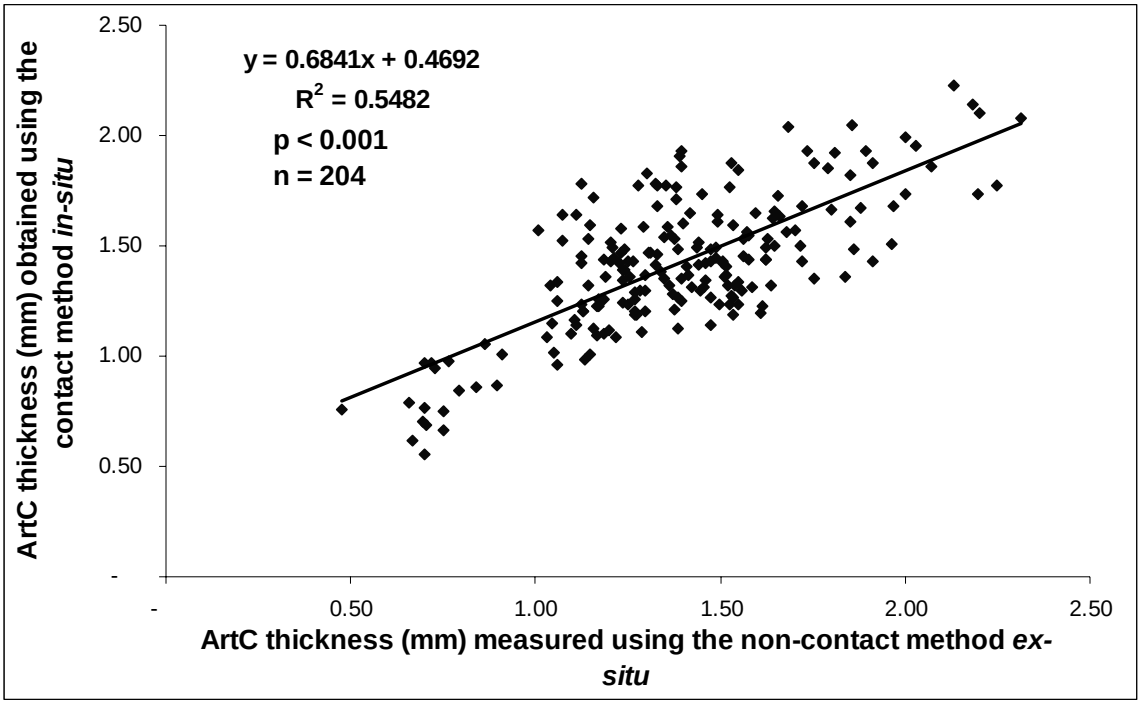

Figure 24. The artC thickness obtained using the contact measurement *in-situ* correlated significantly ($p < 0.001$, $n = 204$) with the thickness obtained using the non-contact *ex-situ*.

Thickness. The thickness of artC at each of the 25 locations on the patella measured by the contact method *in-situ* and the non-contact method *ex-situ* is shown in Fig 21b. The sound speed measured using the non-contact method was used for the calculation of the thickness of the corresponding location for the contact measurement. The overall mean thickness of the patellar artC obtained using the *in-situ* contact measurement was 1.45±0.33 mm (range: 0.55 – 2.59 mm) and that obtained using the non-contact measurement was 1.34±0.34 mm (range: 0.47 – 2.31 mm). A significant correlation ($r^2 = 0.5$, $p < 0.001$, $n = 204$) was observed between the artC thickness obtained using the two US measurements (Fig 24). However, significant ($p < 0.01$, Single-factor ANOVA) difference were noted between the results obtained by the two US measurements. Overall

speaking, the thickness measured by the contact method *in-situ* was 14% larger than that measured by non-contact method *ex-situ*. The maximum mean thickness of 10 patellae measured using either method was located on the ML quadrant (1.37±0.40), which had the lowest sound speed. The other three quadrants had similar thickness (range: 1.30±0.39 – 1.31±0.35 mm). However, no significant difference was obtained in the thickness among the 25 locations and also among the 4 quadrants. Both measurement techniques revealed a relatively similar topography for the artC thickness of the patellae. A 3D contour was also plotted to observe the surface variation of artC throughout the patella surface (Fig 23b). It appears that the diagonal line shown in Figure 23 can separate the patella into two regions with the artC thickness distinctively different. After re-grouping the data in such a way a significant difference ($p < 0.01$) of the artC thickness was demonstrated between the upper region (1.27±0.11 mm) and the lower region (1.31±0.41 mm) of the patellae.

3.7 Strain Dependence Results

A typical stress-relaxation response after a step-wise compression (2.5% strain of 8 steps) is shown in Fig 25a. It was observed that the stress-relaxation period of 15 min appeared not enough for the force to achieve an equilibrium state, particularly for the cases with the overall strain larger than 10%. Fig 25b shows a typical stress-relaxation response when the artC specimen was allowed to undergo a relaxation time of approximately 60 min after a single ramp compression of 20%. The result showed that the force value was almost constant after 60 min relaxation with a force change rate of 0.0004±0.0001 N/s.

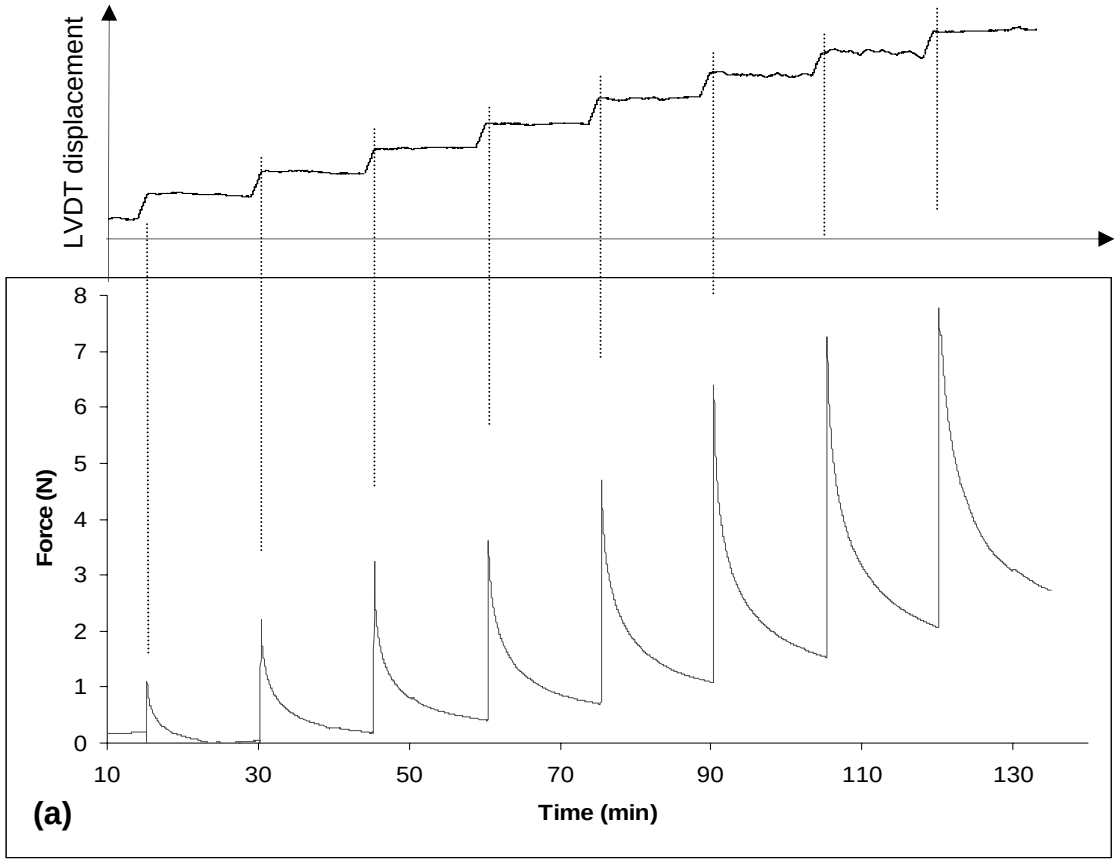

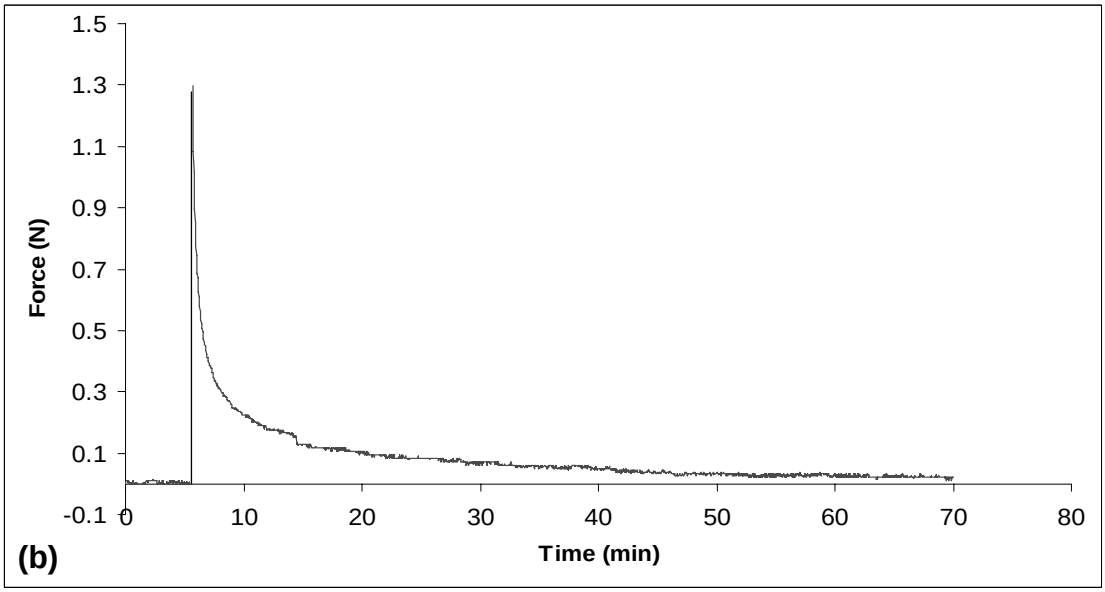

Figure 25. (a) Typical behavior of artC in step-wise stress-relaxation experiment as a function of time in the unconfined compression and the corresponding displacement data by the LVDT sensor **(b)** The type response stress-relaxation of a single step compression when the artC specimen was allowed to relax for 60 min.

Sound Speed. It was noted that the sound speed at the moment with the maximum force after each compression was not significantly ($p > 0.05$) different from that measured after 15 min stress-relaxation. Therefore, the average of the sound speed measured at the instantaneous phase and after 15 min stress-relaxation was used for the subsequent analysis. In addition, the test on the 5 additional artC specimens with 60 min stress-relaxation did not demonstrate a significant difference ($p > 0.05$) between the sound speeds measured after 15 min and 60 min relaxation, though a slight increase of the sound speed was observed with increase stress-relaxation time. The values of sound speed, and Young's modulus measured at various compression levels are summarized in Table 11. The sound speed in artC changed by 7.8% (from 1581±36 m/s to 1671±56 m/s) when the compression was changed from 0% to 20%. The sound speed in artC significantly increased as the increase of the applied strain ($r^2 = 0.98$, $p < 0.001$). A quadratic relationship between the sound speed in artC and the percentage compression was demonstrated ($r^2 = 0.98$) (Fig 26).

Table 11. Averaged values (n = 20) of the sound speed, the instantaneous Young's modulus and the modulus obtained after 15 min stress-relaxation for the 8 compression levels ranged from 2.5 to 20%.

		% artC compression (n = 20)								
		0	**2.5**	**5**	**7.5**	**10**	**12.5**	**15**	**17.5**	**20**
Sound speed (m/s)	**Mean**	1581	1585	1593	1605	1616	1626	1641	1659	1671
	SD	36	43	46	42	44	44	47	49	56
Instantan--eous Modulus (MPa)	**Mean**		0.21	0.39	0.62	0.90	1.11	1.60	2.42	2.86
	SD		0.28	0.53	0.86	1.05	1.10	1.50	1.92	2.64
Modulus after 15min of relaxation(MPa)	**Mean**		0.05	0.13	0.19	0.28	0.37	0.54	0.70	0.87
	SD		0.06	0.08	0.16	0.21	0.29	0.37	0.51	0.81

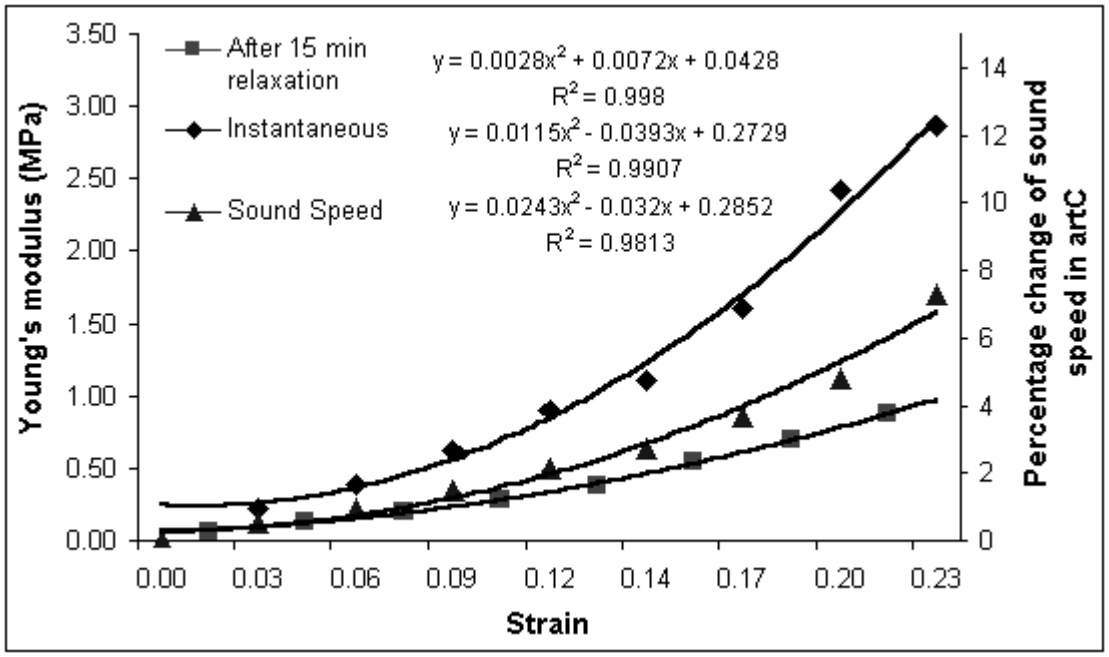

Figure 26. The relationship between the applied compression on artC and the percentage changes of the sound speed, the instantaneous moduli, and the moduli obtained after 15 min stress-relaxation. A quadratic function was used to fit each set of data. Large variation among individual specimens was observed. To make the figure easier to read, the error bar had not been included, the reader can refer to Table 11 for the SD for each data set.

Mechanical Properties. Fig 27 shows the overall stress-strain relationship of artC averaged from the 20 specimens. It was noted that the quadratic functions could very well fit the stress-strain relationship of the data collected instantly after the compression (r^2 = 0.99) as well as after the 15 min stress-relaxation (r^2 = 0.99). The instantaneous Young's modulus changed from 0.21±0.28 MPa to 2.86±2.64 MPa when the applied strain changed from 2.5% to 20%. Similarly, the Young's modulus measured after 15 min stress-relaxation changed from 0.058±0.064 MPa to 0.87±0.81 MPa. Even though large individual variation was observed, high correlation were obtained between the applied strain and the instantaneous modulus (r^2 = 0.99) as well as the modulus obtained after 15 min stress-relaxation (r^2 = 0.99) (Fig 26). Quadratic functions could well represent their nonlinear relationship as shown in Fig 26. The changing rate of the instantaneous modulus was much larger than that of the modulus after 15 min stress-relaxation. It was found that there was a very good linear relationship between the instantaneous Young's modulus and the modulus measured after 15 min stress-relaxation (r^2 = 0.99, $p < 0.001$) (Fig 28).

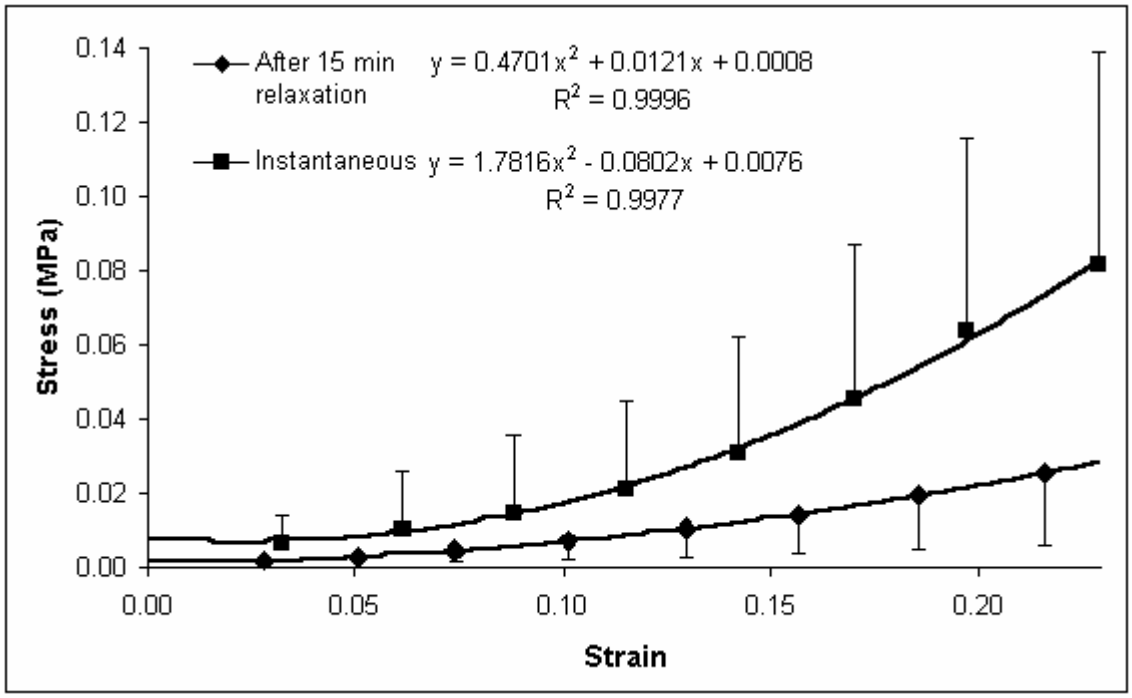

Figure 27. The relationship between the strain and the mean instantaneous stress as well as stress after 15 min stress-relaxation. The error bars represent the SD of the stress at each strain level among the 20 specimens.

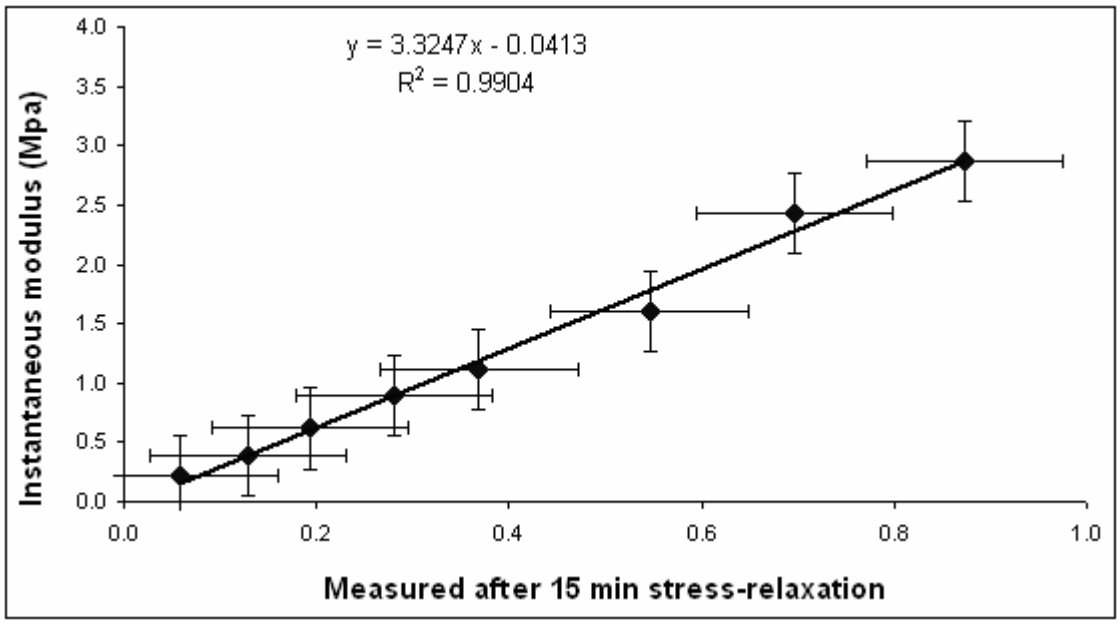

Figure 28. The relationship between the instantaneous modulus of artC and the modulus obtained after 15 min stress relaxation. The error bars represent the SD of the results of the 20 specimens.

Correlation between sound speed and modulus. It was found that the modulus as well as the sound speed both increased nonlinearly with the increase of the strain applied on artC. Fig 29 represents the correlation between the change of the sound speed and the instantaneous Young's modulus and the modulus measured after 15 min stress-relaxation. Good linear relationships were observed between the change of the sound speed and the different moduli of artC (r^2 = 0.97). Even though the instantaneous modulus and the modulus obtained after 15 min stress-relaxation were dramatically different (Table 11, Fig 26), sound speeds did not show any significant difference. It implied that the water redistribution during the stress-relaxation phase might not significantly alter the sound speed in artC. The issue was further discussed in the discussion section.

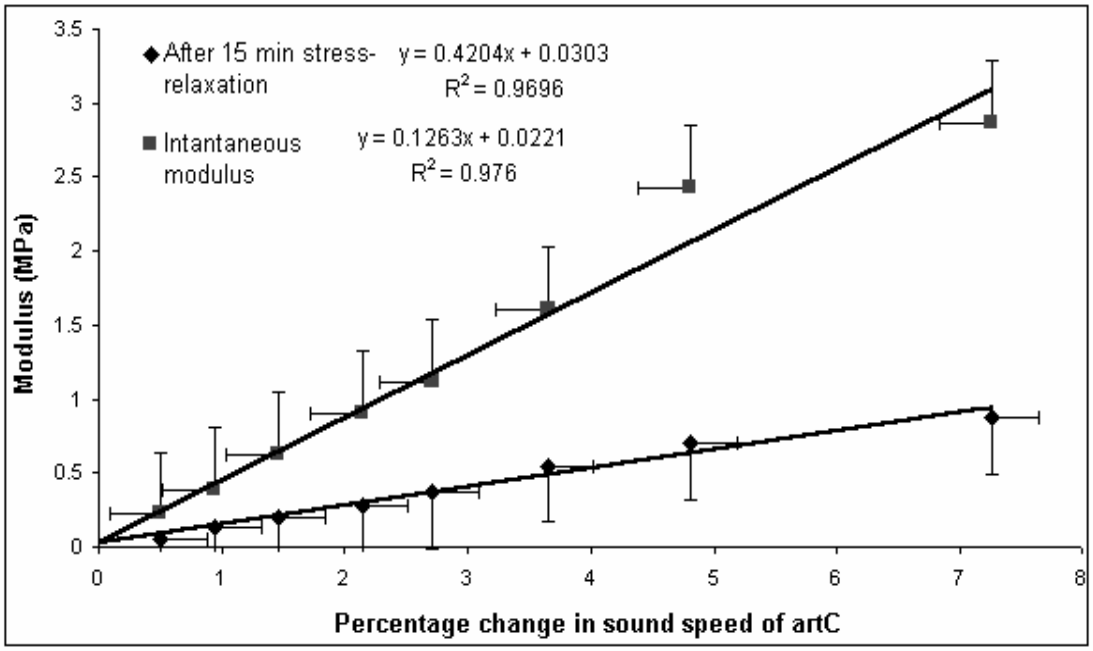

Figure 29. The relationship between the change of the sound speed in artC and the instantaneous Young's modulus and the modulus measured after 15 min stress-relaxation. The error bars represent the SD among the 20 specimens.

4. Discussion

The present study aimed to conduct systematic investigation on the sound speed in artC under various conditions. It is observed from the values reported in the literature that the US measurement of artC is usually performed under the assumption of constant sound speeds. However there are evidences that the US properties of artC are different at different depths because of the spatial variation of the water content, the PG concentration and the orientation of the collagen fibril. The changes in the sound speed due to the variation in inhomogeneous structure of artC, pathological state, environmental variation during experiments and anatomical location may affect the accuracy in the ultrasonic measurements of artC. This study provided an investigation of the sound speed in artC by varying the tissue depth, measurement direction, anatomical site, type of degeneration, the testing temperature, and applied stress. Almost all the factors affecting the sound speed of artC during *in-vitro* measurements have been considered and experiments have been conducted accordingly. Before beginning the discussion on the various experimental results, a brief discussion is provided on three issues that were common for all the experiments.

ArtC Swelling. It has been reported earlier that when artC is detached from bone, it tends to curl and swell. Hence, it is obvious that the swelling effects on the sound speed must be taken into account when the detached specimens are used. We demonstrated that most of the changes of the sound speed happened within first 5 min after the artC specimen was detached from the subchondral bone. The sound speed changed by 1.2% at 15 min after artC was detached from bone, and changed very slightly after that (up to 60 min as measured in this study). In this study all artC specimens were tested at least 15

min after detaching from the subchondral bone. Despite of the fact that our results of the sound speed in artC measured under various conditions might be affected by the swelling effects due to detachment from the bone, they should still have reference values in the context that majority of the sound speed measurement reported in the past were based on detached specimens. In addition, it appears that measuring *in-situ* depth- orientation- or other dependences of sound speed in artC is still difficult using available technology. More systematic studies on swelling effects should be followed and the results may benefit the research area on ultrasonic and biomechanical measurements where detached specimens are normally used.

RF versus envelope signal. A-mode US signal were used in the experiments performed in this study. It was noted that the waveforms of the US echoes distorted for different degrees after it propagated through the artC specimens. This distortion was caused by the artC's frequency-dependent attenuation (Joiner et al 2001) and possible nonlinear acoustic properties (Zheng et al 1999). A cross-correlation algorithm was used to measure the time-of-flight of the US signal in artC by matching the RF signal of the echoes reflected from different interfaces. The distortion of the echoes could potentially affect the cross-correlation matching (Ragozzino 1981). Wherever necessary the RF signal was transformed to an envelope signal using Hilbert transform to achieve a good correlation among various echoes. High correlations ($r^2 = 0.9$) between the echoes could be achieved for most of the specimens in this study. It was verified that the results obtained using the RF signal and corresponding envelope signal matched very well (within 0.1%) for the cases with small phase distortion. When the waveforms

significantly distorted, the echoes to be matched would be first manually located and the cross-correlation approach was then used to optimize the matching.

Sound speed of full-thickness artC. Six different experiments were conducted in this study. The sound speed measurement was the main focus in all the experiments under various conditions. The sound speed in artC at room temperature and at physiological saline condition measured in different experiments showed no significant difference ($p > 0.05$). The overall mean of the sound speed in full-thickness artC measured in all the experiments was (1648±75 m/s, 327 specimens of 87 different patellae). The sound speeds obtained from various experiments is summarized in Table 12 and discussed in the following sections.

Table 12. Summary of the sound speed in artC under various conditions.

	Sound Speed Dependences (m/s)						
	Depth	**Saline Concentration**	**Temperature**	**Degeneration**	**Site**	**Strain**	
Full - Thickness	1636	1675		1651	1626	1581	**Full - Thickness**
Superficial	1562			1662			**PBS**
Middle	1623			1577			**Chondrotinase**
Deep	1703			1564			**Collagenase**
				1575			**Trypsin**
0M		1681					
0.15M		1675			1633		**Central Region**
2.5M		1816			1621		**Peripheral Region**
15°C			1430			1585	**2.5%**
21°C			1496			1616	**10%**
40°C			1667			1671	**20%**

4.1 Measurement Techniques

In most of the previous investigations on US propagation in artC, the sound speeds were either assumed to be constant or measured with the artC thickness measured by another approach. Many studies have demonstrated that the sound speed in artC varied under various conditions. Therefore, using a constant sound speed is not proper under many situations. In this study, a non-contact US method was successfully used for the simultaneous measurement of the sound speed and the thickness of artC specimens *in-vitro*. This non-contact US technique was successfully used in the past to measure the sound speed and thickness of hard materials such as steel and plastic (Kuo et al 1990; Hsu and Hughes 1992). Our measurements demonstrated that this non-contact technique could be reliably used for the measurement of artC *in-vitro* (ICC = 0.97).

In using this non-contact technique the orientation of the specimen with respect to the focused US beam is critical to ensure accurate thickness measurement. If the specimen is not aligned perpendicular to the US beam, errors may occur in the thickness measurement. The device used in this study consisted of three pairs of parallel plates to hold the specimen at its two ends while the measurements were conducted at the middle portion of the specimen. These holdings plates and the fixation rubber bands helped to maintain a perpendicular alignment between the US beam and the specimens. In addition, the amplitude of the US echoes obtained from the artC surface was used as an indicator for the perpendicular condition, i.e. highest amplitude indicating the best perpendicular alignment.

4.2 Sound Speed Variations

Depth and Dire`ction Dependences.

It was demonstrated that the sound speed in artC significantly depended on the tissue depth. The sound speed measured with the US beam parallel and perpendicular to the artC surface both increased from the superficial to the deep layer. The sound speed measured with the beam perpendicular to the artC surface (overall mean for different depths 1629±71 m/s) (mean±SD) was significantly larger than that measured with the beam parallel to the artC surface (1535±18 m/s). Similar results have been reported previously but with only two specimens (Agemura et al 1990). The increasing trends of sound speed in both directions might be related to depth-dependent mechanical properties and structural components of artC. Similarly, the anisotropic behavior of the sound speed in artC might be due to the anisotropic mechanical properties and micro-structures of artC (Kempson et al 1980; Mow et al 1991; Mankin et al 1994). The sound speed of the full-thickness artC was (1636$\pm$25 m/s) within the similar range of the averaged sound speed of the three horizontal slices (1629$\pm$71 m/s). The sound speed (1636±25 m/s) measured in the present study with the 50 MHz US beam perpendicular to the artC surface and under room temperature was within the similar range as reported in most of the previous studies for bovine and human artC's. The sound speeds of full-thickness artC reported in the previous studies have been summarized in Table 4.

The theoretical relationship between the longitudinal sound speed and mechanical parameters is shown in eqn (20).

$$c = \sqrt{(K + 4/3G)/\rho} \qquad (20)$$

where c is the longitudinal sound speed, K is the bulk modulus, G is the shear modulus, and ρ is the density of the material (Stanley 1968). Equation (21) and eqn (22) give the relationship between the bulk modulus K, shear modulus G, Young's modulus E, and Poisson's ratio ν of an isotropic material.

$$K = \frac{E}{3(1-2\nu)} \tag{21}$$

$$G = \frac{E}{2(1+\nu)} \tag{22}$$

It has been reported that the Young's modulus of artC tissue increased from superficial layer to the deep layer (Guilak et al 1995; Schinagl et al 1996; Zheng et al 2002; Wang et al 2002; Laasanen et al 2003a). The increasing trend of the sound speed of artC at depths from the artC surface to the bone appeared to agree with increasing trend of equilibrium Young's modulus. Recently, Laasanen et al (2003a) reported that the middle region of the bovine knee artC had much larger Poisson's ratio (up to 0.4) in compression with that in the superficial and deep regions (low to 0.1). Wang et al (2003) showed that the equilibrium compressive moduli of artC were significantly different when measured in different directions. Their results showed that the modulus of the superficial region measured with the compressing direction perpendicular to the artC surface was significantly smaller than that measured with the compression in other two orthogonal directions. However, the artC tissue of the deep region showed a reversed feature. Due to the complexity of mechanical properties of artC, it appears that the correlation between the anisotropy and depth-dependence of the equilibrium compressive modulus of artC and its longitudinal sound speed was not so straightforward. In addition to Young's modulus and Poisson's ratio the contents of the fluid phase and the shear modulus of artC

are not constant from the superficial region to the deep region (Athanasiou et al 1991). Even though there are few studies (Joseph et al 1999) reported on the density of artC, it is reasonable to predict that artC density is also depth-dependent considering the depth-dependent water contents and other components. Therefore, it appears difficult to have a simple relationship between the depth-dependent Young's modulus and the sound speed.

Another difficulty is that material properties obtained in conventional mechanical tests could not be directly used for eqn (20). According to the artC density (1050 kg/m3) reported by Joseph et al (1999), the instantaneous Young's modulus for bovine patellar artC (8.5 MPa, Laasanen et al 2003, measured with 2 mm/s compression rate for 10% deformation), and the instantaneous Poisson's ratio of 0.4 for bovine patellar artC (Fortin et al 2003, measured with a 2 s ramp compression), the sound speed calculated using eqn (20) is only 132 m/s. This value was much smaller than that measured in the present and all the previous studies. The main reason is that artC is a viscoelastic (biphasic poroelastic) material so it is difficult to measure its real instantaneous modulus and Poisson's ratio, which is involved in the acoustic wave propagation as well as in eqn (20). The compression rate for measuring the instantaneous modulus and Poisson's ratio as reported is much smaller as compared with that in the ultrasonic wave. In other words, the real instantaneous modulus of artC should be much larger than those reported in the literature.

Toyras et al (2003) reported that the sound speed of full-thickness artC significantly depends on the equilibrium Young's modulus, water content and other artC composition. Agemura et al (1990) reported that the differences in sound speed among different regions of artC to its dissimilar fibril organization. In the superficial, middle and

deep region, the collagen fibers are parallel, random and perpendicularly oriented to the surface of the artC, respectively (Mow et al 1991; Mankin et al 1994). Agemura et al (1990) concluded with a limited number of specimens that the US appeared to propagate faster across the long axis of collagen fibrils than along them. In the present study the measured sound speed significantly increased from the superficial region to the deep region. A study with fine slice preparation is necessary to further clarify the correlation between the collagen fibril orientation and the sound speed in artC.

Strain Dependence

In this study, the sound speed and Young's modulus of artC were measured using a custom-made US compression device. Experimental measurement demonstrated non linear behavior of the sound speed and Young's modulus of artC in the direction perpendicular to artC surface. Significant change of the sound speed in artC was observed with the increase of the strain. The instantaneous modulus and the modulus measured after 15 min of each stress-relaxation also significantly depended on the applied strain. The sound speed increased nonlinearly with the increase of the strain. Similar results were observed for the instantaneous modulus as well as for the modulus measured after 15 min stress-relaxation. At the low compression levels, the artC disk appeared to be softer. As the compression level increased, artC became much stiffer. Similar results have been widely reported in the literature (Toyras et al 2003). According to Fig 26, a quadratic function can better represent the relationship between the sound speed and the Young's modulus, except the data point of 20% strain. The relationship agreed with eqn 20.

As described earlier, this relationship can become more complicated by many other factors such as the density of artC. In this study, we observed that the sound speed did not change significantly throughout the 15 min stress-relaxation phase for each compression level. It is obvious that most of the fluid content in artC flowed out of the tissue with the increased compression. This experiment indicates that the sound speed might be mostly governed by the solid matrix of artC. To further confirm these findings, a long stress-relaxation period of 60 min was applied on 5 additional artC specimens. The results revealed that the sound speed in artC remained nearly constant from 15 min to 60 min during the stress-relaxation.

It was demonstrated in this study that the sound speed increased by 7.8% when the applied strain was changed from 0% to 20%. If a constant sound speed was used in the US indentation (Zheng and Mak 1996; Toyras et al 2003), the potential errors caused by this assumption on the artC thickness and indentation measurement would be in the same percentage range. Toyras et al (2003) reported that use of constant sound speed in artC for the measurement of artC modulus could generate an error of approximately 1-7% on the thickness of artC and dynamic modulus measurement. Considering the strain-dependent sound speed demonstrated in artC, the potential error should be larger. It is therefore suggested that the strain dependence of the sound speed should be taken into account in the future in the experimental studies as well as theoretical modeling of artC, such as US indentation, US compression, and mechano-acoustic assessment.

The sound speed in the full-thickness artC measured under 0% compression in this experiment was 1581±36 m/s. It was significantly smaller than those measured in other experiments in the present study. It implied that some systematic error might exist

in the measurement of the initial sound speed (0% compression) using the US compression system. In the US compression method, two flat unfocused US transducers with a frequency of 5 MHz were used for the contact measurement. This configuration was different than that used in other experiments, where a 50MHz focused US transducer was used for non-contact measurement. Further studies are required to find out what causes the difference in the measurement of the sound speed between the two systems. The main focus in using this US compression method was to demonstrate the strain-dependence of the sound speed in artC. Therefore, the percentage change of the sound speed was used to avoid the influence of this potential systematic error.

Temperature and Saline Concentration Dependence

Weissler and Grosso (1951) performed experiments in laboratory for the measurement of the sound speed in sea water. They demonstrated large differences between the sound speeds obtained in the different salt solutions and at variable temperatures. Similar findings were demonstrated by Marks (1959). In the present study, the temperature and saline concentration dependences of the sound speed in artC were studied. Significant ($p < 0.001$) changes in the sound speed were demonstrated when the temperature was varied from 15°C to 40°C or the concentration of saline solution was varied from 0M to 2.5M. Weissler and Grosso (1951) reported similar results. Their value of sound speed in the normal saline (range: 1516-1522 m/s) at 30°C agreed with the value obtained at the same temperature in our study of temperature dependence (1530 m/s). While varying the temperature at fix saline concentration of 0.15M, the sound speed in

artC changed approximately 11 m/s per 1°C change in temperature, indicating that the room temperature can dramatically affect the results of US measurement of artC.

It has been reported that artC swells when it is kept in hypotonic saline solution and shrinks when kept in hypertonic saline solution. This phenomenon occurs since PG's are associated with negative charges and tend to attract mobile cations such as sodium and calcium, to maintain electro-neutrality within the interstitial fluid. Therefore, the total ion concentration inside the tissue is usually greater than the ion concentration of the external bathing solution. The imbalance of ions creates a substantial pressure known as Donnan osmotic pressure. Therefore, artC is in swollen state in its normal form. In the present study the concentration of saline solution surrounding the artC specimen was increased stepwise. It is understood that artC shrunk with the increasing concentration of saline solution and the water is drawn out of artC because of osmosis. Therefore, the artC tends to be denser and the time taken by US to travel in the tissue decreases so that the sound speed in artC increases. Our results agreed with this phenomenon.

Temperature-dependent and saline-concentration-dependent studies were of different nature as the former was performed under a dynamic basis and the later under equilibrium conditions. This might be one of the reasons for the difference between the sound speeds obtained at 0.15M saline concentration in the temperature-dependent experiment at 21°C temperature and at the same temperature in the saline concentration-dependent experiment. Further studies need to be followed to use step-wise temperature variation, i.e. allow the saline and the artC specimen reach equilibrium before adjusting the temperature, so as to clarify the reasons for the difference of sound speed measured in these two experiments.

We observed that the sound speed at lower concentrations was highly fluctuating and nonlinear in the saline concentration dependence study. As the concentration increased, the relationship became linear (especially after 0.15M). It was observed that the sound speed in artC in both the temperature and saline dependence studies was mainly controlled by the sound speed in saline. It might indicate that the effect of temperature on the sound speed was more on the water content in artC (which contributes to approximately 70% of artC volume) than on the solid matrix of artC. It is know that the interstitial water is distributed non-uniformly throughout the depth of articular cartilage. Due to the inflow and outflow of the water content of the artC due to change in concentration of saline the biomechanical properties of artC changes i.e. the more the water inside the tissue the less stiff the artC allowing more deformation of the tissue and vice versa. The sound speed dependence of artC on the water content agreed with the conclusion made by Toyras et al (2003) in which the specimens were allowed to naturally digest. It was concluded that the water content *per se* is one of the strong contender to determine the sound speed. Previously, our group conducted experiments to investigate the swelling properties of artC with changes in the saline solution concentration (Zheng et al 2004). Further research is being conducted in our laboratory to find out the dynamic diffusion of saline and various enzymes in artC in order to investigate its swelling properties. These results would provide additional support to the findings of this study.

The thickness of artC decreased with the increase in the concentration of saline solution. This result agrees well with the previous studies (Mow and Schoonbeck 1984, Myers et al 1984, Lai et al 1991). Tissue shrinkage in higher concentrations and mild expansion in lower concentrations was observed by Parsons and Black (1979). Our

results showed no significant decrease in the thickness of artC when the concentration of the bathing solution was increased, though a decreasing trend was observed. The tissue gained the maximum expansion at 0 M concentration and shrank to the minimum at 2.5 M concentration.

Enzyme Digestion

The enzymatic degradation using three enzymes caused specific alterations and induced structural changes in artC. Based on the enzyme-dependent study with 20 specimens, it was observed that a significant decrease in the artC sound speed occurred for all the three enzyme digestions. Out of the 5 slices from a single plug, one slice was used as a 1st control slice, another one was kept in the PBS solution at 37°C as a 2nd control and remainders were digested with the respective enzymes at 37°C. The reason behind keeping one specimen immersed in PBS solution was to find whether there was any change in the sound speed in artC after storing it for 24 hrs at 37°C and immersed in PBS. The changes of the sound speed in artC induced by the digestion of specific components of artC were also studied. No significant difference of the sound speed as well as thickness was observed in the two control slices A and B (Table 9). It was also observed that the thickness of artC remained similar in both A and B cases before and after measurements. These results were consistent with those reported by Toyras et al (1999). In their study, the 0 hrs control specimen was used for mechanical measurements immediately after specimen preparation. Another specimen was measured after 44 hrs incubation at 37°C. They found no significant decrease in the thickness of the artC specimen. However in the present study, the thickness of the digested specimen

significantly decreased. The percentage decreases were 10.8%, 11.4%, and 11.2% for chondrotinase, collagenase, and trypsin digestion, respectively. There was no significant difference in the changes of the sound speed among the specimens digested with different enzymes.

It was demonstrated that the sound speed of artC changed significantly in the specimens digested with three enzymes. This agreed with previous studies (Toyras et al 1999; Joiner et al 2001; Laasanen et al 2002; Nieminen et al 2002). The sound speed obtained for the control as well as the digested specimens agreed well with the above mentioned studies. It was reported that the sound speed in the degenerated artC decreased but poorly reflected the artC composition (Myers et al 1995). This finding was confirmed in the present study as the significant decrease in the sound speed of degenerated artC did not reflect any significant difference of the sound speed among the specimens treated with the three enzymes. In our results, collagenase digestion caused the maximum decrease (5.3%) of the sound speed. This agreed with the findings of Toyras et al (1999) that the sound speed mainly depends upon collagen fibers within the solid matrix of artC (Agemura et al 1990). The decrease of the sound speed in the specimens after digestion with chondrotinase and trypsin were (4.4%) and (4.7%), respectively.

Site dependence

The site-dependent experiments of the sound speed showed significant differences between the middle and outer (peripheral) region over the patellar artC. In addition, large variations were observed among different sites. Similar large variation of the sound speed was obtained at different anatomical locations for human artC (Yao and Seedhom 1999),

though their results might be partially affected by the uncertainty of the thickness measurement due to the use of needle punching technique. On the other hand, many earlier studies have shown significant site-dependent variation in the dynamic modulus of bovine artC (Laasanen et al 2002b) and canine artC (Arokoski et al 1999; Korhonen et al 2002) using unconfined and compression indentation test. The averaged sound speed of artC obtained in this study was consistent with the results of the earlier studies. In the present study, thickness was measured using the non-contact method together with the sound speed, *ex-situ* and also using contact probe *in-situ*. In the calculation of thickness measurement, the result of *in-situ* contact method was 14% larger than that measured using non-contact method *ex-situ*. Several studies have reported the mean values of artC thickness in various aspects of the knee joint using various *in-vivo* and *in-vitro* studies (Buckland-Wright et al 1995; Adam et al 1998). The value of thickness obtained in their studies (2.6±0.36 mm, Range: 1.7 – 3.1 mm) was found higher than that obtained in our study using contact approach (1.45±0.33 mm, Range: 0.5 – 2.5 mm). This might be due to the difference of pathological state of artC or specimens obtained from different locations. Swelling of artC after excision from the bone layer can also be one of the reasons behind this difference in thickness. Another main reason might be that the artC layer had not been totally cut from the subchondral bone. Further studies are required to confirm what caused the significant difference. The sound speed mapping of the patella obtained in our study from the US measurements showed significantly different values between the middle region of the patella and the surrounding region as indicated in Fig 22. Different results were obtained in the results of thickness measurement using US, in

which the thickness in the LU region was significantly low than the other parts of the patella where a relatively uniform distribution of artC thickness was obtained.

5. Conclusions and Future Research Directions

It was concluded that the non-contact US method introduced in the present study was reliable and reproducible for the measurement of sound speed in artC *in-vitro*. The swelling effect needs to be considered when the results obtained from *in-situ* and *ex-situ* experiments are compared. It was also demonstrated that the measurement of sound speed in artC could be affected by various structural and environmental parameters with the details summarized as follows.

- The depth dependence result showed that the sound speed of artC changed significantly ($p < 0.001$) with the depth and the measurement directions. The sound speed at superficial, middle, and deep regions were 1518±17 (mean±SD), 1532±26, and 1554±42 m/s with the US beam parallel to the artC surface and 1562±23, 1623±33, and 1703±50 m/s with the US beam perpendicular to the artC surface, respectively. The sound speed of the full-thickness artC layer ($n = 18$) was 1636±25 m/s.
- The sound speed in artC changed from 1681±50 m/s to 1816±54 m/s and 1521±03 m/s to 1674±03 m/s in artC and saline, respectively. The sound speed in artC changed significantly ($p < 0.001$) when the saline concentrations varied from 0 to 2.5 M. The sound speed of the full-thickness artC layer ($n = 19$) at 0.15 M was 1675±51 m/s.
- The sound speed in artC significantly ($p < 0.001$) changed from 1430±39 to 1667±68 when the temperature varied from 15°C to 40°C. The rate of change of the sound speed was 11 m/s per 1°C in the 0.15 M saline solution.
- The sound speed in artC significantly ($p < 0.001$) decreased after treated by chondrotinase, collagenase, and trypsin, from 1653±40 m/s to 1577±32, 1564±33 and 1575±38, respectively. The percentage decrease of the sound speed in artC after enzyme

degradation was 4%, 5%, and 4% in the chondrotinase, collagenase, and trypsin enzymes, respectively. The sound speed of the full-thickness artC layer (n = 20) was 1653±40 m/s.

- The sound speed in artC varied from 1507 – 1830 m/s at the 25 locations on the patella. Significant (p < 0.01) site dependence of the sound speed in artC was demonstrated between the middle and the peripheral region of patellar artC. The average full-thickness sound speed in artC layer (n = 20) was 1626±86 m/s.
- The sound speed in artC significantly (p < 0.001) increased from 1581±36 m/s at 0% strain to 1671±56 m/s at 20% strain applied on artC. The full-thickness sound speed in artC layer at 0% compression was (n = 20) 1581±36 m/s.
- The sound speed in full-thickness artC obtained in most of the experiments matched and agreed with previous studies, except in the case of site dependence. The sound speed obtained in the strain dependence study was significantly smaller than that obtained in other dependence studies. As discussed earlier, the potential reason might be the system error existed among different measurement approaches (non-contact v/s contact, focused v/s unfocused US beam, high frequency v/s low frequency US).
- In summary, the sound speed in artC was systematically measured under various conditions in the present study. The results suggested that the environmental temperature, bathing saline concentration, specimen location, applied strain, tissue depth and degeneration status should be taken into account in the investigation of the sound speed in artC or when the sound speed is used for the calculation of other parameters.
- The sudden change in the artC thickness at lower saline concentrations needs to be further studied using several saline concentrations within the range of 0M to 0.0082M. In the present study, the saline concentration and temperature were considered separately

and experiments were performed with one parameter fixed. However, based on the significance difference obtained in the sound speed, it is suggested that experiments should be conducted by considering both parameters simultaneously. The proposed study will not only help to reveal the relationship between the artC acoustic properties and the changes in temperature and concentration of saline but also to explore the effect of temperature on the artC swelling. The study can be further extended to the swelling of artC after the treatment of various enzymes.

- The results of the present study demonstrated that the sound speed as well as thickness of artC significantly decreased after digestion of enzymes. Therefore, it would be interesting to study whether this finding maintained under different concentration of saline. Although our results of site dependence study are consistent with those reported in earlier studies, it would be too early to conclude that less variation of the sound speed occurred in a confined area (patella). A high standard deviation was observed inter- and intra-locations suggesting the site dependence topic is still open for research. Due to time constraints, this study used only 10 bovine patellae for the experiments. It is suggested that more patellae should be used in the future studies.
- The dependences of the sound speed in artC on various parameters have been demonstrated in the present study, including measurement direction, depth, site, strain applied, saline concentration, degeneration, and temperature. In the present study, the effects of these parameters were investigated separately. It would be interesting to perform experiments by varying two or more of the above parameters simultaneously. Such experiments may provide information on the interdependence of these parameters while measuring the sound speed in artC.

- The present study mainly focused on the change of the sound speed with the variation of these parameters. The effects of the variations of these parameters on other acoustical properties, such as attenuation and backscatter, should be further investigated for the US characterization of artC.
- The swelling effects of artC due to the separation from the subchondral bone need to be further studied using more specimens. In addition, the depth-dependent swelling of artC is also an important topic for further research, considering the depth dependence contains fiber-orientation and mechanical properties.
- It was noted that the artC specimens swelled quickly after detaching from the subchondral bone. Therefore, it is very important to find out an approach to measure the sound speed *in-situ*. The *in-situ* method introduced by Suh et al (2001) was complicated by the depth dependence of the sound speed in artC. Further research can be targeted to find out a better solution for this purpose.

References

Adam C, Eckstein F, Milz S, Schulte E, Becker C, and Putz R. The distribution of cartilage thickness in the knee-joints of old-aged individuals – measurement by A-mode ultrasound. Clinical Biomechanics. 1998; 13: 1-10.

Agemura DH, O'Brien WD Jr, Olerud JE, Chun LE, and Eyre DE. Ultrasonic propagation properties of articular cartilage at 100 MHz. Journal of Acoustic Society of America. 1990; 87: 1786-1791.

Appleyard RC, Burkhardt D, Ghosh P, Read R, Cake M, Swain MV, and Murrell GAC. Topographical analysis of the structural, biochemical and dynamic biomechanical properties of cartilage in an ovine model of osteoarthritis. Osteoarthritis cartilage. 2003; 11: 65-77.

Akizuki S, Mow VC, Muller F, Pita JC, Howell DS, and Manicourt DH. Tensile properties of human knee joint articular cartilage: I. Influence of ionic conditions, weight bearing, and fibrillation on the tensile modulus. Journal of Orthopaedic Research. 1986; 4: 379–392.

Armstrong CG and Mow VC. Variation in intrinsic mechanical property of human articular cartilage with age, degeneration and water content. Journal of Bone Joint Surgery. 1982; 64: 88-94.

Arokoski JP, Hyttinen MM, Helminen HJ, and Jurvelin JS. Biomechanical and structural characteristics of canine femoral and tibial cartilage. Journal of Biomedical Materials Research. 1999; 48: 99-107.

Athanasiou KA, Rosenwasser MP, Buckwalter JA, Malinin TI, and Mow VC. Interspecies comparison of in situ intrinsic mechanical properties of distal femoral cartilage. Journal of Orthopaedic Research. 1997; 9: 330-340.

Athesian GA and Soslowsky LJ. Human knee joint anatomy and cartilage thickness. Transaction of Orthopaedic Research Society. 1992; 17: 619.

Berkenblit SI, Frank EH, Salant EP, and Grodzinsky AJ. Nondestructive detection of cartilage degeneration using electromechanical surface spectroscopy. Journal of Biomechanical Engineering. 1994; 116: 384-92.

Blankvoort L, Kuiper JH, Huiskes R and Grootenboer HJ. Articular contact in a three dimensional model of the knee. Journal of Biomechanics. 1991; 24:1019-1031.

Borelli Jr J, Torzilli PA, Grigiene R, and Helfet DL. Effect of impact load on articular cartilage: development of an intraarticular fracture model. Journal of Orthopaedic Trauma 11. 1997; 319–326.

Broom ND. Structural consequences of traumatising articular cartilage. Annals of the Rheumatic Diseases. 1986; 45: 225–234.

Buckwalter J and Mankin H. Articular Cartilage Degeneration and osteoarthritis, repair, regeneration, and transplantation - part II. Journal of Bone Joint Surgery. 1997; 79: 612–632.

Buckland-Wright JC, Macfarlane DG, Lynch JA, Jasani MK, and Bradshaw CR. Joint space width measures cartilage thickness in osteoarthritis of the knee: High resolution plain film and double contrast macroradiographic investigation. Annuals of the Rheumatic Diseases. 1995; 54: 263-268.

Bursac PM, Obitz TW, Esienberg SR, and Stamenovic. Confined and unconfined stress relaxation of articular cartilage: appropriateness of a transversely isotropic analysis. Journal of Biomechanics. 1999; 32: 1125-1130.

Burstein D, Bashir A, and Gray ML. MRI techniques in early stages of cartilage disease. Investigation in radiology. 2000; 35: 622-638.

Chen AC and Sah RL. Deformation of articulating cartilage: Ultrasound analysis. Proceedings of 46th Annual meeting Orthopedics Research Society. 2000; 0887: 12-15.

Chen CT, Burton-Wurster N, Lust G, Bank RA and Tekoppele JM. Compositional and Metabolic Changes in Damaged Cartilage are Peak stress, Stress-rate, and Loading-duration Dependent. Journal of Orthopedic Research. 1999; 17: 870–879.

Cooper C, McAlindon T, Coggon D, Egger P, and Dieppe P. Occupational activity and osteoarthritis of the knee. Annals of Rheumatic Diseases. 1994; 53: 90-93.

D'Astous FT and Forster FS. Frequency dependence of ultrasound attenuation and backscatter in breast tissue. Ultrasound in Medicine and Biology. 1986; 12: 795-808.

Disler P. MR imaging of articular cartilage. Skeletal Radiology. 2000; 29: 367-377.

Duda GN, Haisch A, Endres M, Gebert C, Schroeder D, Hoffmann JE, and Sittinger M. Mechanical quality of tissue engineered cartilage: results after 6 and 12 weeks in vivo. Journal of Biomedical Materials Research. 2000; 53: 673-677.

Eisenberg SR, Grodzinsky AJ. The kinetics of chemically induced nonequilibrium swelling of articular cartilage and corneal stroma. Journal of Biomechanical Engineering. 1987; 109: 79-89.

Elliott DM, Narmoneva DA, and Setton LA. Direct measurement of the Poisson's ratio of human patella articular cartilage in tension. Journal of Biomechanical Engineering. 2002; 124: 223–228.

Fortin M, Soulhat J, Shirazi-Adl A, Hunziker EB, and Buschmann MD. Unconfined compression of articular cartilage: nonlinear behavior and comparison with a fibril reinforced biphasic model. Journal of Biomechanical Engineering. 2000; 122: 189-195.

Fry H and Robertson WV. Interlocked stresses in cartilage. Nature. 1967; 215: 53-54.

Fu FH, Youn I and Suh J-K. Clinical evaluation of mechanical properties of articular cartilage using a newly developed arthroscopic ultrasonic indentation probe. 2nd Symposium of the International Cartialge Repair Society (Boston, 16-18 November 1998).

Fukui N, Purple CR, and Sandell LJ. Cell biology of osteoarthritis: The chondorcyte's response to injury. Current Rheumatology Reports. 2001; 3: 496-505.

Fung YC. Microcirculation Dynamics. Biomedical Science Instrumentation. 1968; 4: 310-320.

Garon M, Légaré A, Quenneville E, Hurtig MB, and Buschmann MD. Streaming potential based arthroscopic instrument distinguishes site-specific properties of equine articular cartilage. 49th Annual Meeting of the Orthopaedic Research Societ. 2002, Paper #025. Biomedical & Chemical Engineering, Ecole Polytechnique, Montreal, Quebec, Canada

Gill HS and O'Connor JJ. Biarticualting teo-dimensional computer model of the human patellofemoral joint. Clinical Biomechanics. 1996; 11: 81-89.

Grodzinsky AJ. Electromechanical and physicochemical properties of connective tissue. Critical Review in Biomedical Engineering. 1983; 9: 133-199.

Grodzinsky AJ, Roth V, Myers E, Grossman WD, and Mow VC. The significance of electromechanical and osmotic forces in the non equilibrium swelling behavior of articular cartilage in tension. Journal of Biomechanical Engineering. 1981; 103: 221-31.

Guilak F, Ratcliffe A, and Mow VC. Chondrocyte deformation and local tissue strain in articular cartilage: A Confocal microscopy study. Journal of Orthopaedic Research. 1995; 13: 410-421.

Harris ED Jr, Parker HG, Radin EL and Krane SM. Effects of proteolytic enzymes on structural and mechanical properties of cartilage. Arthritis Rheumatology. 1972;15: 497–503.

Harkness RD. Mechanical properties of collagen tissues. In: Gould BS, ed. Biology of Collagen 2. New York: London, Academic Press. 1968: 247-310.

Hayes WC, Keer LM, Herrmann G, and Mockros LF. A mathematical analysis of indentation tests of articular cartilage. Journal of Biomechanics. 1972; 5: 541-51.

Heegard J, Leyvraz PF, Curnier A, Rakotomanana L and Huiskes R. The biomechanics of the human paella during passive knee flexion. Journal of Biomechanics. 1995; 28: 1265-1279.

Herrmann JM, Pitris C, Bouma BE, Boppart SA, Jesser CA, Stamper DL, Fujimoto JG, and Brezinski ME. High resolution imaging of normal and osteoarthritic cartilage with optical coherence tomography. Journal of Rheumatology. 1999; 26: 627-635.

Hsu DK and Hughes MS. Simultaneous ultrasound velocity and sample thickness measurement and application in composites. Journal of Acoustic Society of America. 1992; 92: 669-675.

Jeffrey JE, Gregory DW, and Aspend RM. Matrix damage and chondrocyte viability following a single impact load on articular cartilage. Archives of Biochemistry and Biophysics. 1995; 322: 87–96.

Joiner GA, Bogoch ER, Pritzker KP, Buschmann MD, Chevrier A, and Foster FS. High frequency acoustic parameters of human and bovine articular cartilage following experimentally-induced matrix degradation. Ultrasonic Imaging. 2001; 23: 106-116.

Joseph D, Gu WY, Mao XG, Lai WM, and Mow VC. True density of normal and encymatically treated bovine articular cartilage. Proceedings of 45th Annual Meeting of Orthopaedic Research Society, Feb 1999, Anaheim, CA, US. p642.

Jurvelin JS, Rasanen, Kolmonen P, and Lyyra T. Comparison of optical, needle probe and ultrasonic techniques for the measurement of articular cartilage thickness. Journal of Biomechanics. 1995; 28: 231-235.

Jurvelin JS, Buschmann MD, and Hunziker E. Mechanical anisotropy of human knee articular cartilage in compression. Transaction of Orthopaedic Research Society. 1996; 21: 340–347.

Jurvelin JS, Arokoski PA, Hunziker EB, and Helminen HJ. Topographical variation of the elastic properties of articular cartilage in the canine knee. Journal of Biomechanics. 2000: 33: 669–675.

Jurvelin JS, Buschmann MD, and Hunziker EB. Mechanical anisotropy of the human knee AC in compression. Proceedings of Institute of Mechanical Engineering. 2003; 217: 215–219.

Kawchuk GN, Fauvel OR, and Dmowski J. Ultrasonic quantification of osseous displacements resulting from skin surface indentation loading of bovine para-spinal tissue. Clinical Biomechnics. 2000; 15: 228-233.

Kempson GE, Muir H, Pollard C, and Tuke M. The tensile property of cartilage of human femoral condyles related to contents of collagen and glycosaminoglycans. Biochimica et Biophysica Acta. 1973; 297: 456-472.

Kempson GE. The mechanical properties of articular cartilage. In: Sokoloff L, ed. The Joints and Synovial Fluid, vol. II. New York: Academic Press. 1980; 177-238.

Kempson GE. Relationship between the tensile properties of articular cartilage from the human knee and age. Annals of the Rheumatic Diseases. 1982, 41: 508-11.

Kerin AJ, Wisnom MR, and Adams MA. The compressive strength of articular cartilage. Proceedings of the Institution of Mechanical Engineers. 1998; 212: 273–280.

Kiefer GN, Sundby K, McAllister D, Shrive NG, Frank CB, Lam T, and Schachar NS. The effect of Cryopreservation on the biomechanical behaviour of bovine articular cartilage. Journal of Orthopaedic Research. 1989; 7: 494-501.

Kim HK, Babyn PS, Harasiewicz KA, and Foster FS. Imaging of immature articular cartilage using ultrasound backscatter microscopy at 50MHz. Journal of Orthopaedic Research. 1995; 13: 963-970.

Koehler T, Szeri AZ, and Buchanan TS. An inhomogeneous, anisotropic spring model of articular cartilage. 25th Annual Meeting of the American Society of Biomechanics. 2001; 118.

Korhonen RK, Laasanen MS, Toyras J, Lappalainen R, Helminen HJ, and Jurvelin JS. Fibril reinforced poroelastic model predicts specifically mechanical behavior of normal, proteoglycan depleted and collagen degraded articular cartilage, Journal of Biomechanics. 2003; 36: 1373-1379

Korhonen RK, Laasanen MS, Toyras J, Rieppo J, Hirvonen J, Helminen HJ, and Jurvelin JS. Comparison of the equilibrium response of articular cartilage in unconfined compression, confined compression and indentation. Journal of Biomechanics. 2002a; 35: 903-909

Korhonen RK, Wong M, Arokoski J, Lindgren R, Helminen HJ, Hunziker EB, and Jurvelin JS. Importance of the superficial tissue layer for the indentation stiffness of articular cartilage. Medical Engineering & Physics. 2002b, 24: 99-108.

Korhonen RK, Töyräs J, and Nieminen MT. Effect of ionic environment on the compression-tension nonlinearity of articular cartilage in the direction perpenticular to articular surface. Transaction of Orthopaedic Research Society. 2001; 26: 439.

Kuo IK, Hete B, and Shung KK. A novel method for the measurement of acoustic speed. Journal of Acoustic Soceity of America. 1990; 88: 1679-1682.

Lai WM, Hou JS, and Mow VC. A triphasic theory for the swelling and deformation behaviors of articular cartilage. Journal of Biomechanical Engineering. 1991; 113: 245-258.

Lane JM, Chisena E, and Black J. Experimental knee instability: early mechanical property changes in articular cartilage in a rabbit model. Clinical Orthopaedics. 1979; 140: 262-265.

Laasanen MS, Toyras J, Hirvonen J, Saarakkala S, Korhonen RK, Nieminen MT, Kiviranta I, and Jurvelin JS. Novel mechano-acoustic technique and instrument for diagnosis of cartilage degeneration. Physiological Measurement. 2002; 23: 491-503.

Laasanen MS, Toyras J, Korhonen RK, Rieppo J, Saarakkala S, Nieminen MT, Hirvonen J, and Jurvelin JS. Biomechanical properties of knee articular cartilage. Biorheology. 2003a; 40: 133-140.

Laasanen MS, Toyras J, Vasara AI, Hyttinen MM, Saarakkala S, Hirvonen J, Jurvelin JS, and Kiviranta I. Mechano-Acoustic diagnosis of cartilage degenration and repair. The Journal of Bone and Joint Surgery. 2003b; 85-A Suppl 2: 78-84.

Legare A, Garon M, Guardo R, Savard P, Poole AR, and Buschmann MD. Detection and analysis of cartilage degeneration by spatially resolved streaming potentials in articular cartilage. Journal of Orthopaedic Research. 2002; 20: 819–826.

Lengsfeld M. Stresses at the meniscofemoral joint: elastostatic investigations on the applicability of interface elements. Journal of Biomechanical Engineering. 1993; 15: 324-328.

Li LP, Buschmann MD, and Shirazi-Adl A. Strain-rate dependent stiffness of articular cartilage in unconfined compression. Journal of Biomechanical Engineering. 2003; 125: 566.

Lyyra T, Jurvelin J, Pitkanen P, Vaatainen U, and Kiviranta I. Indentation instrument for the measurement of cartilage stiffness under arthroscopic control. Medical Engineering and Physics. 1995; 17: 395-399.

Lyyra T, Kiviranta I, Vaatainen U, Helminen HJ, and Jurvelin JS. In vivo characterization of indentation stiffness of AC in the normal human knee. Journal of Biomedical Material Research. 1999: 48: 482–487.

Macirowski T,Tepic S, and Mann RW Cartilage stresses in the human hip joint. Journal of Biomechanical Engineering. 1994; 116: 10-18.

Mankin HJ, Mow VC, Buckwalter JA, Iannotti JP, and Ratcliffe A. Form and function of articular cartilage. In: Simnon SR, ed. Orthopaedic Basic Science. American Academy of Orthopaedic Surgeons,.1994; 2-44.

Mann RW, Shepherd DET, and Seedhom BB. Discussion on: A technique for measuring the compressive modulus of articular cartilage under physiological loading rates with preliminary results. Proc Instn Mech Engrs: J Engr Medicine. 2001; 215: 123-124.

Marks GW. Variation of acoustic velocity with temperature in aqueous solution of certain inorganic sulphates. The Journal of Acoustical Society of America. 1959; 31: 936-947.

Maroudas A. Balance between swelling pressure and collagen tension in normal and degenerate cartilage. Nature.1976; 260: 808-9.

McDevitt CA. Biochemistry of articular cartilage. Nature of proteoglycans and collagen of articular cartilage and their role in ageing and in osteoarthrosis. Annals of Rheumatic Diseases. 1973; 32: 364-78

McGibbon CA. Inter-rater and intra-rater reliability of subchondral bone and cartialge thickness measurement from MRI. Magnetic Resonance Imaging. 2003; 21: 707-714.

Modest VE, Murphy MC, and Mann RW. Optical verification of a technique for in situ ultrasonic measurement of articular cartilage thickness. Journal of Biomechanics. 1989; 22: 171-176.

Mow VC and Schoonbeck JM. Contribution of donan osmotic pressure towards the biphasic compressive modulus of articular cartilage. Transcations of Orthopaedic Research Society. 1984; 9: 262.

Mow VC, Zhu W, and Ratcliffe A. Structure and function of articular cartilage and meniscus. In: Mow VC, and Hayes WC, ed. Basic Othopaedic Biomechanics. New York: Raven Press. 1991; 143-198.

Myers ER, Lai WM, and Mow VC. A continuum theory and an experiment for the ion-induced swelling behavior of articular cartialge. Journal of Biomechanical Engineering. 1984; 106: 151-158.

Myers SL, Dines K, Brandt DA, Brandt KD, and Alvrecht ME. Experimental assessment by high frequency ultrasound of articular cartilage thickness and osteoarthritic changes. Journal of Rheumatology. 1995; 22: 109-116.

Nambu T, Gasser B, Schneider E, Bandi W and Perren SM. Deformation of the distal femur: a contribution towards the pathogenesis of osteochondrosis dissecans in the knee joint. Journal of Biomechanics. 1991; 24: 421-433.

Njeh CF, Hans D, Fuerst T, Gluer CC, and Genant HK. Quantitative US: Assessment of osteoporosis and bone status. Martin Dunitz Ltd, London, 1999.

Nieminen HJ, Toyras J, Rieppo J, Nieminen MT, Hirvonen J, Korhonen R, and Jurvelin JS. Real-time ultrasound analysis of articular cartilage degradation in vitro. Ultrasound in Medicine and Biology. 2002; 28: 519-525.

Parsons JR and Black J. Mechanical behavior of articular cartilage: Quantitaive changes with alteration of ionic environment. Journal of Biomechanics. 1979; 12: 765-773.

Pocock NA, Babichev A, Culton N, Graney K, Rooney J, Bell D, and Chu J. Temperature dependency of quantitative ultrasound. Osteoporosis International. 2000; 11: 316-20.

Quinn TM, Grodzinsky AJ, Hunziker EB, and Sandy JD. Effects of injurious compression on matrix turnover around individual cells in calf articular cartilage explants. Journal of Orthopaedic Research. 1998; 16: 490–499.

Ragozzino M. Analysis of the error in measurement of ultrasound speed in tissue due to waveform deformation by frequency-dependent attenuation. Ultrasonics. 1981; 19: 135-138.

Repo RU and Finlay JB. Survival of articular cartilage after controlled impact. Journal of Bone and Joint Surgery. 1977; 59-A: 1068–1076.

Roth V and Mow VC. The intrinsic tensile behavior of the matrix of bovine articular cartilage and its variation with age. Journal of Bone Joint Surgery. 1980; 62: 1102–1117.

Rushfeldt PD, Mann RW, and Harris WH. Improved techniques for measuring in vitro geometery and presssure distribution in the human acetabulum: Ultrasonic measurement of acetabular surface, sphericity and cartilage thickness. Journal of Biomechanics. 1981; 14: 253-260.

Sachs JR, Grodzinsky AJ. Electromechanical spectroscopy of cartilage using a surface probe with applied mechanical displacement. Journal of Biomechanics. 1995; 28: 963-76.

Saied A, Cherin E, Gaucher H, Laugier P, Gillet P, Floquet J, Netter P, and Berger G. Assessment of articular cartilage and subchondral bone: subtle and progressive changes in experimental osteoarthritis using 50MHz echography in vitro. Journal of Bone and Mineral Research. 1997; 12: 1378-1386.

Schinagl RM, Ting MK, Price JH, and Sah RL. Video microscopy to quantitate the inhomogeneous equilibrium strain within articular cartilage during confined compression. Annals of Biomedical Engineering. 1996; 24: 500-512.

Schinagl RM, Gurskis D, Chen AC, and Sah RL. Depth-dependent confined compression modulus of full-thickness bovine articular cartilage. Journal of Orthopaedic Research. 1997, 15: 499-506.

Setton LA, Tohyama H, and Mow VC. Swelling and curling behaviors of articular cartilage. Journal of Biomechanical Engineering. 1998; 120: 355-361.

Shen Y, Rangayyan RM, Bell GD, Frank CB, Zhang YT, and Ladly KO. Localization of knee joint cartilage pathology by multichannel vibroarthrography. Medical Engineering and Physics. 1995; 17: 583-94.

Shingleton WD, Hodges DJ, Brick P and Cawston TE. Collagenase: a key enzyme in collagen turnover. Biochem. Cell Biol. 1996; 74: 759–75.

Suh JKF, Youn I, and Fu FH. An in situ calibration of an ultrasound transducer: a potential application for an ultrasonic indentation test of articular cartilage. Journal of Biomechanics. 2001; 34: 1347-1353.

Swann AC, and Seedhom BB. Improved techniques for measuring the indentation and thickness of articular cartilage. Proceedings of Institution Mechanical Engineers. 1989; 203: 143-150.

Tavathia S, Rangayyan RM, Frank CB, Bell GD, Ladly KO, and Zhang YT. Analysis of knee vibration signals using linear prediction. IEEE Trans Biomed Eng. 1992; 39: 959-70.

Torzilli PA, Grigiene R, Borelli J, and Helfet DL. Effect of impact load on articular cartilage: cell metabolism and viability, and matrix water content. Journal of Biomechanical Engineering. 1999; 121: 433–441.

Toyras J, Rieppo J, Nieminen MT, Helminen HJ, and Jurvelin JS. Characterization of enzymatically induced degradation of articular cartilage using high frequency ultrasound. Physics in Medicine and Biology. 1999; 44: 2723-2733.

Toyras J, Lyyra-Laitinen T, Niinimaki M, Lindgren R, Nieminen MT, Kiviranta I, and Jurvelin JS. Estimation of the Young's modulus of articular cartilage using an arthroscopic indentation instrument and ultrasound measurement of tissue thickness. Journal of Biomechanics. 2001; 34: 251-256.

Toyras J, Laasanen MS, Saarakkala S, Lammi MJ, Rieppo J, Kurkijarvi J, Lappalainen R, and Jurvelin JS. Speed of sound in normal and degenrated bovine articular cartilage. Ultrasund in Medicine and Biology. 2003; 29: 447-454.

Wilson A, Forster FK, Clark J, and Notzli H. Development of automated ultrasonic measurements of articular cartilage thickness and surface morphology. In Proc. of the 15th Annual Intl. Conf. of the IEEE Engineering in Medicine and Biology. 1993. 1122–1123.

Wang CCB, Deng JM, Ateshian GA, and Hung CT. An automated approach for direct measurement of two-dimensional strain distributions within articular cartilage under unconfined compression. Journal of Biomechanical Engineering. 2002; 124: 557-567.

Wang CCB, Chahine NO, Hung CT, and Ateshian GA. Optical determination of anisotropic material properties of bovine articular cartilage in compression. Journal of Biomechanics. 2003; 36: 339-353.

Weiss C, and Mirow S. An ultrastructural study of osteoarthritis changes in the articular cartilage of human knees. Journal Bone Joint Surgery of America. 1972; 54: 954-72.

Weissler A, and Grosso DV. The velocity of sound in sea water. The Journal of Acoustical Society of America. 1951; 23: 219-223.

Wu JZ, and Herzog W. Mechanical anisotropy of articular cartilage is associated with variations in microstructures. 24th Annual Meeting of the American Society of Biomechanics. 2001; 275.

Yamagata T, Saito H, Habuchi O and Suzuki S. Purification and properties of bacterial chondroitinases and chondrosulfatases. J. Biol. Chem. 1968; 243: 1523–35

Yao JQ, and Seedhom BB. Ultrasonic measurement of thickness of human articular cartilage in situ. Rheumatology. 1999; 38: 1269-1271.

Youn I, and Suh JK. Acoustic charateristics of collagen and glycosaminoglycan in articular cartilage. Proceedings of 47th Annual Meeting Orthopedics Research Society. 2001; 0435: 25-28.

Zhang YT, Rangayyan RM, Frank CB, and Bell GD. Adaptive cancellation of muscle contraction interference in vibroarthrographic signals. IEEE Transaction of Biomedical Engineering. 1994; 41: 181-91.

Zheng YP, and Mak AFT. An ultrasound indentation system for biomechanical properties assessment of soft tissues in vivo. IEEE Transactions on Biomedical Engineering. 1996; 43: 912-918.

Zheng YP, Maev RG, and Solodov Iyu. Nonlinear acoustic applications for material characterization: a review. Canadian Journal of Physics. 1999; 77: 1-41.

Zheng YP, Ding CX, Bai J, Mak AFT, and Qin L. Measurement of the layered compressive properties of trypsin-treated articular cartilage: an ultrasound investigation. Medical and Biological Engineering and Computing. 2001; 34: 534-541.

Zheng YP, Mak AFT, Lau KP, and Qin L. Ultrasonic measurement for in-vitro depth-dependent equilibrium strains of articular cartilage in compression. Physics in Medicine and Biology. 2002; 47: 3165-3180.

Zheng YP, Shi J, Qin L, et al. Dynamic depth-dependent osmotic swelling and solute diffusion in articular cartilage monitored using real-time ultrasound. Ultrasound in Medicine and Biology. 2004a; 30: 841-9.

Zheng YP, Bridal SL, Shi J, Saied A, Lu MH, Jaffre B, Mak AFT, and Laugier P. High resolution ultrasound elastomicroscopy imaging of soft tissue: System development and feasibility. Physics in Medicine and Biology. 2004b; 49: 3925-2938.

Zheng YP, Niu HJ, Mak AFT, and Huang YP. Ultrasonic measurement of depth-dependent transient behaviors of articular cartilage under compression. Journal of Biomechanics. 2004c; In print.

****